

**Dissertation zur Erlangung des Doktorgrades
der Fakultät für Chemie und Pharmazie
der Ludwig-Maximilians-Universität München**

**New strategies for the application of
Adeno-Associated Virus type 2 targeting vectors**



**Daniela Goldnau
aus
Duisburg**

2006

Erklärung

Diese Dissertation wurde im Sinne von § 13 Abs. 3 bzw. 4 der Promotionsordnung vom 29. Januar 1998 von Herrn Prof. Dr. Michael Hallek betreut und von Herrn Prof. Dr. Horst Domdey vor der Fakultät für Chemie und Pharmazie vertreten.

Ehrenwörtliche Versicherung

Diese Dissertation wurde selbständig, ohne unerlaubte Hilfe erarbeitet.

München, am 31.3.2006

Daniela Goldnau

Dissertation eingereicht am: 07.04.2006

1. Gutachter: Prof. Dr. Horst Domdey
2. Gutachter: Prof. Dr. Michael Hallek

Mündliche Prüfung am: 23.5.2006

Danksagung

Ich danke Herrn Prof. Dr. Michael Hallek für die Möglichkeit meine Doktorarbeit in seiner Arbeitsgruppe durchzuführen und die Bereitstellung eines sehr interessanten Themen- und Aufgabengebiets.

Herrn Prof. Dr. Horst Domdey danke ich, als meinem Doktorvater, für die Möglichkeit in der Fakultät der Chemie meine Doktorarbeit anzufertigen.

Mein besonderer Dank gilt Frau Dr. Hildegard Büning, die diese Doktorarbeit betreut und mich vom ersten bis zum letzten Tag begleitet und unterstützt hat.

Besonderer Dank gilt Prof. Patrick Cramer, der das Genzentrum seit Juni 2004 mit innovativer Kraft leitet und die Weiterarbeit an dieser Arbeit in den Räumen des Genzentrums ermöglicht hat.

Mein Dank gilt der Firma Medigene, die ein viel versprechendes Projekt weiterverfolgt und unterstützt hat. Besonderer Dank gilt hier Markus Hörer und den Mitgliedern seiner Gruppe für kritische und hilfreiche Diskussionen und Unterstützung auch im praktischen Bereich.

Für die Unterstützung bei der Durchführung der Experimente zur Kopplung über Maleimide Bindung sowie für anregende Diskussion und die Bereitstellung verschiedener Materialien möchte ich mich ganz herzlich bei Dr. Florian Kreppel, Universität Ulm, bedanken.

Bedanken möchte ich mich auch bei meinen Mitstreitern Kerstin und Jan, die für Diskussion und auch viel Spaß im Labor gesorgt haben. Ebenso bedanken möchte ich mich bei den ehemaligen Mitglieder der AG Hallek, hier insbesondere Kristin und Nadja, die mich ebenfalls bis zum Schluss begleitet haben und immer ein offenes Ohr und einen guten Rat parat hatten.

Ein ganz lieber Dank geht auch an Sigi Kastenmüller, Frau Mewes und Frau Fulde, die immer eine große Hilfe bei verwaltungstechnischen Dingen waren.

Innigsten Dank möchte ich meinen Eltern für ihre großartige Unterstützung in jeglicher Hinsicht und für alles, was sie mir mit auf den Weg gegeben haben, aussprechen.

Mein ganz besonderer Dank gilt meinem Freund Torsten, für seine Liebe, Verständnis, seine Motivation, Freundschaft und fürs einfach nur da sein. Schön, dass es Dich gibt!

Die vorliegende Arbeit wurde in der Zeit von Dezember 2001 bis März 2006 am Institut für Biochemie der Ludwig-Maximilians-Universität München unter der Anleitung von Prof. Dr. Michael Hallek angefertigt.

Im Verlauf dieser Arbeit wurden folgende Veröffentlichungen angefertigt:

Kerstin Lux, Nico Görlitz, Stefanie Schlemminger, Luca Perabo, **Daniela Goldnau**, Jan Endell, Kristin Leike, David M. Kofler, Stefan Finke, Michael Hallek, Hildegard Büning
"Green Fluorescent Protein-Tagged Adeno-Associated Virus (AAV) Particles Allow the Study of Cytosolic and Nuclear Trafficking"; J Virol. 2005 Sep 79(18):11776-87.

Luca Perabo, Jan Endell, Susan King, Kerstin Lux, **Daniela Goldnau**, Michael Hallek, Hildegard Büning
"Combinatorial Engineering of a Gene Therapy Vector: Directed Evolution of Adeno-Associated Virus"; J Gene Med. 2006 Feb;8(2):155-62.

Daniela Goldnau, Jan Endell, Luca Perabo, and Kathryn White, Jorge Boucas, Sibille Humme, Lorraine Work, Hanna Janicki, Michael Hallek, Andrew H. Baker, Hildegard Büning
"HSPG binding properties of Adeno-Associated Virus (AAV) retargeting mutants and consequences for their *in vivo* tropism"; in revision, J Virol, January 2006.

Hildegard Büning, John Nieland, Luca Perabo, Daniela Goldnau, Kerstin Lux, and Michael Hallek
"AAV anti-idiotypic vaccine", eingereicht als Erfindungsmeldung, 2005

"Our deepest fear is not that we are inadequate. Our deepest fear is that we are powerful beyond measure. It is our light, not our darkness, that most frightens us. We ask ourselves, who am I to be brilliant, gorgeous, talented and fabulous? Actually, who are you not to be?"

From Nelson Mandela's inaugural speech as President of South Africa - May 1994

Für meine Großeltern

Summary

Vectors based on adeno-associated virus type 2 (AAV) offer considerable promise for the somatic gene therapy of various diseases (e.g. cystic fibrosis, hemophilia B, cancer) and new applications such as vaccination. Limitations, however, still exist and require further improvements, especially in the field of cell specific gene transfer. The study presented here addresses ways of generating an universal rAAV retargeting vector and an AAV based anti-idiotypic vaccine approach.

Due to its primary receptor heparan sulphate proteoglycan (HSPG), wtAAV shows a broad tissue tropism. To generate tissue specific rAAV vectors, different targeting approaches were used, including the insertion of a targeting peptide into exposed sites on the AAV capsid. For *in vivo* application an universal targeting vector, which does not demand the production of a new AAV mutant each time, would be of great advantage. Two different strategies were applied for the generation of an universal AAV retargeting vector, either containing a polyionic insertion and a cysteine (AAV-Glu) or only cysteine flanked by glycines (AAV-Cys), both at the exposed insertion site 587.

The accessibility and the reactivity of the thiol groups of the inserted cysteine of AAV-Glu were demonstrated by conjugation of AAV-Glu to a thiol reactive dye. But conjugation to the polyionic ligand SIG could not be verified in transduction experiments. AAV-Cys did not show conjugation ability to 5k-Polyethylenglykol-Mal (5k-PEG-Mal) ligand. In the following six new cysteine mutants were generated, this time by amino acid exchange with cysteine at different exposed sites in the capsid surface. These mutants are currently evaluated for their conjugation ability and showed promising results in preliminary experiments.

Many AAV targeting vectors have been generated by peptide insertions at position 587/588 of the capsid. This is likely to interfere with the heparan sulphate proteoglycan binding ability of at least two (R585 and R588) of the five positively charged amino acids of the recently identified HSPG binding motif, explaining the ablation of HSPG binding of some targeting vectors. In some cases, however, binding was only partially affected, or even restored. To investigate molecular mechanisms responsible for these differences, a library of AAV capsids mutants carrying insertions of 7 randomized amino acids at position 587 were applied to a heparin affinity column to separate binding from non-binding mutants. This resulted in a model explaining the HSPG binding and non-binding

phenotypes of AAV targeting mutants. Furthermore, the inability to bind to heparin/HSPG correlated with liver and spleen detargeting in *in vivo* studies after systemic application, suggesting several strategies to improve efficiency of AAV-2 retargeting to alternative tissues in the future.

Many passive immunization approaches using monoclonal antibodies against a variety of diseases have reached the drug market in the recent years. Here we present a strategy to develop vaccines for active immunization based on anti-idiotypic AAV library mutants selected on antibody epitopes. Selections were performed with the AAV library, containing a random insertion of seven amino acids at the exposed site 587. Two antibodies were tested, the IgE binding antibody Omalizumab (Xolair[®]) and mouse anti-KLH IgG, directed against Keyhole Limpet Hemocyanin (KLH). Mutants could be selected for Omalizumab as well as for anti-KLH IgG. Two out of three selected sequences for Omalizumab showed specificity for the antibody in Dot Blot analysis and four out of five on anti-KLH IgG selected sequences demonstrated specificity for anti-KLH. This proof of principle indicates that the selection of AAV library mutants on antibodies is in general possible and provides the basis for new generation of vaccines. Immunization experiments in rabbits are currently ongoing.

Taken together, these results should be useful for the design and selection of improved recombinant AAV vectors for retargeting and a new generation of active immunization vaccines.

Contents

SUMMARY	1
1. INTRODUCTION.....	5
1.1. ADENO-ASSOCIATED VIRUS AS VECTOR FOR HUMAN GENE THERAPY	5
1.2. GENOMIC AND STRUCTURAL ORGANIZATION OF AAV	8
1.3. AAV TARGETING VECTORS	12
2. CHAPTER I - UNIVERSAL TARGETING OF AAV	14
2.1. INTRODUCTION CHAPTER I	14
2.2. RESULTS CHAPTER 1	18
Insertion of cysteine as reaction partner into the AAV capsid.....	18
Coupling of rAAV to ligands via polyionic fusion peptides.....	21
Coupling by maleimide reaction.....	25
2.3. DISCUSSION CHAPTER 1	28
AAV-2 tolerates insertion of polyionic sequence and cysteine into the capsid structure.....	28
AAV-Glu can be conjugated to Oregon Green dye by thiol maleimide reaction.....	29
Conjugation of AAV-Glu did not result in efficient transduction of target cells.....	29
Conjugation of AAV-Cys to ligands by maleimide reaction.....	31
3. CHAPTER II - DEVELOPMENT OF AN AAV BASED ANTI-IDIOTYPIC VACCINE.....	33
3.1. INTRODUCTION CHAPTER II.....	33
IgE as Therapeutic Target in Allergic Diseases.....	33
3.2. RESULTS CHAPTER II.....	37
Coupling of geno- and phenotype.....	37
Selection of AAV particles with specific affinity for a target antibody from the coupled viral library	46
3.3. DISCUSSION AND OUTLOOK CHAPTER II	55
Uptake seems to allow unspecific internalization of AAV	55
Homogeneous library mutants result from coupling through uptake or infection	57
Selection of anti-idiotypic AAV mutants on antibodies by solid phase.....	61
Outlook.....	65
4. CHAPTER III - APPLICATION OF THE COUPLED AAV LIBRARY FOR SELECTION OF GENE THERAPY VECTORS.....	66
4.1. INTRODUCTION CHAPTER III	66
AAV heparin Binder and Nonbinder pool.....	66
4.2. RESULTS CHAPTER III	67
Separation of Binders and Nonbinders by Heparin binding affinity	67
In vivo biodistribution of heparin Binders and Nonbinders	71
Selection on Hepatocytes with the Nonbinder library	73
Selection procedure on Hepatocytes	74
4.3. DISCUSSION AND OUTLOOK CHAPTER III	75
AAV Library can be divided into heparin binders and Nonbinders with specific binding properties.....	75
In vivo biodistribution of Binder and Nonbinder pool.....	76
Nonbinder library allows the selection of heparin-independent targeting mutants on Hepatocytes.....	77
Outlook.....	78
5. MATERIAL AND METHODS	79
5.1. MATERIAL	79
Cell lines.....	79
Viruses and vectors	80
Bacteria	80
Plasmids.....	81

Enzymes	82
Antibodies.....	82
Synthetic Oligonucleotides.....	82
Chemicals and other Material.....	82
Primers.....	84
Standards and Kits.....	84
Buffer and Solutions	85
Equipment.....	87
5.2. METHODS	87
General Methods	87
Established Methods	93
6. ABBREVIATIONS.....	99
7. REFERENCES.....	101

1. Introduction

1.1. Adeno-Associated Virus as vector for Human Gene Therapy

Presently available gene delivery vehicles for somatic gene transfer can be broadly divided into two categories: viral and nonviral vectors (Table 1). The nonviral vectors, also known as synthetic gene delivery systems, represent a category of delivery vehicles which rely on direct delivery of either naked DNA or RNA with cationic lipids. Nonviral vectors do not share the safety risks of the viral transfer systems, but suffer from low efficiency of gene transfer and only transient expression of the delivered genes. Based on the nature of their genome, viral vectors can be divided into RNA (retroviruses) and DNA (adeno-associated virus, adenovirus, herpes simplex virus, pox virus) viral vectors. Viruses are intracellular parasites that have developed efficient strategies to invade host cells, and in most cases, transport their genetic information into the nucleus.

Table 1. Gene Therapy Trials world wide (www.wiley.co.uk/genmed/clinical)

Vector	Trials ¹	Example of diseases	
Viral			
Adeno-Associated Virus (AAV)	38 (3.3%)	Cystic fibrosis, hemophilia B, prostate cancer, neurological disorders, muscular dystrophy	
Adenovirus	287 (25.1%)	Many cancers, peripheral artery disease, cystic fibrosis, Canavan disease	
Herpes simplex Virus (HSV)	38 (3.3%)	Brain tumor, colon carcinoma	
Pox Virus	59 (5.2%)	Many cancers	
Retrovirus	276 (24.1%)	Many cancers, AIDS, SCID, rheumatic arthritis, graft-versus-host disease, multiple sclerosis, osteodysplasia, hemophilia	
Nonviral			
Gene Gun ²	5 (0.4%)	Melanoma, sarcoma	
Lipofection ³	95 (8.3%)	Many cancers, cystic fibrosis, coronary artery disease, restenosis	
Naked DNA (plasmid)	192 (16.8%)	Many cancers, peripheral artery disease, coronary artery disease, peripheral neuropathy, open bone fractures	
RNA transfer	14 (1.2%)	Many cancers	
Other	136 (12.3%)		

¹ Number of clinical trials conducted worldwide (March 2006)

² DNA coated on small gold particles and shot with a special gun into target tissue

³ Includes liposomes and various packages of lipid, polymer, and other molecules

The major advantages of viral vectors are their high transduction efficiency and the potential stable expression of the therapeutic gene (retroviruses, adeno-associated virus).

A limitation, however, is the risk of toxicity of the vector and induction of immunological reactions against the vector (e.g. adenoviral vectors) or its transgene.

The Adeno-Associated Virus (AAV), which was utilized in the present work, is a particularly promising delivery system for human gene therapy and the number of clinical trials using AAV based vectors is constantly increasing since 1994, when AAV based vectors were utilized in a gene therapy trial dealing with cystic fibrosis (Flotte and Carter, 1995). One major reason why AAV vectors receive increasing attention is the safety of this vector: no known pathogenicity has been related to AAV infection. Moreover, AAV vectors are replication deficient and fail to unleash cellular immune responses (Hernandez et al. 1999, Joos et al. 1998, Zaiss et al. 2002). This has been attributed to the poor ability of AAV to infect dendritic cells (Bessis et al.), but newer studies show that cell-mediated immunity can occur against the AAV capsid and were responsible for the decline of the Factor IX transgene gene (Manno et al. 2006)

AAV, the primary virus, is a member of the parvovirus family. Viruses of this family have a single-stranded DNA genome of approximately 5kb and a non-enveloped icosahedral capsid. With a diameter of only 18 to 30nm the parvoviruses are among the smallest known viruses. For its progeny production adeno-associated viruses naturally depend on co-infection of an unrelated helper virus, e.g. adenovirus (Ad), herpesvirus (HSV), human cytomegalovirus, or papillomavirus (for review see (Muzyczka and Berns, 2001). Originally, AAV was found as a contaminant in laboratory stocks of adenovirus, hence the name “adeno-associated virus” (Atchison, Casto, and Hammon, 1965; Hoggan, Blacklow, and Rowe, 1966). Up to now eleven serotypes (AAV type 1 – AAV type 11), which share different levels of sequence homology, have been identified (Gao et al. 2002, Gao et al. 2004, Mori et al. 2004). Although the other serotypes have attracted increasing attention during recent years, AAV type 2 is the most prominent serotype for gene therapy, being the best characterized. All following descriptions will refer to AAV type 2, it will be termed AAV throughout this work.

The life cycle of AAV has two distinct intracellular phases (Figure 1). In the absence of co-infection by a helper virus the latent cycle is initiated. AAV enters the cell, and after a limited expression of viral regulatory proteins (Rep proteins), the virion integrates preferentially into the host genome in the q arm of chromosome 19 at a specific

locus (AAVS1). After super-infection with a helper virus, the integrated genome is activated by entering the lytic cycle, leading to viral gene expression, rescue and replication of the AAV genome with subsequent production of viral progeny (Berns and Giraud, 1996). Besides helper virus also genotoxic agents (e.g. UV-irradiation, γ -irradiation, hydroxyurea, topoisomerase inhibitors, and various chemical carcinogens) can support a productive infection (Heilbronn et al., 1985; Russell, Alexander, and Miller, 1995; Yakobson et al., 1989; Yalkinoglu, Zentgraf, and Hubscher, 1991; Yalklinoglu et al., 1988). These observations led to the conclusion that the role of helper functions is rather the induction of the appropriate cellular milieu (expression of stress response genes) required for AAV DNA replication than direct involvement of helper virus gene products (Yakobson, Koch, and Winocour, 1987).

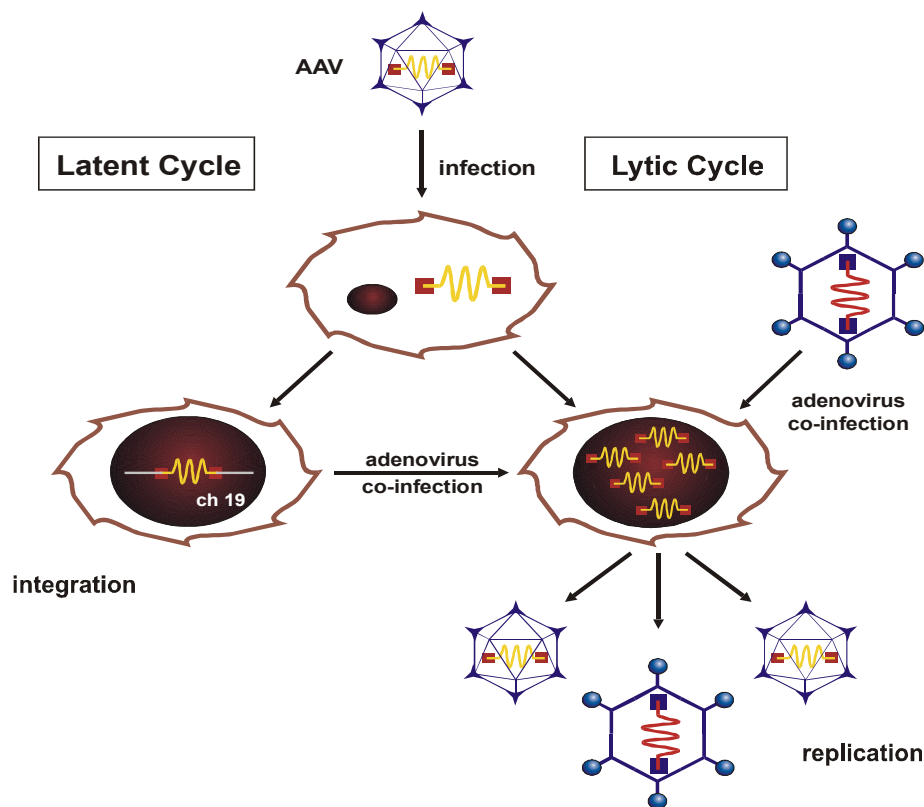


Figure 1. The biphasic life cycle of AAV. In the presence of a helper virus, e.g. adenovirus or herpesvirus, AAV enters the lytic cycle and undergoes a productive infection. Lacking a helper virus the AAV DNA can stably integrate preferentially into chromosome 19 of the host genome (AAVS1). After super-infection with a helper virus AAV can be rescued from the latent state and reenter the lytic cycle. (Figure kindly provided by Nadja Huttner)

The natural route for AAV infections is assumed to occur via the respiratory or gastrointestinal route as is the case for Ad, because *in vivo* AAV has been typically found as a contaminant of Ad isolates (Blacklow et al., 1971). However, it is not yet clear what tissue or organ is a preferred site of latency in humans. Nevertheless, recombinant AAV vectors have demonstrated infection and long-term gene expression in a wide variety of

tissues, including brain, liver, muscle, lung, and retina in animals (Fisher et al., 1997; Flannery et al., 1997; Flotte et al., 1993; Kaplitt et al., 1994; Snyder et al., 1997; Xiao, Li, and Samulski, 1996). Although AAV is widespread, no disease has been associated with the virus (Berns and Linden, 1995). On the contrary, AAV seems to be protective against bovine papillomavirus and Ad mediated cellular transformation (de la Maza and Carter, 1981; Hermonat, 1989; Khleif et al., 1991; Mayor, Houlditch, and Mumford, 1973), and seems to have cytotoxic effects in malignant cells (Raj et al. 2001).

1.2. Genomic and Structural Organization of AAV

The wild-type AAV (wtAAV) has a single-stranded DNA genome of 4680 nucleotides and consists of two large open reading frames (ORF). These ORFs are flanked by palindromic sequences, the inverted terminal repeats (ITRs) (Figure 2).

The 145 nucleotide long inverted terminal repeats (ITR) form a T-shaped structure on either side of the genome. They contain a Rep binding site (RBS) and a specific cleavage site for the bound Rep protein (terminal resolution site, TRS) (Im and Muzyczka, 1990; McCarty et al., 1994; Snyder et al., 1993; Snyder, Samulski, and Muzyczka, 1990). They constitute an important *cis*-acting signal which serves as origin of replication (*ori*) and primer for initiation of DNA synthesis. Furthermore they are critical for regulation of gene expression, and essential for site-specific integration of AAV and rescue of the viral genome from the integrated state (Labow and Berns, 1988; McLaughlin et al., 1988; Samulski, Chang, and Shenk, 1987).

The 5'-ORF *rep* encodes the non-structural, regulatory Rep proteins. Two promoters, p5 and p19, direct expression of the *rep* gene. A common intron results in the production of four Rep proteins: p5 promoter controls transcription of Rep78 and its splice variant Rep68, whereas transcription of Rep52 and its splice variant Rep40 is controlled by the p19 promoter. Rep78 and Rep68 are multifunctional proteins with diverse biochemical activities, including DNA binding, DNA ligase, ATPase, DNA helicase, and strand- and site-specific endonuclease activities (Im and Muzyczka, 1990; Im and Muzyczka, 1992; Smith and Kotin, 2000; Zhou et al., 1999). They are involved in AAV DNA replication, transcriptional control and targeted integration. The two smaller proteins, Rep52 and Rep40, appear to be involved directly in the accumulation and encapsidation of single-

stranded genomes into preformed capsids (Chejanovsky and Carter, 1989; Dubielzig et al., 1999; King et al., 2001; Smith and Kotin, 1998). The Rep proteins can act as both repressors and transactivators of AAV transcription by regulating the activities of the three viral promoters. In the absence of helper virus, all Rep proteins have been observed to repress p5 and p19 transcription (Kyostio et al., 1994).

The 3'-ORF *cap* encodes three structural proteins with overlapping amino acid sequences, VP1, VP2, and VP3, which form the viral capsid. They are all transcribed from the p40 promoter and expressed in a ratio of approximately 1:1:20 (Kronenberg, Kleinschmidt, and Bottcher, 2001) and use a common stop codon. The molecular weight of VP1, VP2, and VP3 is 90kDa, 72kDa, and 60kDa, respectively. While VP3 alone is sufficient for capsid formation and VP2 capsid protein is non essential for viral infectivity (Warrington et al. 2004), VP1 is required for viral infection (Hermonat et al., 1984; Smuda and Carter, 1991; Tratschin, Miller, and Carter, 1984).

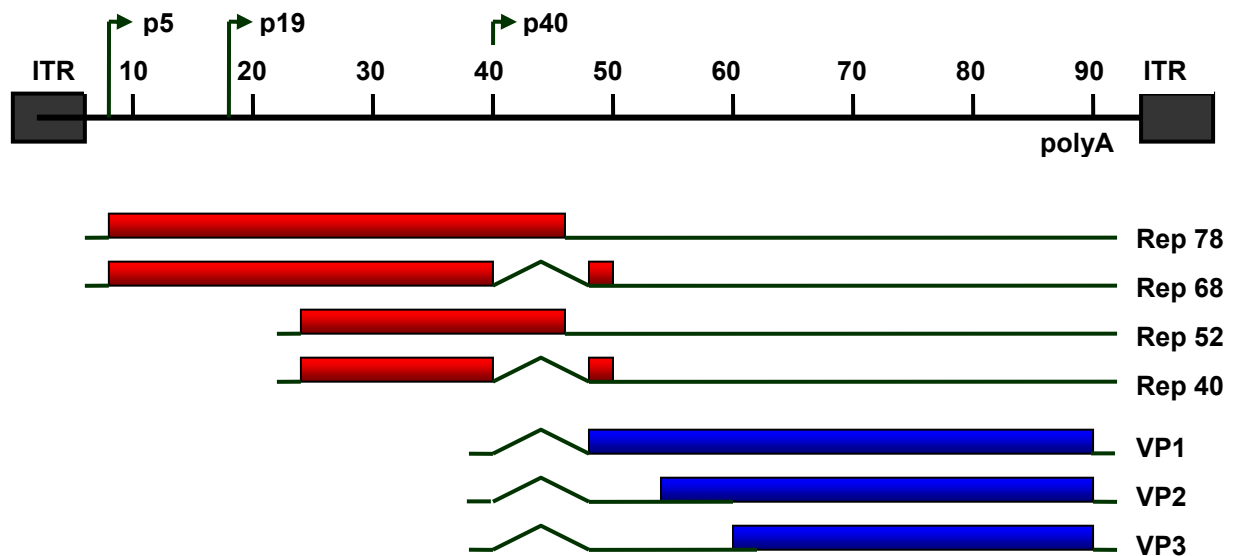


Figure 2. Map of the AAV genome. The AAV genome encompasses 4680 nucleotides, divided into 100 map units. Indicated are the two inverted terminal repeats (ITRs), the three viral promoters at map position 5, 19, and 40 (p5, p19, and p40) and the polyadenylation signal at map position 96 (poly A). The open reading frames are represented by rectangles, untranslated regions by solid lines and the introns by carats. Large Rep proteins (Rep78 and Rep68) under the control of the p5 promoter and small Rep proteins (Rep52 and Rep40) driven by the p19 promoter exist in spliced and unspliced isoforms. The *cap* genes encoding the three different capsid proteins VP1, VP2, and VP3 are under control of the p40 promoter.

The AAV particle has a molecular weight between 5.4 and 6.0×10^6 g/mol (de la Maza et al. 1980). Approximately 70% of the mass is protein, and the remaining is DNA. AAV particles are very resistant to inactivation. They are stable between pH 3 and 9 and at 56°C for 60 min. Inactivation of the virus is possible by formalin, β -propiolactone, hydroxylamine, and oxidizing agents (Berns et al., 2000).

While the atomic structures of related autonomous parvoviruses, including canine parvovirus (CPV), feline panleukopenia virus (FPV), minute virus of mice (MVM), Aleutian mink disease virus (ADV), and the human parvovirus B19, have been resolved during the past decade, the three-dimensional structure of the AAV capsid remained unknown (Agbandje et al., 1994; Agbandje-McKenna et al., 1998; Chang, Sgro, and Parrish, 1992; Chapman and Rossmann, 1993; Chipman et al., 1996; McKenna et al., 1999; Strassheim et al., 1994; Tsao et al., 1991). Instead, alignments of these related parvoviruses with AAV had led to hypothetical models of the AAV capsid. Random and systematic mutagenesis approaches helped to identify functional sites on the capsid, including putative binding sites for the primary receptor HSPG, immunogenic epitopes and flexible loop regions at the capsid surface that accept the insertion of targeting ligands (Girod et al., 1999; Rabinowitz, Xiao, and Samulski, 1999; Wobus et al., 2000; Wu et al., 2000). In 2002 the atomic structure of AAV has been determined to 3Å resolution by x-ray crystallography (Xie et al., 2002).

Each viral capsid is composed of 60 subunits arranged with T=1 icosahedral symmetry (Xie et al., 2002). The three structural proteins VP1, VP2, and VP3, which share overlapping sequences and differ only at their N-termini (Figure 2), build the AAV capsid with a relative stoichiometry of about 1:1:20 (Kronenberg, Kleinschmidt, and Bottcher, 2001). The central motif of each subunit is an anti-parallel β -barrel which is highly conserved among parvoviruses. This β -barrel motif forms elongated smooth lumps at the inner surface of the capsid at the 2-fold symmetry axis (Kronenberg, Kleinschmidt, and Bottcher, 2001). Between the strands of the β -barrel core large loop insertions are found that share only low similarity among the parvovirus family. These loops comprise two-thirds of the capsid structure and constitute the capsid surface features that interact with antibodies and cellular receptors. These surface features include a hollow cylinder at the 5-fold axis of symmetry which is surrounded by a circular depression (canyon), and a depression spanning the 2-fold axis (dimple). The most prominent features of the capsid are the 3-fold-proximal peaks, which cluster around the 3-fold symmetry axis. The peaks are not derived from one capsid subunit protein but from the interaction of two adjacent subunits. Other interactions between loops of neighboring subunits are found at the 5-fold cylinder. Overall, the outside surface of AAV is positively charged with clusters of positive charges in the canyon, surrounding the 5-fold cylinder, and at the 3-fold symmetry axis. Regions of negative charges are mainly found at the top of the 5-fold cylinder and at the sides of the 2-fold dimple facing the 3-fold axes.

After resolution of the crystal structure of AAV important functions obtained from genetic data could be mapped to the structure. At the 3-fold-proximal peaks, in the valleys separating the three peaks of one 3-fold axis, clusters of positive charges are located, which are implicated in receptor binding. Although no definitive HSPG binding motif has been found on the capsid surface so far, mutational analyses have identified these locations being involved in binding to the primary receptor HSPG (Wu et al., 2000). Especially the basic amino acids (aa) R487, R585, and R588, which are at the side of the peak, seem to play a crucial role (Grifman et al., 2001; Wu et al., 2000; Xie et al., 2002). Interestingly, the separation between these clusters at the side of the peaks is 20 Å, consistent with binding neighboring disaccharides of the heparan sulfate moiety. The epitope of an AAV-neutralizing antibody, A20, could also be mapped to the 3-fold spike region. It is situated in the valley between the peaks of one 3-fold axis (Wobus et al., 2000).

1.3. AAV Targeting Vectors

The development of safe and efficient gene transfer vectors is crucial for the success of gene therapy. The adeno-associated virus is a promising vector for human somatic gene therapy, however, its broad tissue tropism, which is based on the widely spread of its primary receptor HSPG, is a disadvantage, if a tissue and organ-selective gene transfer after systemic application is desired. Although, AAV is known to infect diverse organs such as brain, liver, muscle, lung, retina and heart muscle (Carter and Samulski, 2000), the vector has to be administered directly to reach clinically relevant gene expression (Monahan and Samulski, 2000; Tal, 2000).

Therefore, increasing efforts have been made to target AAV-based vectors to specific receptors. So far, the most promising approach is the genetic modification of the viral capsid.

The first successful demonstration that a genetic capsid modification can be used to retarget AAV was described by Girod et al. (1999). A sequence alignment of AAV and CPV identified six sites aa positions (261, 381, 447, 534, 573, 587) that were expected to be exposed on the surface of the virus capsid and to accept the insertion of a ligand without disrupting functions essential for the viral life cycle. At these positions, the sequence for the 14 amino-acid peptide L14 (QAGTFALRGDNPQG) was inserted into the capsid gene. The L14 peptide contains the RGD motif of the laminin fragment P1 and is the target for

several cellular integrin receptors, besides also serving as a viral receptor. An efficient transduction of B16F10 cells was observed using the AAV insertion mutant I-587 expressing Rep or β -galactosidase (Girod et al, 1999). Grifman et al. (2001) inserted the Myc epitope and a CD13 (NGR receptor expressed on angiogenic vasculature and in many tumor cell lines) specific peptide with the sequence NGRAHA, identified by phage display, into positions 448 and 587. The insertion into 587 allowed a cell-specific targeting to different cell lines (KS1767 (Kaposi sarcoma) and RD (rhabdomyosarcoma)).

Other approaches for efficient retargeting of AAV include the targeting by bispecific antibodies which mediate the interaction between virus and target cell and was first demonstrated by Bartlett et al (1999). The antibody used was generated by a chemical crosslink of the Fab arms of monoclonal antibodies against the $\alpha_{IIb}\beta_3$ integrin (AP-2 antibody) and the intact AAV capsid (A20 antibody). The major ligand for $\alpha_{IIb}\beta_3$ is fibrinogen, which becomes internalized via endocytosis. Therefore, AAV targeted to this integrin was expected to become internalized via receptor-mediated endocytosis, similar to wild-type virus. This targeting vector transduced MO7e and DAMI cells, which are not permissive for wild-type AAV infection (70-fold above background). In contrast, a 90% reduction in AAV transduction was seen on cells negative for the targeting receptor. It remains to be determined whether this reduction was because of steric hindrance or some other mechanism. Another issue that remains to be resolved is the stability of the virus-bispecific antibody complexes *in vivo*.

Wu et al. (2000) inserted the receptor specific ligand of the HA epitope YPVDVDPDYA into the N-terminal regions of VP1, VP2 and VP3 and the C-terminus of the *cap* ORF. They observed that the insertion of this and other epitopes at the N-termini of VP1 and VP3 and at the C-terminus of the *cap* ORF resulted in either no detectable particles (for VP3 and the *cap* ORF) or in a 2-3 log decrease of infectious and physical particle titers. In agreement with Yang et al. (1998) only the insertion at the N-terminus of VP2 was tolerated. Moreover exchanging the HA epitope by the serpin receptor ligand KFNKPFVFLI78 resulted in a 15-fold higher infection of the lung epithelial cell line IB3 than by wild-type AAV.

Studies demonstrating a successful *in vivo* retargeting of AAV vectors for other organs than the liver include the targeting of coronary endothelial cells (Muller et al. 2005) and human vascular endothelial cells (Nicklin et al. 2001, Shi and Bartlett 2003). To efficiently retarget AAV vectors, a better understanding of the infectious biology of AAV

will be required. This includes the virus-cell surface interactions, mechanism of uptake, endosomal processing and release, nuclear transport and mechanisms leading to gene expression.

Another important issue is the identification of the optimal ligand or targeting receptor. Length and sequence of the ligand can be critical in insertion vectors, as the insertion of a peptide may result in profound alterations of the three dimensional capsid structure. This problem might be overcome by the combination of the insertion with one or more deletions or with the insertion of a sequence that is able to form its own secondary structure, for example, a loop closed by a cysteine bridge (Shi and Bartlett 2003; Wang et al. 2005).

To identify new ligands, phage display is a valid approach. However, the ligand sequences are selected in an architectural context that is different from that of the final vector. This means that once inserted in the context of AAV, they could destabilize the capsid structure (resulting in low packaging efficiency) or lose their biological properties (resulting in low infectious titers). To overcome these difficulties the screening for new retargeting peptides to be inserted was done in the context of the AAV capsid itself, where a pool of randomized peptide sequences was inserted into the capsid sequence and the viral pool was then screened directly on target cells (Perabo et al. 2003).

Perabo et al. applied the AAV library for selection of receptor-specific targeting mutants on different cell lines that were resistant to infection by wtAAV. Three mutants were obtained which transduced target cells with an up to 100-fold increased efficiency, in a receptor-specific manner and without interacting with the primary receptor for wtAAV. Extension of the library by randomizing the viral capsid by error prone PCR showed that mutants with improved phenotype can be obtained which are less efficiently neutralized by human antibodies and can, therefore, be used to generate novel vectors for the treatment of patients with pre-existing immunity to AAV (Perabo and Endell et al. 2006).

Overall, the adeno-associated viruses are very promising gene transfer vehicles for the treatment of multiple diseases. The increasing interest in AAV as vector system and the rising amount of gene therapy trials which are currently under investigation argue for its potential as human gene therapy vector. Hurdles, however, still exist and have to be overcome, including specific and selective transduction of the target tissue and potential immune responses to the vector and/or the transgene.

2. Chapter I - Universal Targeting of AAV

2.1. Introduction Chapter I

The primary receptor of AAV is heparan sulphate proteoglycan (HSPG). Since HSPG is displayed on a wide variety of cells, AAV shows a broad tissue tropism. This limits cell-specific transduction of target tissue after systemic application and therefore targeting of AAV vectors plays an important role.

In principle, two different strategies are possible to achieve a receptor targeting of AAV (Cosset and Russell, 1996):

1. **Indirect targeting:** In contrast to wild type (Fig. 1A) the interaction between the viral vector and the target cell is mediated by an associated molecule (e.g. a bispecific antibody) which is bound to the viral surface and interacts with a specific cell surface molecule (Miller, 1996) (Fig. 1B).
2. **Direct targeting:** The cell specific targeting of the vector is mediated by a ligand which is directly inserted into the viral capsid (Walter and Stein, 1996) (Fig. 1C).

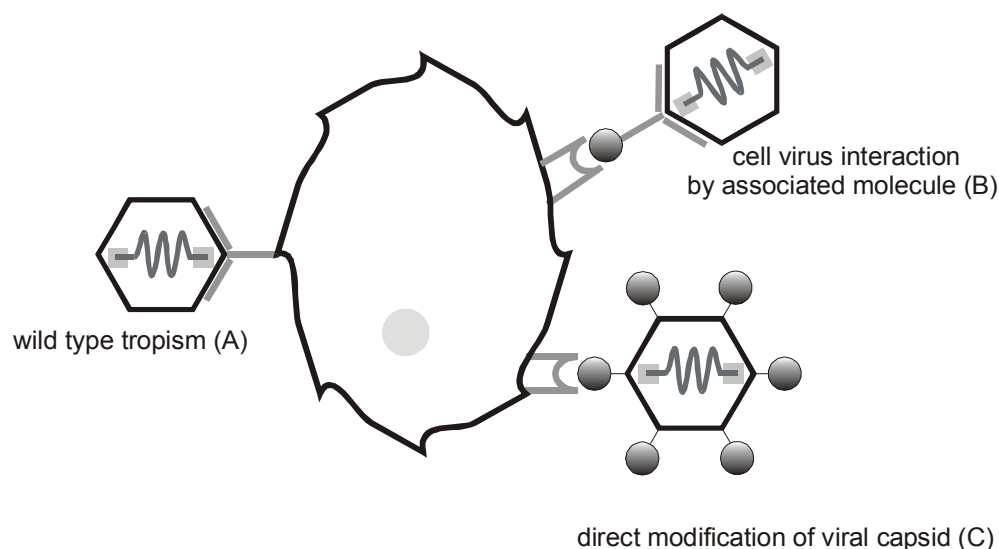


Figure 1: Possibilities of viral vector targeting (Büning et al. 2003).

Viral vectors with wild type tropism (A) show a direct binding of structural capsid components to the cell surface receptor. In targeting vectors, the virus-cell interaction is mediated by a molecule associated with the capsid (indirect targeting, B) or by a ligand directly inserted into the capsid (direct targeting, C).

For indirect targeting it is not necessary to know the three-dimensional structure of the viral surface if high affinity viral surface binding molecules such as monoclonal

antibodies are available. For this strategy, the stability of the interaction of the virus with the intermediate molecule and the efficiency by which the complex is generated are rate limiting. In addition, the intermediate molecules must bind to cell-specific receptors which allow the uptake and correct intracellular processing of the virus.

A combination of two important parameters is required for the successful generation of a targeting vector by direct modifications of the capsid:

The first parameter is a good choice of the insertion site to ensure that packaging of the mutant virus remains efficient and the inserted ligand is exposed on the virus surface. Different strategies have been used for AAV to identify candidate positions for insertion of heterologous ligand: a) sequence alignment between AAV and other parvoviruses for which the X-ray crystal structure is known (Girod et al. 1999; Grifman et al. 2001); b) a systematic, insertional mutagenesis of the whole AAV capsid (Rabinowitz and Samulski, 1999; Shi and Bartlett 2001; Wu et al. 2000). Since the X-ray crystal structure of AAV has been solved in 2002 (Xie et al. 2002), the selection of insertion sites can now be performed by educated guesses.

The second important parameter is the choice of the targeting peptide. It is difficult to predict the secondary structure of the ligand inserted into the AAV capsid. Therefore, the ligand should be structure-independent and not too large to avoid the destabilization of the entire capsid. Finally, the ligand-receptor complex should be internalized in a way that allows an efficient transport of the virus and the release of the viral DNA into the cell nucleus.

Direct and indirect targeting approaches and a combination thereof have been used to successfully retarget AAV (Bartlett et al. 1999; Girod et al. 1999; Grifman et al. 2001; Nicklin et al. 2001; Ried et al. 2002; Shi and Bartlett 2001; Wu et al. 2000; Yang et al. 1998, Perabo et al. 2003, Muller et al. 2005, Stachler et al. 2006, Work et al. 2006).

The basis of the current project was the work of Ried et al, who tried to create an universal targeting vector using a truncated 34 amino acid peptide, Z34C, from protein A of *Staphylococcus aureus* (Ried et al., 2002). Protein A recognizes and binds the Fc part of immunoglobulins (Ig), but not the variable region, which therefore remains free to bind the antigen. Z34C is derived from the protein A subunit B, which encompasses 56 amino acids and binds the Fc portion with a dissociation constant of about 10-50 nM (Sinha, Sengupta, and Ray, 1999). Z34C was inserted at position 587, previously described as retargeting site by Girod et al. (1999), into the AAV capsid (rAAV-587Z34C). This insertion allowed a functional expression of the IgG binding domain, as shown by binding studies using

various antibodies. Coupling 587Z34C AAV vector with different antibodies e.g. against CD29 (β 1-integrin), CD117 (c-kit-receptor) or CXCR4 resulted in a specific, antibody mediated transduction of hematopoietic cell lines. No transduction could be detected without antibody, whereas the targeted infection was blocked with soluble protein A or with IgG molecules. In addition, no inhibition of transduction by the targeting vector was observed with heparin, demonstrating that the interaction of the 587Z34C mutants with the natural AAV receptor heparan sulphate proteoglycan (HSPG) was not essential for infection or transduction. Thus an universal targeting vector had been generated which allowed to exchange the respective tropism by simply exchanging the ligand coupled to the modified vector.

However, vector titers (10-fold decrease in packaging efficiency) and transduction efficiency of the respective target cells were relatively low. The decreased packaging efficiency is most likely due to the size of the insertion (34 amino acids inserted into each of the 60 proteins of the AAV capsid) whereas the stability of the interaction between the antibody and coupling domain hampers from the fact that it is based only on non covalent interaction and could be one of the reasons for low transduction efficiency obtained.

In 2001 Stubenrauch et al. described a specific coupling of an antibody fragment to the surface of polyoma VLPs via polyionic fusion peptides by complementary charge. Stability was increased by a disulfide bridge which covalently coupled the antibody fragment and the VLP. The antibody utilized in this study was the tumour-specific anti-(Lewis Y) antibody fragment. This approach led to a retargeting of the modified polyoma particles towards antigen-presenting cells, thus demonstrating the basic concept for the development of a cell-type-specific, non-viral vector system. However, also in this study the transfection efficiencies were rather low, probably due to the degradation of polyoma VLP in lysosomes after cellular uptake (Stubenrauch et al. 2001).

Kreppel et al. recently described a novel virus vector-targeting platform based on a unique combination of genetic and chemical vector particle modifications to overcome typical restrictions in virus vector targeting. (Kreppel et al. 2005). They genetically introduced cysteines into the HI loop of adenovirus, which is solvent-exposed position. The corresponding thiol groups were highly reactive, and they established procedures for controlled covalent coupling of protein and nonprotein ligands to them. After the coupling of apo-transferrin, the particles were efficiently targeted to the transferrin receptor pathway. Depending on the chemistry used, ligands could be coupled under the formation of thioether or disulfide bonds, the latter allowing for separation of ligand and particle after

cell entry into the endosome. Furthermore, this technology could be efficiently combined with vector shielding for true retargeting: after amino-PEGylation of the vector particles the genetically introduced thiols were still accessible for ligand coupling, and particles could be retargeted to the transferrin receptor.

In the work described here, we tried to improve the concept of an universal AAV targeting vector by introducing a covalent linkage between the modified AAV vector (carrying a coupling domain) and the ligand (which defines the tropism). Two different strategies were applied: a) specific coupling via polyionic fusion peptides combined with the introduction of cysteines for controlled covalent coupling and b) just the insertion of cysteine.

2.1. Results Chapter I

Insertion of cysteine as reaction partner into the AAV capsid

First, in analogy to Stubenrauch et al. (2001), the following strategy was performed to try to optimize the interaction between virus and ligand: a sequence of eight glutamic acids and one cysteine was inserted C-terminal of the amino acid position 587 into the AAV capsid utilizing standard cloning techniques. As counterpart the ligand (SIG peptide, see below) to be coupled was synthesized as fusion with a sequence of eight arginines and one cysteine. A first contact between ligand and vector capsid should be mediated by the polyionic sequences, followed by a covalent linkage due to disulfide bridging by cysteine.

The AAV mutant, AAV-Glu, was packaged in 293 cells and purified by iodixanol step gradient (details see Material and Methods). After purification AAV-Glu preparation was characterized. For genomic titer determination the Dot Blot method was used and capsid titer was determined by ELISA, utilizing an antibody (A20) which recognizes only intact AAV capsids. Both titers (4×10^8 genomic particles/ μl and 1×10^9 capsid particles/ μl , respectively) showed that the mutant could be packaged to titers comparable to wtAAV.

To further purify the virus solution, purification by gel filtration and/or by anion exchange column were established and applied. Fractions of gel filtration were eluted with PBS and purified virus could be obtained from three fractions with high genomic and capsid titers (3×10^8 genomic particles/ μl). Due to the inserted charged amino acids, an anion exchange chromatography (HiTrap ANX FF high sub, Amersham) could be performed. This was a first proof that the inserted negative charged amino acids are accessible on the capsid surface. The bound fractions were eluted with 1M NaCl. The high salt concentration was removed by gel filtration where necessary.

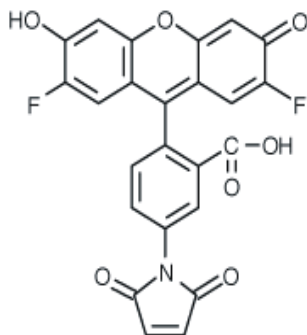


Figure 2:
Oregon Green 488 maleimide
(Molecular Probes)

To analyse if the inserted cysteine is accessible for coupling, AAV-Glu was coupled to a thiol reactive dye, Oregon Green 488 maleimide (Figure 2).

The coupling was conducted as described according to the protocol for thiol-reactive probes by Molecular Probes. Briefly, the thiol groups, introduced into the capsid of AAV-Glu, were reduced by 10-fold

molar excess of Tris(2-carboxyethyl) phosphine hydrochloride (TCEP). TCEP was chosen, because it does not interfere with the conjugation reaction to maleimides. The Oregon Green dye was added again in a 10-fold molar excess and incubated at room temperature for 2h. Excess dye was removed by dialysis. After dialysis the capsid titers were determined by A20-ELISA and same capsid particles (1×10^{10} capsid particles) were analyzed by SDS PAGE.

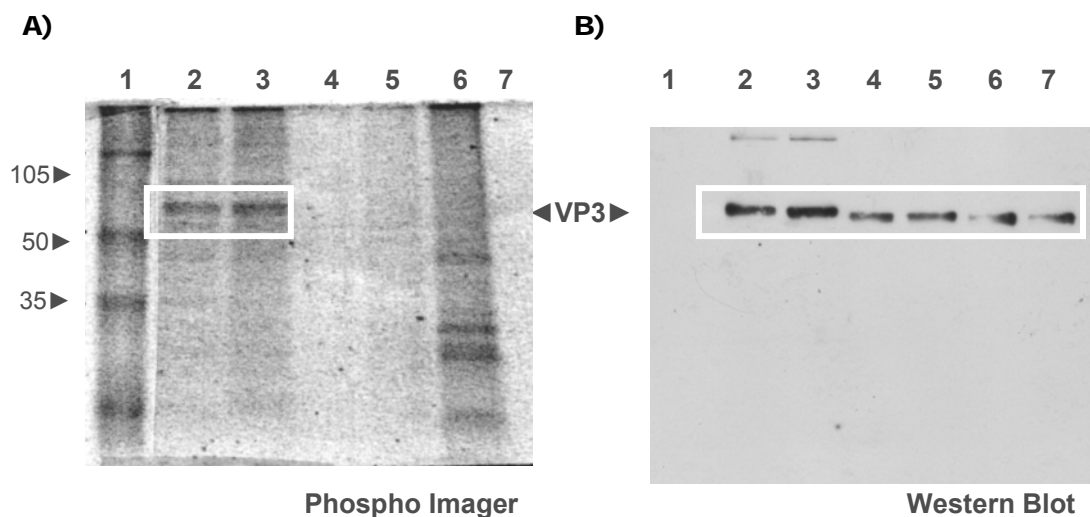


Figure 3: Conjugation of Oregon Green to AAV-Glu

AAV-Glu and wtAAV were coupled to Oregon Green and dialyzed against PBS. Capsid titers were determined and same particles of all samples were applied to separation by SDS PAGE. Before blotting the SDS gel was analyzed by Phospho Imager using the blue channel (450nm) to detect Oregon Green. The gel was blotted to nylon membrane by semi-dry membrane transfer and the AAV capsid proteins were detected with B1 antibody.

Lane 1: Marker; **Lane 2,3:** AAV-Glu +Oregon Green; **Lane 4,5:** AAV-A3 (HSPG knock out, Wu et al. 2000); **Lane 6:** wtAAV +Oregon Green; **Lane 7:** wtAAV w/o Oregon Green

Phospho Imager allows the detection of Oregon Green dyes. When applying the SDS-Gel to the Phospho Imager for analysis, labelled bands were detectable (Figure 3A). The gel was then blotted and incubated with B1 antibody. B1 antibody is able to recognize unassembled viral capsid proteins (VP) 1, 2, and 3 of AAV (Bleker et al. 2005). In the Western Blot analysis (Figure 3B) only the VP3 could be detected for all vectors used. This is most probably due to the detection limit, since VP1, VP2 and VP3 are building up the AAV capsid in a 1:1:20 ratio (Rabinowitz et al. 1999) and already the VP3 signal was relatively weak. By comparing the bands detected in the Western Blot (Figure 3B) with the image taken with the Phospho Imager of the same SDS gel before blotting (Figure 3A), a labelled band for VP3 was detectable in the sample of AAV-Glu which had been coupled to Oregon Green. wtAAV, which was used as a control and had also been incubated with

Oregon Green, showed labelled bands in the Phospho Imager picture. However, none of these bands corresponded in size to the AAV VP proteins.

These results show that the cysteine inserted in AAV-Glu is accessible for coupling.

In the optimal situation, the interaction between the targeting vector and its target is only dictated by the inserted ligand (knock out for natural ligand:receptor interaction of the original virus). To determine the tropism of AAV-Glu, the transduction efficiency of AAV-Glu was determined in comparison to rAAV with unmodified capsid on HeLa (cervix carcinoma cell line) and SVEC (endothelial cell line). For this the cells were seeded into 24-well plates 24h before transduction. 4 different amounts of vectors were used (5×10^3 , 1×10^4 , 5×10^4 and 1×10^5 genomic particles per cell). Both vectors encoded the same transgene (enhanced green fluorescent protein). After 48h cells were harvested and analyzed for GFP expression by FACS analysis.

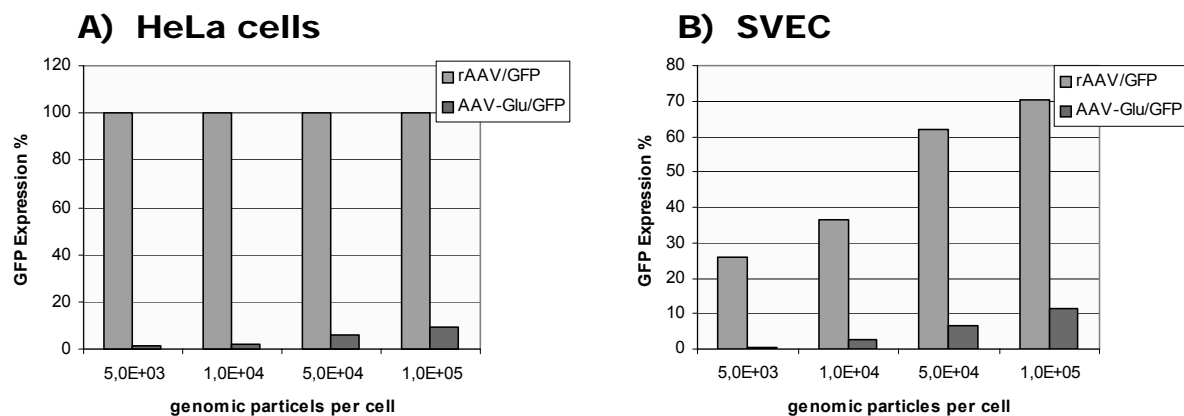


Figure 4: Transduction efficiency of AAV-Glu/GFP and rAAV/GFP on HeLa cells and SVEC
Cells (Hela: 2×10^5 ; SVEC: 1×10^5) were seeded in 24 well plates. After 24h medium was changed, the cells number per well was determined and cells were transduced with genomic particles per cell of 5×10^3 , 1×10^4 , 5×10^4 and 1×10^5 . After 48h cells were harvested and analyzed by FACS for transduction efficiency.

In comparison to rAAV with unmodified capsid, AAV-Glu was not able to transduce neither HeLa nor SVEC cells efficiently, indicating that the natural tropism had been ablated by the insertion of the polyionic sequence into the capsid. This is a very promising basis for the generation of a targeting vector since abolishment of the natural tropism will transfer the targeting properties alone to the coupled ligand.

Coupling of rAAV to ligands via polyionic fusion peptides

Conjugation to the SIG peptide

In a first approach, the peptide SIGYPLP (SIG) was chosen as a coupling ligand. SIG was fished as an endothelial specific peptide by phage display by Nicklin et al (2000) and a SIGYPLP-modified AAV (AAV-SIG), with the SIG peptide inserted in position 587 of the capsid, could be generated. AAV-SIG showed an efficient and selective tropism for endothelial vascular cells (EC) compared with control AAV vectors with wt capsid (Nicklin et al. 2001). Since AAV-SIG, was available as control mutant and had shown specific retargeting of endothelial cells, SIG was chosen in a first approach as coupling ligand.

The peptide was synthesized by Dr. Arnold (Gene Center of LMU Munich) in a way that the SIG peptide was fused with eight arginines and one cysteine at the C-terminus to constitute the counterpart to the negatively charged sequence inserted in AAV-Glu. The polyionic SIG peptide was designed with and without a linker separating the peptide sequence and the polyionic part.

AAV-Glu was coupled to the polyionic peptide with the same protocol as used for the Oregon Green conjugation reaction and the genomic titers were determined after coupling. One sample of a SIG peptide coupled to AAV-Glu was submitted to a further purification step by gel filtration and the genomic titer was determined subsequently.

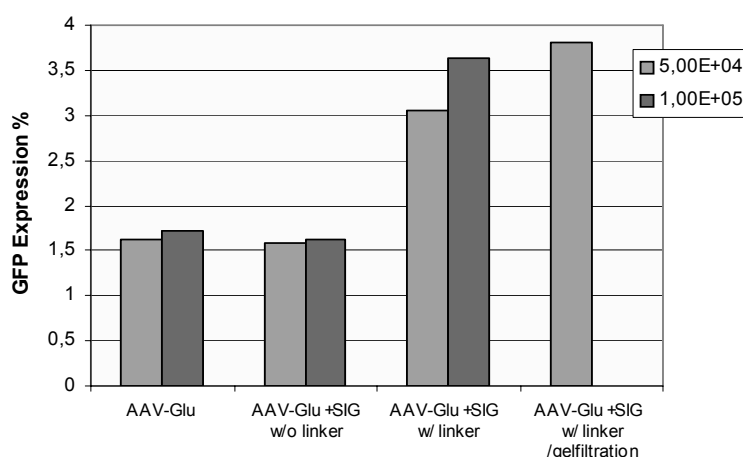


Figure 5: Transduction of SVEC with AAV-Glu/GFP coupled to the SIG peptide

AAV-Glu was coupled to SIG peptide with the same protocol as used for Oregon Green conjugation. One sample was conducted to an additional purification step by gelfiltration. After dialysis and purification the genomic titers were determined and SVECs as target cells were transduced with 5×10^4 and 1×10^5 genomic particles per cell. After 48h cells were harvested and the transduction efficiency was determined by FACS.

As control, AAV-Glu without peptide was incubated under the same conditions to determine if the incubation conditions influenced the vector. SVEC cells were then transduced with genomic particles per cell of 5×10^4 and 1×10^5 for AAV-Glu and AAV-Glu coupled with the polyionic peptide with and without linker (Figure 5).

AAV-Glu coupled to the peptide without linker did not show any enhancement in transduction efficiency compared to AAV-Glu (control; first two columns). The transduction efficiency could be doubled with AAV-Glu coupled to peptide with linker sequence and showed better transduction efficiency after purification by gel filtration. However, only transduction efficiencies of up to 4% (GFP expressing cells) could be detected with 5×10^4 genomic particles per cell. AAV-SIG carrying the same SIG sequence as an inserted peptide in 587 was able to transduce the same cells up to 50% under the same conditions (example see Figure 6).

To determine if the high transduction efficiency on SVEC observed for AAV-SIG was mediated by the inserted peptide, competition experiments utilizing the SIG peptide were performed. For this the AAV-SIG was preincubated with the SIG peptide, the same which was used for the coupling, in 10-fold molar excess and then utilized to transduce SVEC.

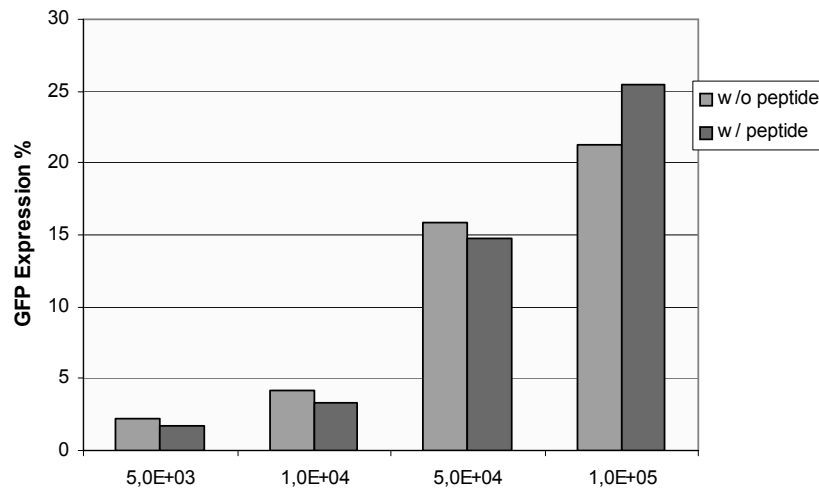


Figure 6: Competition of AAV-Sig on SVEC with SIG peptide

1×10^5 SVECs were seeded into 24 well plates. After 24h cells were transduced with AAV-SIG/GFP preincubated with SIG peptide at genomic particles per cell of 5×10^3 , 1×10^4 , 5×10^4 and 1×10^5 . Cells were harvested after 48h and analyzed by FACS.

Interestingly, incubation with the peptide had no influence on the transduction efficiency for AAV-SIG. Although Nicklin et al. had used heparin to show that AAV-SIG

transduced HUVECs independently of AAVs primary receptor, they never did a peptide competition. Because the receptor for the SIG peptide is still unknown and it was not possible to block AAV-SIG transduction of SVEC by soluble SIG peptide, it was decided to utilize the tumour-specific B3 (Lewis Y) antibody as ligand which was already used by Stubenrauch et al. for the same coupling reaction to establish this coupling procedure with AAV within this project.

Conjugation to the B3 (Lewis) antibody

B3 (Lewis Y) antibody specifically recognizes tumour cells presenting the antigen Lewis Y, a sugar residue found on breast tumours and epidermoid tumour cells (Brinkmann et al. 1991). As already stated, this was the same ligand Stubenrauch and colleagues used for their approach and was kindly provided by Hauke Lilie (University of Halle).

The protocol was varied by addition of Dithiopyridine (DTP), which facilitates the binding of small amounts of thiol groups. The B3-antibody, fused to eight arginines and one cysteine, was activated by incubation with DTP which should help to enhance the binding to the thiol group inserted in the viral capsid (for detailed protocol see Material and Methods). After coupling the solution was submitted to gel filtration to eliminate non reacted free B3-antibody, which might interfere with the transduction experiment. Genomic titers were determined by Dot Blot and MCF-7 cells, a breast carcinoma cell line, were transduced with coupled and uncoupled AAV-Glu and rAAV/GFP (with unmodified capsid) as control.

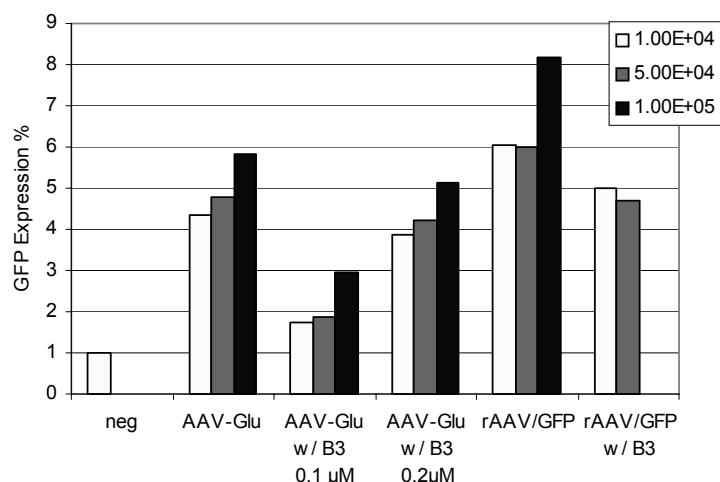


Figure 7: Transduction of MCF-7 cells with AAV-Glu and rAAV/GFP coupled to B3-antibody
AAV-Glu/GFP and rAAV/GFP were coupled to B3-antibody in two different amounts (0.1 μM and 0.2 μM) activated by incubation with DTP (for detailed conjugation protocol see Material and Methods). MCF-7 cells were seeded into 24 well plates and were transduced 24h later with genomic particles per cell of 1×10^4 , 5×10^4 and 1×10^5 . After 48h cells were harvested and analyzed for GFP expression by FACS.

For both coupling approaches, increasing transduction efficiencies were observed with increasing amounts of vectors with the samples containing AAV-Glu after coupling to B3-antibody (Figure 7). However, the transduction efficiency obtained was only comparable with transduction efficiency reached by the uncoupled AAV-Glu. In addition, rAAV with wild type capsid showed the best transduction efficiency. However, transduction efficiency reached in general was very low, only up to 6%. In contrast, Stubenrauch et al. could detect a 5-fold increase in transduction efficiency of their β -galactosidase encoding virus like particles (VLPs) conjugated to B3-antibody. (Stubenrauch et al. 2001)

A new coupling attempt was analyzed by SDS PAGE, followed by silver staining (instead of transduction experiments) to analyse if at least coupled B3-antibody was detectable. To determine the amounts of antibody necessary to detect a signal by silver staining, unbound B3-antibody was also analysed by SDS PAGE in addition. With respect to the coupling approach, AAV-Glu and B3-antibody were conjugated as described before and submitted to gel filtration to separate the coupled virions from free B3-antibody. The coupled virion proteins were separated in a SDS-PAGE under reducing conditions. Subsequently the gel was silver stained (Figure 8). For the B3-antibody a band at 14kDa was expected, as this is the antibody size. For the conjugated AAV-Glu-B3 complex, the VP proteins should be detectable and in addition a signal at 14kDa for the B3-antibody separated by the reducing conditions in the gel.

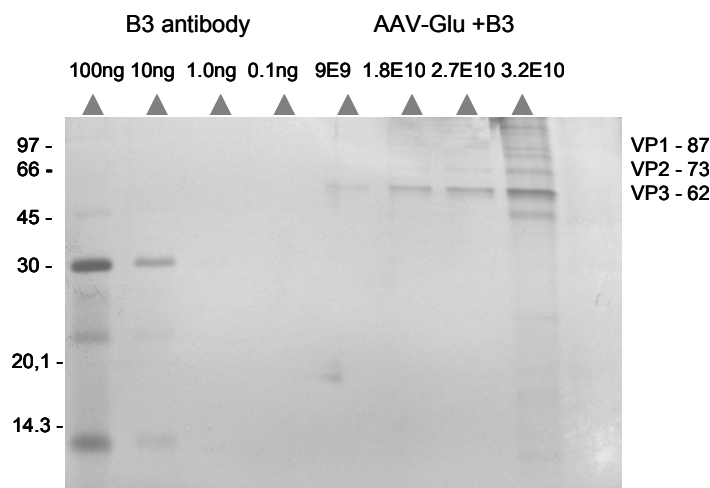


Figure 8: Analysis of AAV-Glu-B3 conjugation attempt

B3-antibody was conjugated to AAV-Glu using the DTP protocol as described above and then separated by SDS-PAGE under reducing conditions. Proteins were detected by silver staining of the gel.

Amounts of 100ng as well as 10ng of B3-antibody were still detectable in the silver stained SDS gel. However, beyond this amount no signal was detectable. For the coupled AAV-Glu 90, 180, 270, and 320 ng had been used, respectively. In case of 3.2×10^{10} AAV particles used and assuming that the antibody is bound to all 60 subunits, a total of 45ng of antibody would be bound to the 3.2×10^{10} AAV particles. Taking into account that only part of the used antibody would have been coupled to AAV-Glu, at least 25% need to be coupled to be detectable. Lower amounts would not be possible to detect by silver staining as might be the case.

Although we could prove that both, the negative charged amino acids and the cysteine of the inserted peptide are accessible at the AAV capsid, we could not demonstrate that an efficient coupling of peptides to AAV-Glu by disulfide bridging via polyionic fusion peptides is possible.

Coupling by maleimide reaction

Since coupling of the inserted cysteines with a maleimide group had been proven by conjugation of the Oregon Green to AAV-Glu before, we decided to use the same reaction to couple a ligand to the AAV capsid.

To perform this reaction another coupling system had to be used, but still the thiol group of the inserted cysteine in AAV capsid could be utilized, but this time with a maleimide group as reaction partner. Maleimide and thiol form a stable thioether under reducing conditions (Figure 9).

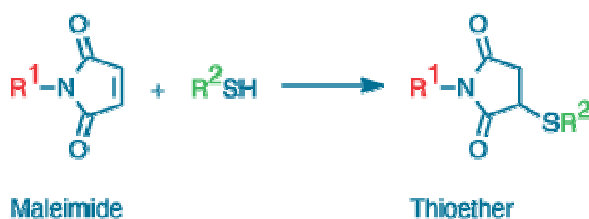


Figure 9: Thioether formation of thiol groups with maleimide (Molecular Probes)

For this approach a cooperation was started with Florian Kreppel (University of Ulm), who applied this coupling system to Adenovirus. Kreppel et al. (2005) were able to introduce a specific chemical reactivity by cysteine at defined positions in the viral capsid

surface of Ad5. This chemical reactivity was, after production of the viral vector from conventional producer cells, used to chemically couple ligands for targeting. For this, a short cysteine containing motif LIGGGCGGGID was inserted into the solvent-exposed fiber HI loop of Ad5. They could show that NANOGOLD monomaleimide particles and monofunctional maleimide-bearing 5k-polyethyleneglycol molecules (5k-PEG-Mal) could be covalently linked to the genetically introduced cysteines. The coupling was detectable in SDS PAGE under reducing conditions and Western Blot. By coupling apo-transferrin ligand, with an introduced thiol-reactive maleimide group, to the Ad-Cys vector, they could show increased transduction efficiency in CAR-deficient K562 cells, which could not be transduced by Ad-Cys alone.

Crucial for the coupling was the chemical reactivity of the genetically introduced thiol groups on the surface of the vector particles. Thiol groups were activated by reducing agents dithiothreitol (DTT) or Tris (2-carboxyethyl) phosphine hydrochloride (TCEP) and Kreppel et al. showed that the reducing agents had no influence on the infectivity of the vector particles. To keep the thiol groups activated the vectors were kept under argon atmosphere to prevent oxidizing events. Once the ligands were coupled to the vector, argon atmosphere was not needed anymore and the coupled vectors could be stored under conventional conditions.

To apply this approach to AAV, a new vector was created by insertion of the peptide LIGGGCGGGID into the 587 site and AAV-Cys was packaged according to the AAV production protocol using oxygen free buffers and was then reduced with TCEP and kept under argon atmosphere (this last part was carried out in Ulm).

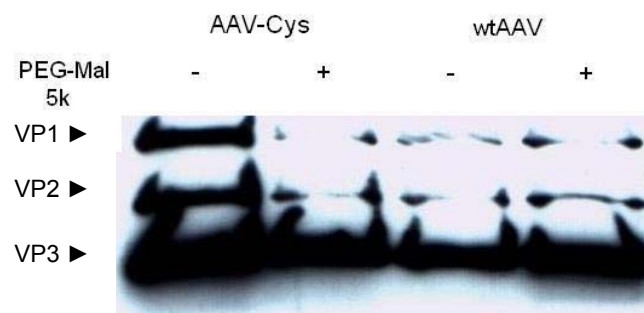


Figure 10: Conjugation of PEG-Mal (5k) to AAV-Cys

Thiol groups AAV-Cys were reduced by TCEP and then conjugated to PEG-Mal in oxygen free atmosphere. Conjugated protein particles were separated by reducing SDS and then transferred to a nylon membrane and AAV VP proteins were detected by B1 antibody in Western Blot. Conjugation and analysis in Western Blot was kindly carried out and the results provided by Florian Kreppel, University of Ulm.

5k-PEG-Mal was coupled to the reduced AAV-Cys and submitted to SDS PAGE under reducing conditions and AAV capsid protein VP1, VP2, and VP3 were detected by B1 antibody in Western Blot. For efficient coupling a shift should be seen in the VP proteins, where the additional cysteines were introduced.

No shift in the VP capsid proteins could be seen after coupling of 5k-PEG-Mal to AAV-Cys. In contrast a shift was seen when coupling 5k-PEG-Mal to Ad-Cys under the same conditions (Kreppel et al. 2005).

Evaluation of new substitution sites for cysteine residues

Since the insertion of cysteine with a short linker motif into 587 did not show coupling efficiency with PEG-Mal in Western Blot analysis, new insertion sites were determined. The reason for this was the hypothesis, that the cysteine within the linker used inserted in 587 was not accessible for the coupling reaction. For this reason, we generated 6 different mutants, in which on exposed sites (according to the crystal structure of Xie and colleagues) an one amino acid substitution towards Cysteine was performed. The following residues were selected for substitution with cysteine: N587C, S452C, G453C, A667C, G265C and S384C. In all cases it was considered that only smaller amino acids and those which play a minor role in structure definition like serine or glycine were exchanged. All the mutants were cloned by PCR cloning, could be successfully packaged with GFP as transgene and purified by Iodixanol step density gradient to genomic (determined by Light Cycler PCR) and capsid titers, which were comparable to the titers obtained for wtAAV (data not shown). The new obtained mutants are currently being tested for efficient conjugation and retargeting with apo-transferrin in cooperation with Florian Kreppel (University of Ulm).

2.3. Discussion Chapter I

The broad tissue tropism of AAV2, mediated by its primary receptor heparan sulphate proteoglycan (HSPG), represents a disadvantage for *in vivo* gene therapy, because after systemic application, viral vector particles are sequestered by a wide variety of HSPG displaying cells and only few particles will reach organs other than liver and spleen.. Strategies to alter the tropism include the insertion of peptides into the AAV capsid, creating targeting mutants useful for one specific receptor-ligand interaction. Universal targeting approaches seek to redirect rAAV binding to specific cell surface receptors by simple coupling of different ligands to its capsid. Bartlett et al. (1999) demonstrated that bispecific antibodies, mediating interaction between AAV vector and a specific cell surface receptor, can redirect the tropism to megakaryocyte cell lines, usually non-permissive for AAV2. Although they were able to overcome the block to transduction of non-permissive cell lines, the level of vector-mediated gene expression was still very low. Ried et al. (2002) inserted a minimized domain of protein A into position 587 to couple various antibodies binding to specific cell surface receptors to the AAV capsid and demonstrated that the infection in target cells was specifically antibody mediated. However also in this case, the transduction efficiency was fairly low. Based on the hypothesis, that the low transduction efficiency observed by Bartlett et al and Ried et al. is maybe caused by the instability of the ligand-capsid interaction, we sought to generate an universal AAV targeting vector by coupling the ligand via a disulfide bridge to the modified AAV capsid.

AAV tolerates insertion of polyionic sequence and cysteine into the capsid structure

Different insertion strategies were tested to incorporate cysteine into the AAV capsid. In a first approach a polyionic peptide (eight glutamic acids and one cysteine) was inserted into position 587. The capsid tolerated the insertion and the vector could be purified to high titers by anion exchange chromatography due to the inserted negatively charged glutamic acids. This negative charge is also responsible for the inability to transduce HeLa or SVEC, which display as most adherent cells, the negatively charged HSPG on their cell surface. HSPG naturally serves as primary receptor of AAV. Based on this, AAV-Glu can be described as a knock-out mutant with ablation of the natural AAV tropism. This is an ideal situation for the generation of targeting vectors.

AAV-Glu can be conjugated to Oregon Green dye by thiol maleimide reaction

To prove that the conjugation to a ligand is mediated by the inserted cysteine, AAV-Glu was coupled to Oregon Green Dye. The maleimide group of Oregon Green had to react with the thiol group of the cysteine introduced into the AAV capsid in AAV-Glu. Only in the AAV-Glu sample which underwent the conjugation reaction with Oregon Green bands were detectable in Phospho Imager after SDS-PAGE which corresponded to the VP3 protein in Western Blot analysis of the very same gel (Figure 3). WtAAV, which were also submitted to the coupling reaction, showed no labelled protein, which corresponded in size to one of the capsid proteins.

These results prove that the cysteine is accessible for coupling (in addition to the negatively charged glutamic acids) (**Figure 3 Conjugation of AAV-Glu to Oregon Green**).

Conjugation of AAV-Glu did not result in efficient transduction of target cells

For conjugation of a target peptide to AAV-Glu, the SIG peptide was chosen in a first approach, which consists of seven amino acids (SIGYPLP) and was fished in phage display as an endothelial specific peptide (Nicklin et al. 2000). The peptide had been incorporated into the AAV capsid into the 587 position by Nicklin et al. (2001) and the mutant AAV-SIG was able to successfully retarget to Human Umbilical Vein Endothelial cells (HUVEC). Specificity of the vector was proven by heparin competition studies on HUVEC, showing that rAAV-SIG is able to transduce these cells independent on AAVs natural primary receptor HSPG. Furthermore, the selective specificity of the binding was shown by infection studies using different non-endothelial cell lines such as HepG2 (Nicklin et al. 2001).

The SIG-peptide was designed with and without a linker region separating the seven amino acids of the targeting sequence and the polyionic coupling sequence. The linker should guarantee a more flexible structure. SIG-peptide was coupled to AAV-Glu according to the protocol used by Stubenrauch et al. (2001) to couple polyoma VP protein to B3 antibody, also using polyionic sequences. When AAV-Glu was coupled to the SIG peptide with linker, the transduction efficiency could be doubled reaching 4% GFP expression compared to AAV-Glu alone. However AAV-SIG, containing the respective peptide inserted in 587 reached transduction efficiencies of about 50%.

To analyse if the high transduction efficiency of AAV-SIG on SVEC is mediated by the inserted peptide, competition studies were performed. Here no reduction in the transduction efficiency could be seen. Although Nicklin et al. (2001) did a detailed analysis of the intracellular interaction of AAV-SIG in endothelial cells utilizing different chemical substances, such as bafilomycin A (inhibitor of the vascular H^+ -ATPase responsible for acidification of endosomal vehicles), no peptide competition experiments were done. Therefore, it can not be excluded that AAV-SIG is utilizing additional ligand:receptor interaction for the transduction of SVEC.

A better characterized ligand receptor system was then chosen, using the B3 (Lewis) antibody for conjugation and MCF-7 as target cell line. The antibody was kindly provided by Hauke Lilie from the University of Halle, whose colleagues were successful in conjugating B3 antibody to the polyoma virus VP1 protein. Using a protocol with Dithiopyridine (DTP) to activate thiol groups of the ligand, the B3 antibody was conjugated to AAV-Glu and the transduction efficiency was tested on MCF-7 cells. Conjugated AAV-Glu did not show better transduction efficiency than AAV-Glu alone.

Conjugated AAV-Glu was then biochemically analysed by performing SDS-PAGE and silver staining to also detect small amounts of antibody. In addition different amounts of B3 antibody were also submitted to SDS PAGE and silver staining to determine what amounts of antibody are still detectable in the gel. 10ng or more of B3 antibody could be easily detected in a silver stained gel. Smaller amounts were not visible anymore. In the conjugated AAV-Glu sample no bands for the antibody were detectable (Figure 8). Although more than 10ng of B3 antibody were used for conjugation of AAV-Glu in the sample analysed, unconjugated antibody had been separated by gel filtration. Since it is very unlikely that all available antibodies were coupled to the vector, the failure to detect B3 antibody in the conjugated AAV-Glu sample is explainable by detection limit. However, this result showed that this method can not be used for our analysis. In contrast, Stubenrauch et al. could show conjugated B3 antibody in Coomassie stained SDS gels. However, they were able to analyse high amounts of VP1 protein and antibody.

Taken together, we could show that AAV-Glu, carrying an insertion of eight glutamic acids and one cysteine, can be generated and purified to high titers. AAV-Glu is a promising basis for a targeting vector, since it is ablated of AAVs natural receptor usage. In addition, the inserted amino acids are accessible, since purification could be performed making use of the inserted negatively charges glutamic acids and Oregon Green maleimide dye could be coupled to the vector via the inserted cysteine (no reaction with wtAAV).

However, neither with the SIG peptide nor with the B3 antibody fragment an enhanced transduction of the respective target cell by the new targeting vector could be detected in comparison to the controls. It can not be excluded that the test system (cell lines, peptide ligands) were not suitable for this approach and we therefore failed to proof the success of this targeting approach. However, also other options have to be taken into accounts as for example repulsion of AAV-Glu by the negatively charged HSPG molecules on the cell surface on the target cell if the inserted 480 negative charges are not completely covered by the coupled ligand.

Conjugation of AAV-Cys to ligands by maleimide reaction

For the AAV-Cys vector, cysteine was inserted into position 587 flanked by spacer amino acids (LIGGGCGGGID (AAV-Cys)). This sequence was previously successfully inserted into the solvent-exposed fiber HI loop of Ad5 by Kreppel and colleagues, who conjugated apo-transferrin to the cysteine containing Ad mutant (2005). The cysteine modified AAV-Cys could be packaged and purified to high titers, but was not able to transduce HeLa cells (data not shown). This might be due to the insertion, which might interfere with the arginines important for HSPG binding in positions 585 and 588 (Opie et al. 2003; Kern et al. 2003) and therefore ablate the natural HSPG binding. That such a mechanism can indeed take place, was shown within this thesis (Endell, Goldnau, Perabo, White et al. in revision and Chapter III).

For the coupling a new ligand system was chosen, this time using a thioether reaction for conjugation. These experiments were performed in cooperation with Florian Kreppel at the University of Ulm, who established this coupling system for adenoviral vectors (Kreppel et al. 2005). The expected shift in the VP proteins of AAV-Cys could not be detected in Western Blot after conjugation to 5k-PEG-Mal ligand, a PEG molecule containing a maleimide group for the thioether reaction, indicating that the conjugation had not been successful. Since the reaction conditions had already been optimized by Florian Kreppel during his experiments with Ad5 (Kreppel et al. 2005), the failure of AAV-Cys to become coupled to PEG-Mal is most likely due to an inaccessibility of the Cys, when inserted within the LIGGGCGGGID sequences in 587. For the studies with Ad this sequences was inserted to the fiber HI-loop, protruding from the viral structure, now it is inserted within the three dimensional structure of a viral capsid. Based on this assumption,

a new insertion strategy was applied, this time only exchanging amino acids at exposed site within the AAV capsid. Only small and uncharged amino acids were exchanged, to avoid major changes in the capsid structure. Six amino acids were selected, which are displayed on the capsid surface according to the crystal structure of AAV (Xie et al. 2002). Amino acids were exchanged for cysteine obtaining the following Cys-mutants G265C, S384C, S452C, G453C, N587C, and A667C. All mutants could be packaged and are currently analysed in cooperation with Florian Kreppel (University of Ulm). The mutants are expected to be conjugated to ligands like 5k-PEG-Mal and apo-transferrin.

Since this approach can integrate clinically diverse molecules as ligands, it may be used for clinical gene therapy and, potentially, also for vaccination in the future.

3. Chapter II - Development of an AAV based anti-idiotypic vaccine

3.1. Introduction Chapter II

IgE as Therapeutic Target in Allergic Diseases

A promising indication for the treatment with anti-idiotypic vaccines are allergic disorders. Allergic diseases, including allergic asthma, are hypersensitivity reactions initiated by immunologic mechanisms. They are usually mediated by Immunoglobulin E (IgE) antibodies, which trigger an inflammation characterized by increased production of T_H2 -type cytokines at mucosal surfaces.

The physiological role of IgE is to protect against helminthic parasites. In allergic reactions IgE triggers a defensive immune response against innocuous antigens by antigen binding to IgE antibodies which are bound to the high affinity receptor $Fc\epsilon RI$ on mast cells. The reactions vary from irritating sniffles of hay fever to life-threatening circulatory collapse and systemic anaphylaxis. In the body IgE is found mostly bound to its high affinity receptor $Fc\epsilon RI$, whereas other antibodies are located mostly in body fluids. The $Fc\epsilon RI$ binds IgE to mast cells, basophils and activated eosinophils. When the cell-bound IgE antibody is cross-linked by a specific antigen, $Fc\epsilon RI$ mediates an activating signal. With high concentration of IgE, the receptor is also upregulated and thus enhancing the sensitivity. On activation, mast cells synthesize and release, besides histamine, other chemokines, lipid mediators such as leukotrienes and platelet-activating factor (PAF), and additional cytokines such as IL-4 and IL-13 which perpetuate the T_H2 response.

The inflammatory response after IgE-mediated mast-cell activation occurs as an immediate reaction, starting within seconds, and a late reaction, which takes up to 8 – 12 hours to develop. The immediate reaction is due to the activity of histamine and other preformed or rapidly synthesized mediators that cause a rapid increase in vascular permeability and the contraction of smooth muscle. The late-phase reaction is characterized by the T_H2 reaction and a more sustained inflammation process.

Allergy can be treated by inhibiting either IgE production by desensitization or the effector pathways activated by cross-linking of cell-surface IgE. In desensitization the aim is to shift the antibody response away from one dominated by IgE toward one dominated by IgG, the latter can bind to the allergen and thus prevent it from activating IgE-mediated

effector pathways. Patients are injected with escalating doses of allergen, starting with tiny amounts. This injection schedule gradually diverts the IgE-dominated response, driven by T_H2 cells, to one driven by T_H1 cells, with the consequence of down regulation of IgE production. A potential complication of the desensitization approach is the risk of inducing IgE-mediated allergic responses.

Another strategy that shows promise in experimental models of allergy is the use of oligodeoxynucleotides rich in unmethylated cytosine guanine dinucleotides (CpG) as adjuvant for desensitization regimes. These oligonucleotides mimic bacterial DNA sequences known as CpG motifs and strongly promote T_H1 responses via Toll-like receptor 9 (TLR9). The direct conjugation of CpG oligonucleotides to allergen may be a potent stimulus to cause allergen desensitization while minimizing potential CpG side effects. (Krieg and Walfield et al. 2002).

Active immunization approaches, which have also not reached clinical trials yet, include vaccination with synthetic IgE peptide (Wang et al. 2003), where Wang and colleagues chose a peptide, which targets the binding site on IgE for the high affinity receptor FcεRI. The chosen peptide was immunopotentiated by linkage to a combinatorial T helper epitope derived from measles virus, UBITH[®] A, to provoke an immune response and allow active immunization. A polyclonal antibody response could be generated in dogs and these antibodies blocked binding to the high affinity receptor FcεRI, and were sufficiently immunogenic to evoke functional anti-dog IgE immune responses in dog.

Other approaches try to interrupt the involved Interleukin pathways, such as IL-13, IL-4 or IL-5. Clinical trials show rather limited beneficial effects for interrupting the IL-4 or the IL-5 pathway. Also the redundancy between some of the activities of these cytokines might make this approach difficult to implement in practice (Jonkers et al. 2005).

Another target for therapeutic intervention might be the high affinity IgE receptor FcεRI itself. An effective competitor for IgE at this receptor could prevent the binding of IgE to the surfaces of mast cells, basophils and eosinophils. Candidate competitors include modified IgE Fc constructs that bind to the receptor, but lack variable regions and thus cannot bind antigen, or humanized anti-IgE monoclonal antibodies, which bind to the Fc part of IgE and block its binding to the receptor. A recombinant humanized monoclonal antibody is Omalizumab (Xolair[®]). Xolair[®] has been on the US market for a couple of years now and has been approved for the German market in November 2005. Xolair[®] is indicated for patients with moderate to severe forms of allergic asthma, who already

depend on the treatment with inhaled corticosteroids (ICS) and β -antagonists and show raised serum IgE levels.

Although Omalizumab already works well in practise, the treatment with monoclonal antibodies bears several disadvantages, since it represents a passive immunization. It has to be applied in short time intervals during the treatment according to the severity of the disorder and the IgE level has to be closely monitored. If injections are stopped, the allergic reactions will reoccur after antibody serum levels are decreased again. The patients depend on a life long treatment. Furthermore, the risk of development of anti-idiotypic antibodies (anti-Omalizumab), which could lead to the loss of efficacy and resistance against the therapy, exists.

Anti-idiotypic vaccines are already in use for the treatment of autoimmune diseases or cancer. These anti-idiotypic antibodies raise antibodies directed against antigens that mediate e.g. autoimmune disease or are expressed by tumour cells and are a major improvement of passive immunization therapies. Furthermore anti-idiotypic antibodies induce a polyclonal antibody response against the target antigen, minimizing the risk of development of therapy resistance, while for passive immunotherapy monoclonal antibodies are used. A disadvantage of anti-idiotypic antibodies as vaccines is that induced antibody titers are often lower due to the low immunogenicity of antibodies.

The combination of the advantages of an anti-idiotypic antibody with a suitable immunogen eliciting a sufficient immune response would represent a new approach with great benefit for the patients suffering from severe allergic disorders.

Viruses bear the necessary polymeric structure which is recognized by the host as immunogenic and can thereby break B-cell tolerance against self-antigens such as IgE (Abbas and Lichtman Basic Immunology 2004). The Adeno-Associated Virus (AAV) is known for its low immunogenicity showing minor T-cell response, but is still able to elicit immune responses on the B-cell level, corroborated by the fact that over 50 to 96% of human beings show antibodies against different AAV serotypes such as AAV type 2 (Chirmule et al. 1999).

If an AAV mutant, resembling an anti-idiotypic sequence to e.g. Omalizumab and, therefore, resembling the Fc ϵ RI binding region of IgE, is selected who is able to stimulate the immune system in a way that suppresses the level of its own IgE by generating antibodies against the Fc ϵ RI binding region of IgE, it can be applied as a vaccine for active immunization and a new treatment is only needed when anti-IgE antibody titers are

decreasing. The treatment possibly has to be refreshed every few years then, in contrast to treatments with monoclonal antibodies every few weeks.

Perabo et al. developed a combinatorial approach based on an AAV virus library for generation of efficient and receptor-specific targeting vectors with desired cell tropism (Perabo et al. 2003). The AAV library, which was in this project utilized for the selection of AAV capsid mutants, able to elicit an anti-IgE immune response, consists of approximately 4×10^6 capsid-modified viral particles carrying random insertions of 7 amino acids at position 587 of the AAV capsid protein. The choice of a 7-mer was empirical and dictated by the need to insert a sequence long enough to generate an acceptable amount of diversity, but without impairing the capsid stability. Typical B-cell epitopes are 5 or 6 amino acids in length (Abbas and Lichtman Basic Immunology 2004), this should be sufficient to induce B-cell responses against the inserted peptide sequence when used as vaccine.

In this study the AAV library is applied to a selection procedure using antibodies coated to a solid phase. By this AAV mutants can be selected which bind specifically to the desired idiootype of the selection antibody and which, therefore, resemble the epitope of the antibody target. Since antibodies are available against a great number of targets, it will allow selection of specific mutants resembling a wide variety of target epitopes.

3.2. Results Chapter II

Coupling of geno- and phenotype

The AAV library contains a pool of AAV capsid mutants, which differ from each other by the random insertion of seven amino acids at position 587 in the VP3 region of all 60 capsid proteins. When packaging the AAV library, a pool of plasmids coding for the mutant capsid proteins, the viral replication proteins Rep, and harbouring the inverted terminal repeats (ITRs), is introduced into 293 cells by transfection (Figure 1).

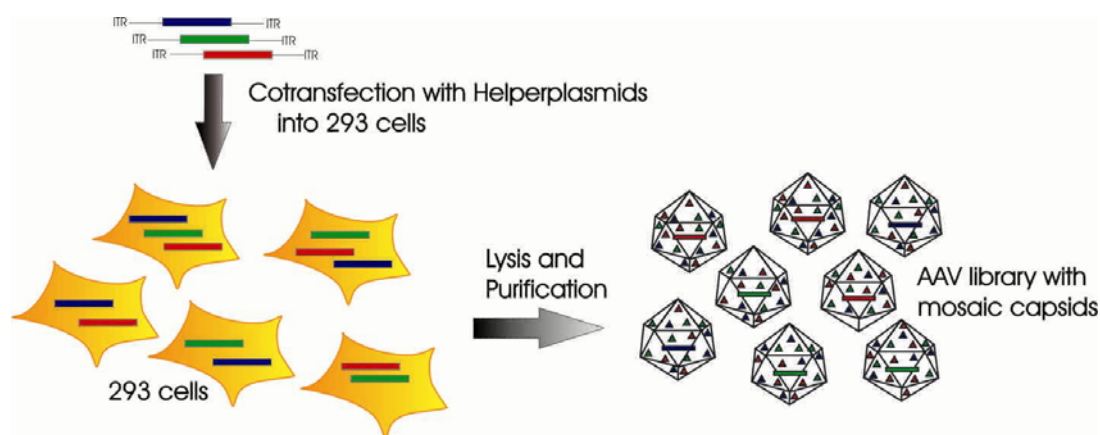


Figure 1: Packaging of the AAV library

Briefly, the DNA library plasmids are transfected into 293 cells together with adenoviral helperplasmid pXX6-80 at a molar ratio of 2:1. After 48h cells are lysed and the viral progeny is purified by iodixanol density gradient.

Transfection of high DNA concentration of a given plasmid results in the introduction of multiple copies per cell, which can replicate and express AAV capsid proteins with different inserted 7mere sequences. 60 capsid proteins build up a mosaic capsid encoding one AAV genome being randomly chosen. Therefore, many if not most of the AAV particles will contain a vector genome which is not related to any of its 60 capsid proteins, geno- and phenotype of this mosaic viruses are uncoupled. As later AAV selection is based on the AAV phenotype (the capsid variant) and because the sequence information for the selected AAV variant can only be gained from the respective AAV genome, a coupling of geno- and phenotype is indispensable. Therefore, the production of homogenous library mutants can not be guaranteed by simply packaging the AAV library using the transfection protocol described above. Based on this, it becomes clear that a coupling step had to be introduced which resulted in a pool of viral mutants each

consisting of a viral capsid displaying only one kind of peptide insertion and containing only the respective viral genome.

Blocking Conditions

For the selection of AAV library mutants on antibodies, the antibodies have to be coated to wells to allow a solid phase selection procedure. To avoid unspecific binding of the AAV library to the plastic material, the blocking conditions were optimized. Three different blocking reagents, Milk Powder (1% Milk Powder/PBS/1% Tween20), BSA (3% BSA/PBS/5% Saccharose/0.05% Tween20), and Casein (1% Casein/PBS/1% Tween20), were tested.

Wells were coated with A20 antibody, which recognizes intact AAV capsids, or PBS, respectively, and then incubated with the above mentioned blocking buffers. As control, PBS was applied instead of a blocking buffer. Wells were then incubated with rAAV/GFP with 1×10^3 genomic particles per cell (GPC) in blocking buffer or PBS, respectively, and after washing HeLa cells were seeded on top and cultured for 48h. GFP expression in AAV transduced cells was determined by FACS analysis. The experiment was repeated at least three times. High transduction efficiency should be observable in wells coated with A20, where the binding of virions to the well was mediated by A20. In wells "coated" with PBS no or only low transduction efficiency should be detectable since AAV binding to the well was impeded by the blocking reagent.

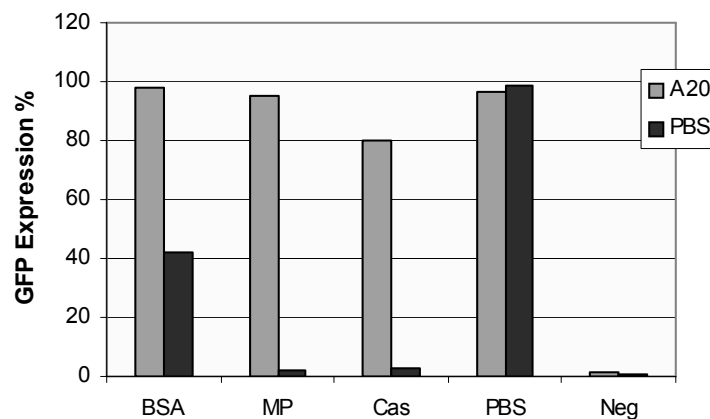


Figure 2: Blocking Buffer Test

Wells were coated with A20 antibody or PBS and blocked with Milk Powder 1%/PBS/Tween20 1% (MP), BSA 3%/PBS/Saccharose 5%/Tween20 0.05%, Casein 1%/PBS/Tween20 1% (Cas) or with PBS as control and incubated with rAAV/GFP (GPC 1×10^3). After washing HeLa cells were seeded into wells and analyzed by FACS after 48h.

As expected, in wells coated with A20, a transduction efficiency of 80 to 100% was achieved in all cases, Casein blocking showed the least expression with 80%. Here the blocking buffer might have interfered with the binding of AAV to A20 leading to a lower GFP expression. Comparing all wells "coated" with PBS, followed by blocking with three different blocking reagents and subsequent AAV incubation, GFP expression was still high (about 40%) in wells blocked with BSA, suggesting that blocking of the plastic material was insufficient in this case allowing for AAV binding to the plastic and subsequent uptake by HeLa. In contrast, blocking of the wells with Milk Powder or Casein was complete as AAV bound to the plastic being subsequently taken up by HeLa only led to GFP expression of 2%. In conclusion Milk Powder seems to be the most suited blocking reagent to avoid unspecific binding of virions to the well material, but allowed specific binding of AAV to the coated antibody.

Therefore, in all following experiments a 10% solution of Milk Powder/PBS/1%Tween 20 was used as blocking reagent.

Coupling of geno- and phenotype: A) unspecific uptake

Prior to AAV selection on antibodies a method was to be developed to ensure the production of homogenous library mutants and to eliminate the problem of not matching geno- and phenotype within one mutant. To achieve replication of only one mutant per cell, coupling through cell transduction with comparatively low virus concentrations was tested. In doing so, two different methods to get the AAV particles into the cell were compared: A) unspecific uptake, and B) receptor-mediated uptake or simple virus infection. The latter method bears the risk that an undesired selection of infectious virus takes place which could lead to a loss of target (antibody-) specific but non-infectious AAV variants.

All viruses must have evolved ways of entering cells to initiate replication and progeny production. In case of AAV the virus enters the host cell through clathrin-mediated endocytosis (Bartlett et al. 2000). The internalization is facilitated by its primary receptor heparan sulfate proteoglycan (HSPG) and the secondary receptors, of which three have been postulated, the fibroblast growth factor receptor I (FGFR), the $\alpha_v\beta_5$ integrin and recently the hepatocyte growth factor receptor (HGFR) (Qing et al. 1999; Summerford et al. 1999; Kashiwakura et al. 2005). Following internalization into the early endosome, the virus encounters a weakly acidic environment which is necessary for endosomal escape into the

cytosol. AAV then accumulates perinuclearly and viral uncoating takes place before or during nuclear entry (Lux et al. 2005).

Other endocytotic pathways include caveolae, macropinocytosis or non-clathrin, non-caveolae pathways. Macropinocytosis is generally considered to be a nonspecific mechanism for internalization, in that it is not reliant on ligand binding to a specific receptor. Instead, formation of endocytotic vesicles occurs as a response to cell stimulation. Such virus mediated signaling has been shown for adenovirus, where integrin-dependent virus binding activates macropinocytosis. Cells, which use macropinocytosis as a major route, are e.g. antigen-presenting cells like dendritic cells (DCs) and in this case not even cell stimulation is required (Sieczkarski et al. 2002).

We hypothesize that it should be possible to couple the geno- and phenotype of the AAV library mutants by induction of an unspecific uptake in the sense of macropinocytosis. To test this hypothesis the following experiment was performed. Virions were bound via antibodies to wells and cells were seeded on top to allow an uptake of all mutants that would be bound to the wells.

To ensure binding of AAV particles, wells were coated with A20 antibody, which recognizes intact AAV capsids (Grimm et al. 1999, Wistuba et al. 1997) independently from their possible insertion in position 587. For proof of principle the wells were incubated with rAAV encoding GFP (rAAV/GFP) with 1×10^3 and 1×10^4 genomic particles per cell (GPC). Unbound rAAV/GFP was removed by a washing step with PBS/1% Tween20 and HeLa cells were seeded into the wells and incubated for 48h. GFP expression was then determined by FACS analysis. The same experiment was performed with A3/GFP, a recombinant AAV, where amino acids R-585 and R-588, which are mainly responsible for HSPG binding and in addition N-587, were substituted to alanine. This mutant is unable to bind to heparin and was described as HSPG knock out mutant (Wu et al., 2000). As a control, infections on HeLa cells were carried out with the same amounts of genomic particles as used for the uptake experiment. Experiments were also performed with an incubation time of 72 hours to analyze if the amount of GFP expressing cells can be improved by prolonging the incubation period. It was assumed that for A3 GFP expression was clearly increased by uptake in contrast to infection, whereas for rAAV/GFP similar results as for the infection were expected.

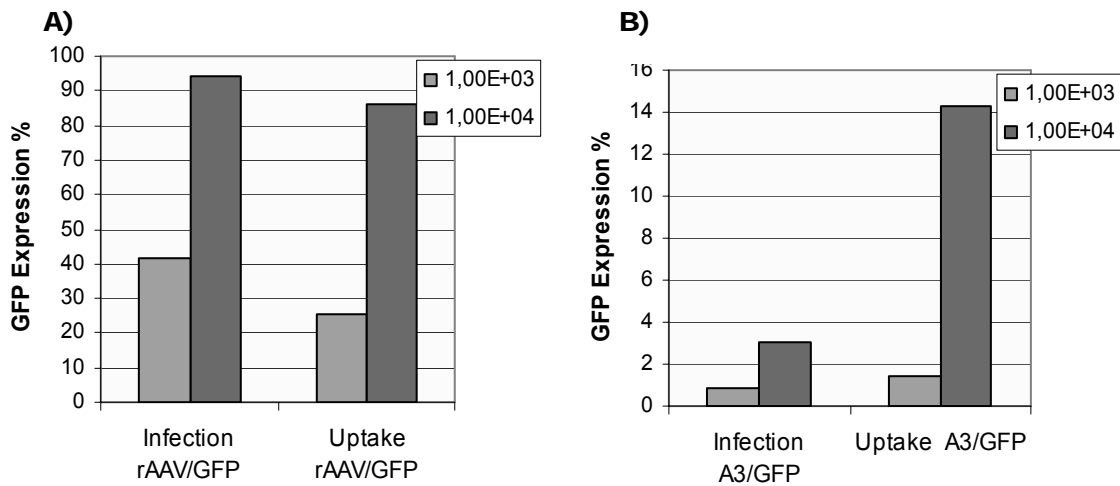


Figure 3: Uptake of rAAV/GFP and A3/GFP versus infection

For uptake wells were coated with A20 antibody and incubated with rAAV/GFP (Figure A) or A3/GFP (Figure B) at GPC of 1×10^3 and 1×10^4 . Wells were washed and then HeLa cells were seeded into the wells. Cells were analyzed by FACS analysis after 48h. For infection HeLa cells were seeded into wells and infected with rAAV/GFP or A3/GFP with GPC of 1×10^3 and 1×10^4 . Cells were analyzed by FACS analysis after 48h.

Regarding rAAV/GFP the uptake with A20 showed a transduction efficiency almost as high as with infection (Figure 3A). Slightly lower expression levels may be due to the loss of virions by the stringent washing step before applying the HeLa cells. For A3/GFP the transduction efficiency by infection was as low as expected for a HSPG knock out mutant and could be enhanced almost five-fold by uptake using 1×10^4 GPC (Figure 3B). Prolonging the incubation time to 72 hours had only little effect on GFP expression in both cases (data not shown). Interestingly, increasing the amount of virus could not increase the GFP expression of A3/GFP to rAAV/GFP levels.

Next, we wanted to analyze if the uptake was an unspecific mechanism or if AAV's primary receptor HSPG played the main part. For this infection and uptake were performed in presence of heparin which is able to block about 90% of infection of wtAAV on HeLa cells. If uptake was unspecific, heparin should not be able to block transduction and therefore GFP expression in these cells.

For infection HeLa cells were seeded into wells and then infected with rAAV/GFP with 1×10^3 GPC, which had been incubated before with heparin solution (425 U/ml). Cells were then incubated for two days and the GFP expression level was determined by FACS analysis. For uptake A20 antibody was coated into wells and rAAV/GFP with 1×10^3 GPC was bound on top. The bound virions were then incubated with heparin and HeLa cells

were seeded on top and incubated for another two days. Again the GFP expression level was determined by FACS analysis. The transduction efficiency of uptake and infection without heparin was set to 100% and the fold reduction as percentage is shown in the diagram.

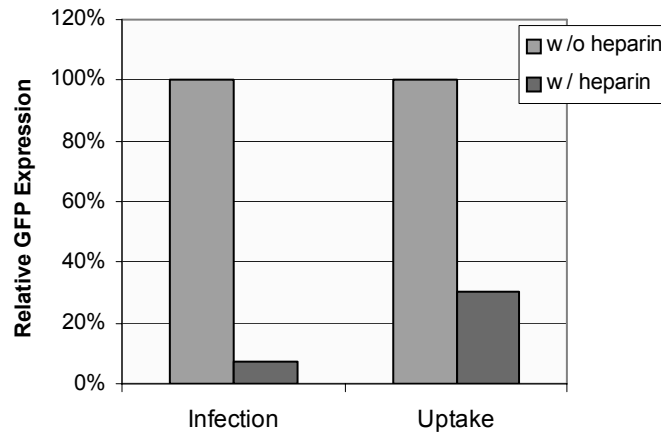


Figure 4: Infection and Uptake of rAAV/GFP w/ and w/o heparin

For uptake experiments wells were coated with A20 antibody and incubated with rAAV/GFP with 1×10^3 GPC. Wells were washed and bound virus was incubated with heparin. HeLa cells were seeded into the wells. Cells were analyzed by FACS analysis after 48h. For infection HeLa cells were seeded into wells and infected with rAAV/GFP with 1×10^3 GPC after preincubation with heparin. Cells were analyzed by FACS analysis after 48h.

As expected the GFP expression for the infection was reduced to 6-8% when heparin was added and infection without heparin was set to 100%. For uptake the reduction was not as unaffected as expected, heparin could still reduce the GFP expression to 30% compared to 100% without heparin. Part of the uptake seemed to be blocked by heparin while one third was not susceptible to the treatment with heparin.

To analyze if a coupling of the AAV library was possible by uptake, an uptake experiment utilizing 15cm^2 plates was performed. Briefly, a cell culture plate was coated with A20 antibody, blocked with Milk Powder (MP), and then incubated with the AAV library with genomic particles per cell of 10, 100 and 1000. Unbound virus was washed away and HeLa cells were seeded onto the bound virions. Adenovirus was added for helper function for AAV replication and packaging. Cells were incubated for two days and then harvested. The cell pellet was resuspended in lysis buffer and treated with repeated thaw/freeze cycles. Viral DNA from virions contained in the lysate was purified, amplified by PCR and cloned into the AAV pRC vector. Plasmids were transformed into bacteria, single clones were picked and at least one hundred clones for each setting were sequenced.

For comparison the region of interest of the DNA library and the original uncoupled viral library obtained after packaging in 293 cells and purification by Iodixanol density gradient were cloned into AAV pRC vector, transformed into bacteria, and sequenced, again at least 100 single clones, and analyzed.

The coupling state is reflected by the amount of stop codons detected, since stop codons would also be packaged if more than one capsid encoding plasmid was transfected into one cell, 12 stop codons in a hundred regarding the codon usage were statistically possible, and 8.6 out of a hundred occurred in the original library.

viral pool uncoupled	Uptake GPC 10	Uptake GPC 100	Uptake GPC 1000
Stopcod.per 100: 8.6	Stopcod.per 100: 1.4	Stopcod.per 100: 2	Stopcod.per 100: 4.6

Table 1: Frequency of stop codons after coupling by uptake (GPC 10, 100 and 1000)

At least 100 sequences were analyzed and the number of stop codons was calculated per 100 sequences.

Utilizing the number of stop codons as an indicator for the coupling state of the library, the number of stop codons should be markedly decreased. In addition, biodiversity of the library should be maintained. An indicator for this was the absence of duplicate sequences.

Regarding single sequences about 40% of sequences in GPC 10 occurred more than once, which is to be regarded as a reduced biodiversity. Presumably, under these conditions not all of the 10^6 different genomes were able to transduce cells, resulting in the enrichment of given sequences. In the uptake experiments utilizing GPC 100 and 1000 there were no duplicate sequences pointing to a better ratio between genomic particles and cells and a better diversity. The number of stop codons was lower as in the original library, which points to a well coupled library. The number of stop codons calculated per 100 sequences increased as expected, when higher GPC were used, since in case of GPC 1000 it was very likely that more than one viral mutant was able to be taken up by one cell. Taken together the uptake with GPC of 100 seemed to be appropriate in terms of the coupling of mutants and the maintenance of an adequate diversity of the AAV library.

Coupling of geno- and phenotype: **B) infection**

Coupling of AAV library by infection without loss of biodiversity will work, if each virion from the non-coupled AAV library contains at least one cell binding motif which renders the AAV particle infections. In addition to the uptake experiments the coupling was therefore also performed by infection. As for the uptake experiment different GPCs were tested to determine the optimal coupling efficiency retaining full biodiversity.

HeLa cells were seeded into cell culture plates and infected with 10, 100 and 1000 genomic particles per cell in the presence of adenovirus to allow replication and packaging of AAV. Cells were harvested and resuspended in lysis buffer. Viral DNA was purified, amplified by PCR and cloned into the AAV pRC vector. Plasmids were transformed into bacteria and single clones were picked and sequenced.

viral pool uncoupled	Infection GPC 10	Infection GPC 100	Infection GPC 1000
Stopcod.per100:8.6	Stopcod.per100:1.2	Stopcod.per100:0	Stopcod.per100:0

Table 2: Frequency of Stop codons in infection experiment with GPC 10, 100 and 1000

At least 100 sequences were analyzed and the number of stop codons was calculated per 100 sequences.

As observed for the coupling by unspecific uptake a comparatively high number of sequences occurred more than once when a GPC of 10 is used. The diversity of the library was clearly higher with GPCs of 100 and 1000 with no duplicate sequences and the number of stop codons, as an indication for the coupling state, was down to zero with GPCs of 100 and 1000 (Table 3). Even with an amount of 1000 genomic particles per cell a coupling of geno- and phenotype was accomplished. Since the coupling rate and biodiversity of the library seemed to be better when coupling was performed by infection (according to the frequency of stop codons per 100 sequences) the library coupled by infection was chosen for all following selection experiments.

Further analysis of geno/phenotype of coupled viral libraries

In the previous experiments it was shown that the coupling of geno- and phenotype could be accomplished, no matter if coupling by infection or uptake was applied.

To further prove that the library was indeed coupled after a first uptake or infection step, the coupled libraries were submitted to another round of infection and uptake, respectively. A clear difference of the 7mer sequences should be seen after submission of a coupled AAV library to an uptake or infection experiment, respectively. No mosaic capsids were expected in case of a coupled library. In general, AAV capsid variants, recovered after infection of cells with a coupled library, should harbour a genome with a higher content of positively charged amino acids. In contrast, the repetition of uptake with a coupled library should not show any significant differences to the sequences obtained from the former round, which in addition would prove the unspecificity of the uptake process.

To investigate this, both libraries coupled by uptake or infection were submitted to a new round of uptake or infection and progeny virus was sequenced as described above. The sequences were analyzed for the overall net charge. Results are exemplarily shown for round II Uptake GPC100 and round II infection GPC 1000 (Table 4).

Uptake II	net charge	Infection II	net charge
VNDRLPS	neutral	SALNLQG	neutral
GIDLARS	neutral	VPPRDER	neutral
NVLGSGQ	neutral	TSATTPR	+
ASTQPQL	neutral	DRSPVVR	+
REQRETA	neutral	STPPSGR	+
IQGSPQG	neutral	PLASNPR	+
NESARSL	neutral	ISPKPQR	+
AEDRVTT	-	NTTLSCR	+
AQRSPQG	+	SRTLTR	+
RAPNGGS	+	NSSGRDR	+
KVVGSGR	+	SGSQSIR	+
TQSPVQR	+	ATPATPK	+
GKARTSE	+	GTRGNLG	+
LARNQSG	+	RGATTGP	+
VKLGAAS	+	GRSGVQI	+
SVRAGSS	+	KLDQMRP	+
ASGSSPR	+	ATGRAPT	+
ANQRGPT	+	STKPGVA	+
RIERLAY	+	SLSQRAP	+
DKTGSKP	+	APSPRSI	+

Table 3: Representative example of 20 insertion sequences detected in round II of uptake GPC 100 and infection GPC 1000

Again the frequency of small amino acids like serine or glycine was increased and the number of bulky ones like phenylalanine or tryptophan was decreased similarly to the results obtained for coupling by uptake or infection. Striking was the increased frequency of arginine at position 7 after the second round of infection. Whereas only 3 out of 20 sequences from the uptake experiment contain an arginine or lysine at position 7 (15% compared to 13% expected when completely random), 55% of the sequences after infection contain positively charged amino acids at position 7. Overall, 80% of all sequences after infection have a net positive charge, 20% are neutral, compared to 61% positively charged, 4% negatively charged and 35% neutral sequences found after uptake. These results, therefore, support that i) the libraries are indeed geno/phenotypically coupled and ii) uptake is rather unspecific.

Selection of AAV particles with specific affinity for a target antibody from the coupled viral library

The AAV library has been initially designed to select retargeting mutants which are able to specifically and efficiently infect a desired cell line. Selections have been successfully performed in the past as Luca Perabo was able to select three receptor-targeting mutants on different target cells. These mutants transduced target cells with an up to 100-fold increased efficiency, in a receptor-specific manner and without interacting with the primary receptor for wt AAV (Perabo et al. 2003). Here, AAV mutants were to be selected which are able to specifically bind to the idiotype of the antibodies they are selected on (Figure 5). Selected AAV mutants should, therefore, carry epi- or mimitopes of the antibody's target (the respective antigen of the antibody used).

In the first step the target antibody was coated to an appropriate cell culture plate at a concentration of 50-750µg per 15cm² plate. The uncoated surface was then blocked with Milk Powder, followed by incubation of the coupled AAV library (see **Coupling of geno- and phenotype by infection**) on the coated antibodies.

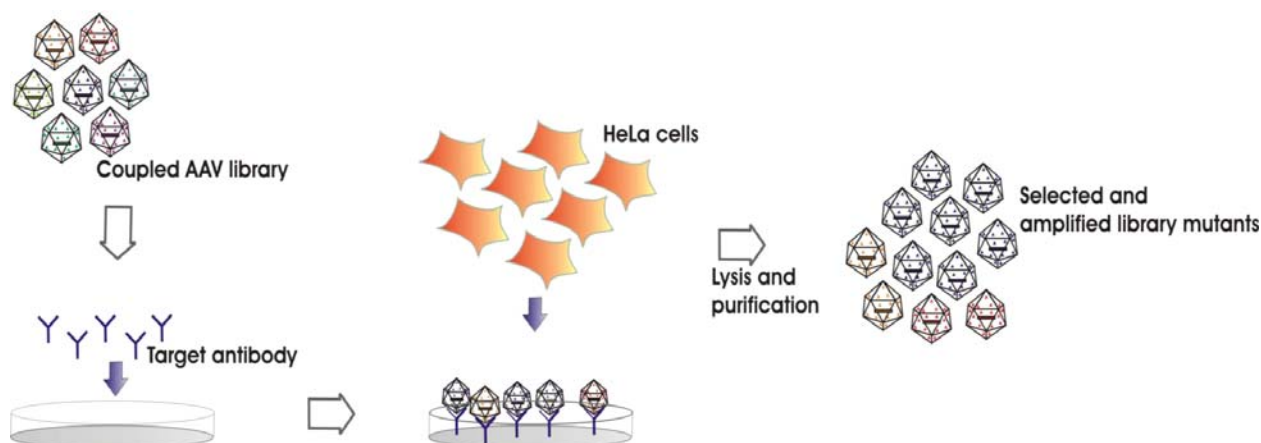


Figure 5: Selection procedure for selection of AAV library mutants specific for antibodies

Antibodies were coated to cell culture plates and after blocking incubated with the AAV library coupled by infection. Cell plate was washed to remove unbound mutants and HeLa cells were seeded into the plate. After 48h cells were harvested, lysed and the viral progeny was analyzed and submitted to another round for further selection.

After adequate washing HeLa cells were seeded into the plate to allow AAV uptake and coinfecting with adenovirus for replication and packaging. Cells were harvested and the lysates containing the virus were used further on as described above. The genomic titers obtained after each round were then quantified and sequences of single mutants were determined by sequencing.

Selection of AAV capsid variants against target antibodies Omalizumab (Xolair[®]) and IgG-KLH

During this thesis the following antibodies were used for the selection of anti-idiotypic AAV vectors. In first experiments the anti-human IgE antibody Omalizumab (Xolair[®]) was chosen, because this antibody has already been approved in therapy against allergic disorders in moderate to severe allergic asthma and specific mutants derived from this selection should be interesting candidates for drug development. The epi/mimotope of IgE bound by Omalizumab is not published and it is not known if it is a linear epitope or if a secondary structure of IgE is necessary for binding of Omalizumab. Furthermore, we used an anti-mouse IgG antibody directed against KLH (Keyhole Limpet Hemocyanin) in order to use an antibody which is known to recognize a linear epitope.

Selection on Omalizumab (Xolair[®])

With regard to developing an AAV based vaccine to treat allergic disorders we used the monoclonal antibody Omalizumab (Xolair[®]). Omalizumab is a humanized monoclonal antibody that selectively binds to human immunoglobulin E (IgE). Omalizumab binds IgE at the same site as the high-affinity receptor FcεRI, thereby reducing the amount of free IgE that is available to bind to the receptor. Levels of free IgE in the serum are reduced and, as consequence, the number of FcεRI receptors on basophils and other effector cells declines.

Before starting with selections, the binding affinity of Omalizumab to the cell culture plate was determined by ELISA. For this, the antibody was coated in serial dilution into 96-well plates from Nunc, the same material that was used for the selections later on.

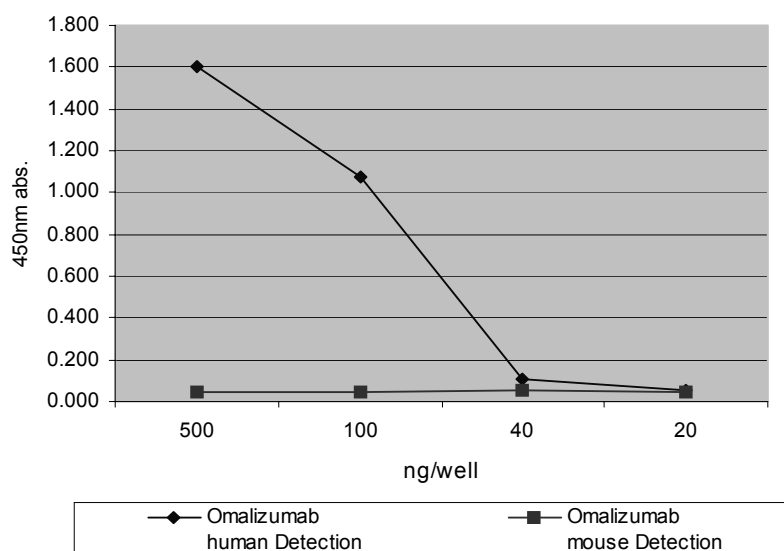


Figure 6: Detection of Omalizumab with anti-human IgG1k and anti mouse IgGy

Omalizumab was coated to Nunc well plates in dilutions from 500ng/well to 20ng/well and incubated with biotin-conjugated anti-human IgG1k and anti-mouse IgGy antibody. Bound antibody was detected and quantified by Streptavidin-POD and subsequent enzyme reaction.

After incubation unbound antibodies were washed away and the wells were incubated with blocking solution (Milk Powder). Coated antibody was incubated with biotinylated anti-human IgG for detection of Omalizumab or anti-mouse IgG as control. Thereafter an enzyme reaction with Streptavidin-POD was performed and quantified, showing that Omalizumab bound well to the cell plate.

Omalizumab was able to coat to the cell culture plates and could be nicely detected by anti-human IgG, but not by anti-mouse IgG as expected.

Next, four selection rounds were performed on Omalizumab with the coupled AAV library generated by infection, monitoring the genomic titers and the selected sequences after each round. In analogy selection rounds on PBS coated plates were carried out as negative control.

The cell lysates, after repeated thaw/freeze cycles of the cell pellet, from each round were used for further analyses. Viral DNA was extracted from AAV capsids in the cell lysates and the genomic titers were determined.

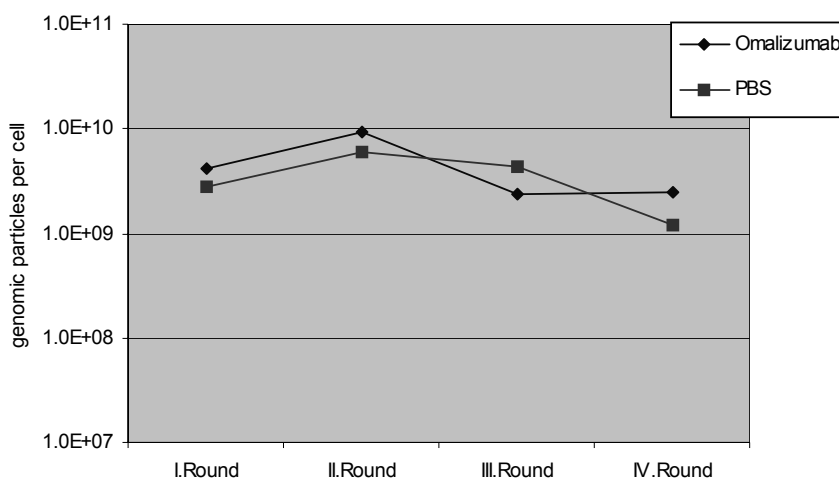


Figure 7: Genomic titers of selected mutants on Omalizumab round I to IV

The figure shows the genomic titers determined after round I to IV of selection for selections carried out on Omalizumab and on PBS coated wells, respectively, with the library coupled by infection.

If one or few variants of the AAV library display a sequence within 587 able to mediate binding to Omalizumab, first a drop in titer is expected, because in the first round the amount of the respective mutants is very low. Then round after round this mutant should be amplified and should show an increase in titer. However, for AAV selection on Omalizumab such an increase in genomic titers could not be detected. Titers yielded did not even exceed the titers that were obtained by selection on PBS.

Characterization and specificity of selected mutants

After each selection round fifty to a hundred clones were analyzed and their sequence was determined. For this the extracted viral DNA from each round was amplified by PCR and cloned into the AAV pRC vector. The plasmids were transformed into bacteria and single colonies were picked and analyzed by sequencing.

With each selection round the diversity of sequences clearly decreased and some sequences became more prominent within the different rounds. After each selection round, other sequences were enriched. Only one single sequence stood up to others in course of the four selection rounds, VYSPTGK, which was identified as a predominant sequence after selection rounds 3 and 4. Another sequence, SDAPLPR, disappeared after the second selection round while being predominant after rounds 1 and 2. Importantly, none of the sequences identified from the Omalizumab selections corresponded to the sequences identified in the control PBS selection.

Omalizumab selection	I. round	II. round	III. round	IV. round
SDAPLPR	69.0%	83.1%	0%	0%
VYSPTGK	16.7%	7.9%	58.4%	100%
TSASRAP	0%	0%	8.3%	0%
others	14.3%	9.0%	33.3%	0%

Table 4: Frequency of occurring sequences

At least one hundred clones were sequenced and analyzed and the amount of each selected sequence was set in relation to the others.

The three most prominent sequences identified were cloned into an AAV-helper plasmid and the respective plasmids were used to package recombinant AAV vectors encoding a self complementary GFP (scGFP) transgene. Self complementary transgene vectors are, in contrast to single stranded AAV transgene vectors, able to bypass second-strand synthesis, which is the rate-limiting step for AAV in host cell DNA synthesis (McCarty et al., 2001). The respective AAV mutants yielded comparable titers to wtAAV and were tested for specific binding to the Omalizumab antibody by Dot Blot. For this IgE antibody as positive control, the intact viral capsids of the selected variants, and wtAAV as negative control were blotted to a nitrocellulose Hybond membrane (Amersham) and then detected by Omalizumab, which was also used for the selection. Bound Omalizumab was detected by anti-human IgG γ HRP and quantified by subsequent enzyme reaction. The blot was then stripped and detection was repeated with the capsid specific antibody A20, as the A20 epitope is not marked by the inserted sequence at position 587, recognizing AAV

capsids. All AAV variants should be detectable by A20, whereas only the selected mutants should bind to Omalizumab if the selection was indeed specific for the idiotype of the selection antibody used.

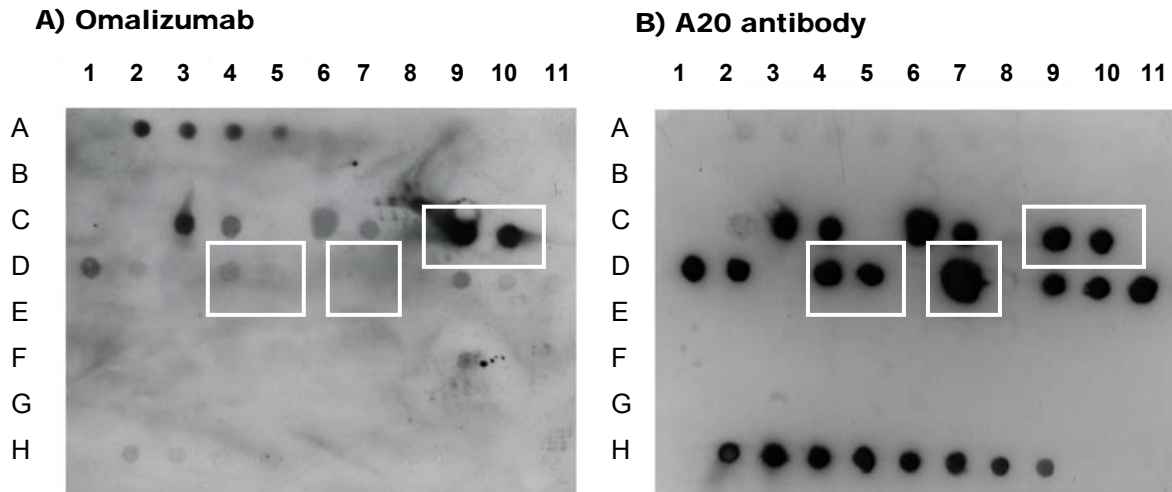


Figure 8: Omalizumab specific Dot Blot

Selected mutants were blotted to nitrocellulose membrane and detected by Omalizumab (A). The blot was stripped and bound mutants were detected by A20 antibody (B). The mutants were blotted in two concentrations, 5×10^{10} capsid particles and 1×10^{10} capsid particles. A2 to A9 shows the IgE positive control and H2 to H9 wtAAV as control. Mutant SDAPLPR is blotted in C9 and C10; mutant TSASRAP in D4 and D5 and mutant VYSPTGK in D7 (Other Dots show mutants not described in this work).

All selected variants were still detectable by A20 antibody (Figure 8B). However, according to the Dot Blot data, there is a clear difference in the affinity for the three sequences analyzed. In this case the variant SDAPLPR was recognized better by Omalizumab as variant TSASRAP and VYSPTGK, indicating that there is a difference in the affinity of the variants to Omalizumab.

Selection on linear epitope of mouse anti-KLH IgG antibody

To proof the concept of selection of anti-idiotype AAV vaccine, selection was performed with an antibody, which was known to recognize a linear epitope. The mouse anti-KLH IgG was obtained from a mouse immunized with purified KLH (Keyhole Limpet Hemocyanin) and is an IgG₁ isotype antibody.

Again the binding affinity of the antibody to the plate was tested by ELISA. Mouse anti-KLH IgG, A20 antibody and PBS as negative control were coated to a Nunc 96-well plate and incubated over night at 4°C. Wells were washed the next day and blocked with BSA. Bound antibodies were detected with biotinylated anti-mouse IgG and quantified by enzyme reaction with Streptavidin-POD.

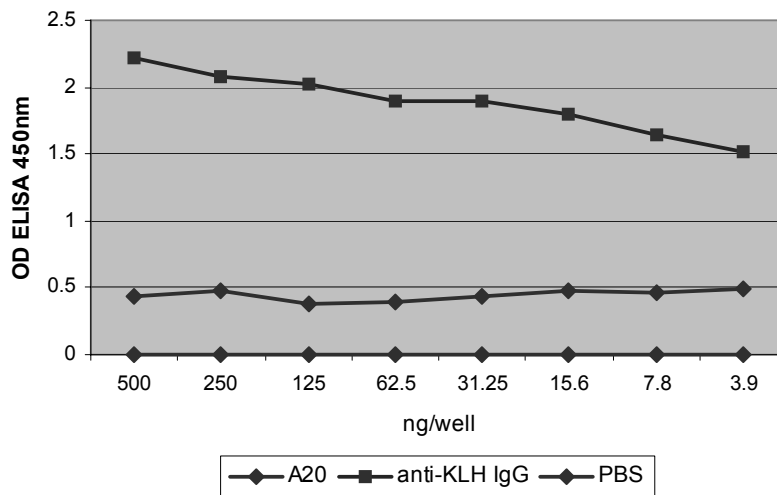


Figure 9: Detection of mouse anti-KLH IgG with anti-mouse IgG

Mouse anti-KLH IgG, A20 and PBS were coated to Nunc well plates in dilutions from 500ng/well to 4ng/well for mouse anti-KLH IgG and incubated with biotin-conjugated anti-mouse IgG antibody. Bound antibodies were detected and quantified by Streptavidin-POD and subsequent enzyme reaction.

Three selection rounds were performed with the AAV library coupled by infection on mouse anti-KLH IgG (see **Coupling of geno- and phenotype by infection**). Again selection rounds on PBS coated plates were performed as a negative control. The viral DNA was extracted from the mutants in the cell lysates and the genomic titers were determined as described above.

Within the three rounds of the selection the genomic titers for the selection on mouse anti-KLH IgG clearly increased this time compared to the PBS control. In the third round no genomic particles were detectable for the PBS control anymore.

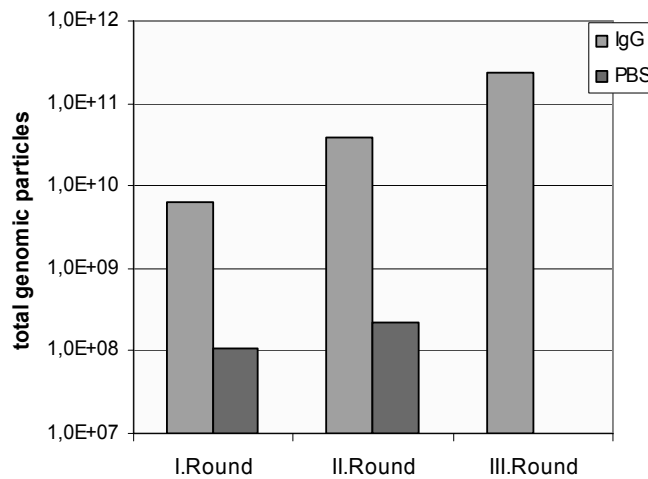


Figure 10: Genomic titers of mutants selected on IgG-KLH

Genomic titers were determined by Light Cycler PCR after each round and the total number of genomic particles after each round was calculated.

Characterization and specificity of selected mutants

Extracted viral DNA from the lysates after the first and the second round was amplified, cloned into the AAV pRC vector and the resulting plasmids were transformed into bacteria. Fifty to a hundred single clones were analyzed to determine the sequences inserted in 587 of the respective clones. For mouse anti-KLH IgG 5 sequences could be determined which were clearly prominent. All sequences, comparing mouse anti-KLH IgG and PBS control selection, were different, arguing for target specificity of the selected clones.

IgG	I. Round	II. Round
ARAGLPG	22%	0% ▼
LRPDARP	15.4%	50% ▲
PRTDSPR	26.4%	45% ▲
PTLTPPR	19.8%	0% ▼
STLAPPA	2.2%	0% ▼
Others	14.2%	5% ▼

Table 5: Frequency of identified sequences

At least one hundred clones were sequenced and analyzed. The amount of each specific sequence was set in relation to the total sequences analyzed.

The selected sequences were cloned into AAV helper plasmid, which were used to package recombinant AAV vectors encoding for scGFP as transgene as described before for the mutants selected against Omalizumab. The titers obtained for the mutants were

comparable to titers determined for wtAAV. These mutants were then tested in anti-KLH specific Dot Blots. For this KLH peptide as positive control, the intact viral capsids of the selected mutants, and wtAAV as negative control were blotted to a nitrocellulose Hybond membrane (Amersham) and then detected by mouse anti-KLH IgG, which was also used for the selection. Bound anti-KLH IgG was detected by anti-mouse IgG γ HRP and quantified by enzyme reaction. The blot was then stripped and detection was repeated with the capsid specific antibody A20. All AAV variants should be detectable by A20, whereas only the selected mutants should bind to the anti-KLH IgG if the selection was indeed specific for the idio type of the selection antibody used.

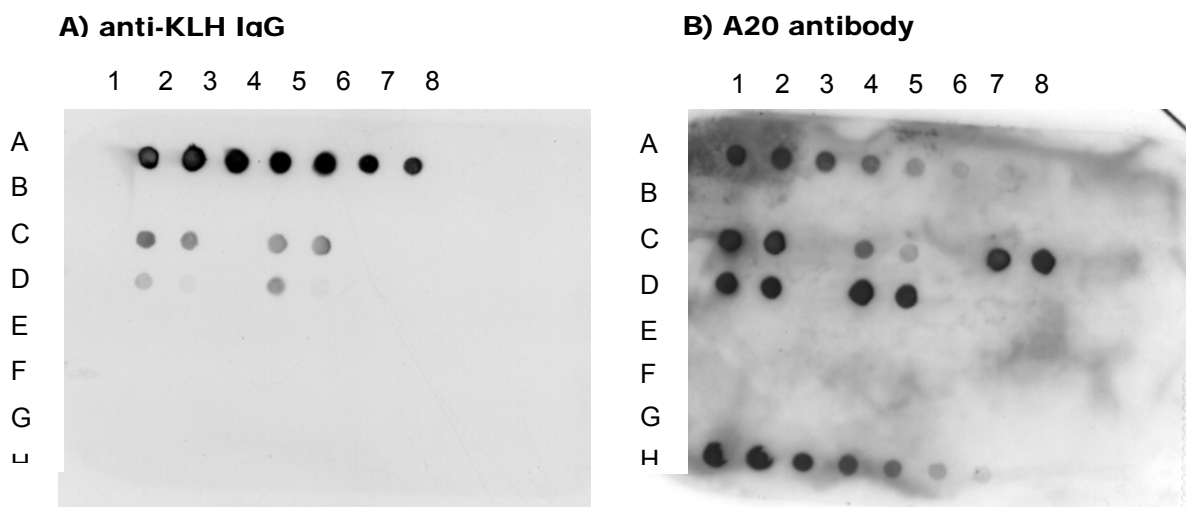


Figure 11: anti-KLH specific Dot Blot

Selected mutants were blotted to nitrocellulose membrane and detected by mouse IgG-KLH (A). The blot was stripped and bound mutants were detected by A20 antibody (B). A1 to A8 shows the KLH positive control and H1 to H8 wtAAV as positive control for A20 antibody. The mutants were blotted in two concentrations, 1×10^{10} capsid particles and 5×10^{10} capsid particles. Mutant ARAGLPG was dotted in C1, C2; LRPDARP in C4, C5; PTLTPPR in C7, C8; PRTDSPR in D1, D2 and STLAPPA in D4, D5.

All five mutants were detectable by A20 antibody, indicating that the intact capsids could be blotted to the membrane. Four mutants also showed a signal with the KLH specific antibody anti-KLH IgG, suggesting that four out of five mutants showed specific binding to the antibody they were selected on, whereas ARAGLPG and LRPDARP showed a higher affinity to anti-KLH IgG in the Dot Blot than the other mutants. Vaccination experiments in rabbits will be performed by Medigene AG with the two mutants in this blot, which showed the best signal with anti-KLH IgG, ARAGLPG and LRPDARP.

3.3. Discussion and Outlook Chapter II

Allergic disorders are one of the increasing diseases of the industrial countries. The prevalence of asthma in Western Europe has doubled in the last decade, leading to an estimated prevalence in the adult population of 10 to 15% (Jonkers et al. 2005). While milder forms like hay fever can be easily treated with today's medicine, such as antihistamines and corticosteroids for moderate forms of asthma, more severe forms like the walnut or bee sting allergy represent life-threatening illnesses for the patient and are greatly interfering with the patient's life quality.

In general the immune system shows tolerance against self antigens, like IgE as in the case for allergies, tumour-associated antigen (TAA) or beta-amyloid, because these antigens are not recognized as immunogenic. For active immunization against these antigens, their antigenic structures, or part of it, can be presented by anti-idiotypic antibodies in another molecular context to induce an immune response against the original self antigen. It was shown that anti-idiotypics can break immune tolerance, but the titers reached were usually fairly low.

An AAV mutant, representing an anti-idiotypic sequence, could combine the advantages of an anti-idiotypic vaccine and an efficient immune response, evoked by the viral polymeric structure.

The AAV library represents a suitable tool to select mutants, which display the desired anti-idiotypic sequence, e.g. by selection on anti-IgE antibodies. Selections here were performed using a diversity of 4×10^6 AAV variants in a solid phase selection procedure.

Since the number of patients with allergic disorders and also the number of severe forms of allergic diseases are dramatically increasing in the industrial countries, a new efficient treatment will be of great value for the patients suffering from these diseases.

Uptake seems to allow unspecific internalization of AAV

AAV infects cells by interaction with its primary receptor HSPG, which is found on a wide variety of cells and therefore establishing AAV's broad tissue tropism (Summerford and Samulski, 1998; Kern et al., 2003). For the performed selection procedure, it had to be guaranteed that the bound mutants were taken up by the host cell for replication, no matter

what tropism the mutant would show. Macropinocytosis is an unspecific mechanism, with which cells are able to take up viruses or other antigens without receptor interaction (Sieczkarski et al. 2002). This mechanism is mostly used by antigen presenting cells, which are responsible for recognizing material which has to be eliminated.

For the selection procedure a similar approach was to be achieved by simply seeding HeLa cells on top of antibody bound mutants. To test if viruses were in fact taken up by HeLa cells independent of HSPG receptor binding and able to replicate within the cell, different uptake experiments were performed (compare **Coupling of geno- and phenotype by uptake**).

To establish the system, rAAV/GFP, which corresponds to a wildtype capsid carrying a GFP transgene expression cassette, was bound to the immobilized A20 antibodies in a first approach. HeLa cells were then seeded on top of the A20-rAAV/GFP complexes, and the transduction efficiency by means of GFP expression was measured 48h later. As positive control, infection of HeLa cells with rAAV/GFP was performed (Figure 3). The results clearly show that the transduction efficiency achieved by uptake was almost as high as with infection. Fairly lower transduction efficiencies in case of uptake might be due to the washing step applied before seeding the HeLa cells. Some virions might get lost, which then cannot contribute to the overall transduction efficiency. To show that uptake is unspecific and thus independent of the capsid sequence (and, therefore, independent of receptor binding), the same experiment was carried out with an A3/GFP mutant, whose heparin binding residues at positions R-585 and R-588, and in addition N-587, were mutated to alanine residues. This mutant is unable to bind to heparin and was described as HSPG knock out mutant (Wu et al., 2000). In fact, in infection experiments A3/GFP was only able to transduce HeLa cells with up to 3% transduction efficiency (GPC of 1000), whereas in uptake experiments, the transduction efficiency was increased to about 15%. This means a five fold increase in transduction efficiency. The fact that GFP expression mediated by uptake of A3/GFP cannot be increased to rAAV/GFP levels, neither by higher virus concentrations nor by prolonging the incubation time of the cells to 72h, might result from inefficient intracellular processing or a different trafficking pathway, that A3/GFP uses once it is internalized by the cells. Wu et al. (2000) first described this mutant as heparin independent and showed that it can only poorly bind to heparin column, but did not test further if A3 is taken up by the cell and able to travel to the nucleus or not. Interestingly, a heparin Nonbinder pool selected from a coupled AAV library which only poorly infected HeLa cells as expected (see **Chapter III Figure 2 Infection and Uptake**

experiments with the Binder and Nonbinder fractions) is able to transduce HeLa cells rather efficient if the uptake technology is applied. This strongly supports the theory that uptake is suitable for efficient, sequence-unspecific cell transduction, and that the specific mutant A3/GFP has unique features which interfere with subsequent intracellular trafficking.

The experiment was repeated with rAAV/GFP, this time using heparin to prevent internalization mediated by the primary receptor of AAV, the heparan sulfate proteoglycan (HSPG). Both infection and uptake were performed in the presence of heparin. Infection could be blocked, up to 92-94% by heparin, whereas uptake was still blocked up to two thirds. The partial blocking of the uptake by heparin could be explained by different uptake routes that the virions might use. Since the cells are seeded on top of the virions, bound to antibodies in the cell plate, macropinocytosis might be an option for the virions to enter the cell. In other events the secondary receptors of AAV may facilitate the uptake. Other virions might still use their primary receptor HSPG, which can then be blocked by heparin. On the other hand heparin itself might prevent other events than just the interaction of AAV with HSPG.

Homogeneous library mutants result from coupling through uptake or infection

The original viral library consists of inhomogeneous mutants with mosaic capsids arising from the fact that many library plasmids are transfected into each cell during the production step of an AAV library in 293 cells. For the application of selection on antibodies, it is absolutely necessary to use mutants which genome encodes the same insertion as the capsid displays. To couple geno- and phenotype of the library for the selection protocol, the virions were submitted to uptake and infection experiments, varying the amounts of genomic particles per cell. To test for coupling efficiency and biodiversity of the new libraries generated, sequences of the resulting libraries were analyzed in terms of frequency of stop codons and diversity and compared to the original library (see **Coupling of geno- and phenotype by A)uptake/B)infection**).

Depending on the GPC used, differences were found when looking at stop codons and repetitive 7-mer sequences. Using 10 genomic particles per cell for uptake and infection, a few sequences were found more than once in a hundred sequences analyzed. The biodiversity was clearly higher when using a GPC ratio of 100 or 1000. Under such conditions no single sequence was found more than once in a hundred sequences analyzed.

The decreased diversity in GPC 10 might be explained by the low multiplicity of infection (MOI) used. The infectious titer of wtAAV is usually lower than the determined genomic particle titer. Transferring this onto the AAV library, not all of the 10 genomic particles per cell will result in genome transcription, explaining why the diversity decreases when GPC 10 is used, in uptake as well as in infection experiments.

The number of stop codons was analyzed to draw conclusions concerning the coupling state of the obtained libraries. The original pool still contained 8 stop codons per 100 sequences, whereas the number of stop codons was clearly reduced in all cases where GPC ratios of 10, 100 or 1000 were used for uptake as well as for infection experiments. In case of uptake experiments 1 to at maximum 4 stop codons (GPC 1000) were found. In case of infection experiments none to just 1 stop codon was found in a hundred sequences analyzed. Obviously, libraries resulting from infection experiments are coupled to a higher degree compared to libraries resulting from uptake experiments.

A reason for this major difference in the coupling state may be due to the coupling procedure used for uptake experiments. Virions are bound to A20 antibodies being coated to the tissue culture dishes. If for some reason the A20-virion complexes are not evenly distributed in the plate, rather a "virion pool" than single virions might be taken up by some cells, whereas other cells do not take up any virus. Such events could lead to the successful packaging of AAV genomes harbouring a stop codon in the inserted 7-mer sequence, despite the fact that these genomes code for non-functional cap proteins. In infection experiments, an even distribution of the virions might be more easily achieved, ensuring that at most one particle is taken up by a single cell.

Importantly, the biodiversity deduced from the number of repetitive sequences was high when using at least 100 genomic particles per cell, both for uptake and infection experiments. As 4 stop codons were found on case of uptake and GPC of 1000, a GPC of 100 should be chosen to couple an AAV viral library without losing biodiversity. In case of coupling by an infection step, a GPC of 1000 should be chosen, as 1 or less stop codons were found for both conditions, GPC 100 and 1000, and as no repetitive sequences were found under both conditions. A higher GPC in this case guarantees a higher degree of biodiversity, although no difference could be found when analyzing only 100 sequences. To have more confidence, ideally 300 to 1000 sequences should be analyzed.

Müller et al. (2001) generated a random AAV peptide library, also containing insertion of 7-mer peptides in position 587, in a three-step system to obtain virions

encoding of the displayed peptides by the packaged genome. In contrast to this approach, they packaged the library containing mutant *cap* genes into capsids, made up partially of wild-type VP proteins, by cotransfecting wildtype *rep-cap* plasmids lacking the inverted terminal repeats (ITRs) required for encapsidation. By this they obtained "AAV library transfer shuttles", which partly resembled wildtype capsid and bound heparin at a level of approximately 60% of wtAAV (Muller et al. 2001). To obtain coupled AAV library mutants, they transduced 293T cells with the AAV transfer shuttles with MOI of 1 to 5. They demonstrated by sequencing of a representative number of randomly selected clones that the resulting AAV library showed a diversity comparable to the plasmid library from which it was generated. A major problem in this approach is the fact that the library production allowed packaging of wtAAV genomes to some degree, probably resulting from homologous recombination taking place during packaging and thereby limiting the application for selection on cell types susceptible to AAV infection. For the selection on antibodies, this might also be disadvantageous, since mutants which can infect the producer cell line, in this case HeLa cells, more efficiently, but show low affinity to the antibody they are selected on, might outweigh high affinity mutants with poor ability to transduce the producer cells.

Interestingly, the coupling by infection experiments with GPC 1000 in this case seemed to result in a good coupling state (low number of stop codons) and without loss of biodiversity, compared to the coupling with AAV transfer shuttles, done by Müller et al.. The coupling of geno- and phenotype of the AAV library will work if each virion of the non-coupled library contains at least one heparin-binding motif which renders the AAV particle infections. A heparin-binding motif is reconstituted if the last amino acid of the random 7-mer sequence contains a positively charged amino acid R or K or an overall net positive charge is achieved by the insertion (compare **Chapter III, Heparin Binder and Nonbinder, Table 1**). Looking at the arginine positions R585 and R588, the insertion of a peptide between R585 and R588 (Figure 12A, B) could cause their spatial separation or sterically block the heparin binding ability. In either case, bulky amino acids are prone to lead to one or both of these events (Figure 12C, D). If the peptide consists of small residues, the insertion could be less invasive and the structure of the HSPG binding motif maintains functional (Figure 12E). Insertion of positively charged peptides could lead to a HSPG binding phenotype in combination with one of the original arginines (Figure 12F) or independently from them (Figure 12G). The proximity of R588 to the last position of the inserted peptide could facilitate reconstitution of a functional motif if an arginine is present

at this latter position (Figure 12H). It should be noted that this behaviour could be due to the particular sequence of the construct that was used, where the 7th position of the randomized peptide and R588 are separated by two residues resembling the wild-type situation. Thus, multiple ways for the generation of a heparin/HSPG binding phenotype exist.

Therefore, most of the non-coupled virions indeed are able to bind to the cell and to be replicated in the cell without the need of an AAV transfer shuttle.

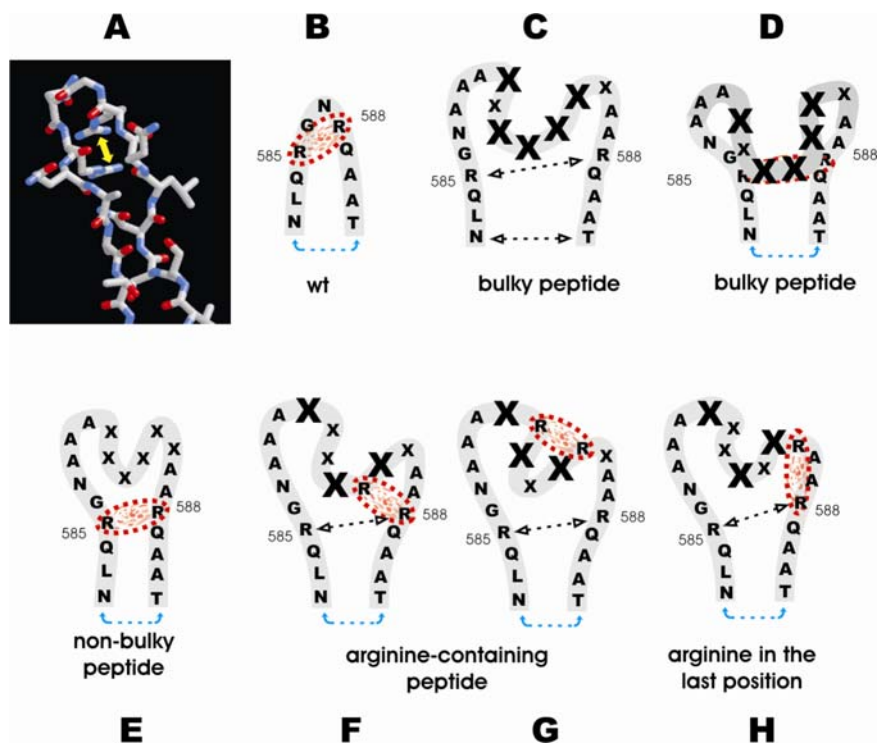


Figure 12: Proposed model for the influence of several peptide classes on capsid stability and on binding to heparin. A) Three dimensional atomic structure of the 587 region. The side chains of R585 and R588 are pointed by the yellow arrow. B) The two arginines are part of the HSPG binding motif. C) A bulky peptide disrupts the heparin binding motif taking the arginines apart. D) A bulky peptide obstructs the HSPG binding motif. E) Small peptides could preserve the original structure of the loop and heparin binding motif. F) and G) The presence of one or more arginines in the inserted peptide restores the heparin binding ability. H) Due to its proximity to R588, an arginine in the last amino acid position of the insertion is prone to restore heparin binding motif. In all panels, a functional heparin binding site is indicated by a red pattern. A loop conformation that confers capsid stability is indicated by the blue arrow. Taken from Goldnau, Endell, Perabo, and White et al, in revision

When the coupled libraries were submitted to a new round of infection or uptake experiments, as expected, the characteristics of the analyzed sequences changed, whereas no significant changes were observed after another round of uptake.

The frequencies of the 20 amino acids and the overall net charge of the inserted 7-mer sequence did not change after performing another round of uptake, indicating that no

major changes in the characteristics of the library happened and proofing that uptake happens in an unspecific manner. In case of infection on the other hand a clear shift to positive amino acids, especially arginine, strikingly at position 7, was observable. The coupled library consists of a homogeneous capsid carrying exactly the same genome encoding these capsid proteins. All particles which are no more able to bind the cell via the inserted sequence or the original R585/R588 if the inserted ligand is not destroying the natural heparin/HSPG binding motif (Figure 12C, D) will be lost. The increased prevalence of arginine or other positively charged amino acids, like the prevalence of small amino acids such as serine or alanine, hint indeed to a conservation of the capsid's ability to bind to heparin by the R585/R588 or a corresponding restored motif (Figure 12).

Selection of anti-idiotypic AAV mutants on antibodies by solid phase

After establishing the conditions for the selection procedure, the AAV library was submitted to selection on the anti-IgE antibody Omalizumab to identify mutants which could then be used for a vaccination approach. Omalizumab was chosen as target antibody as the therapeutic concept of the anti-IgE drug is clinically validated, and this monoclonal antibody is already approved as a passive vaccine in asthmatic patients, both in the USA and in Europe. Four rounds of selection were carried out, using the library coupled by infection. As a control the same selection protocol was applied to plates where instead of the antibody only PBS was coated instead of the antibody. For an ideal selection process one would expect that the genomic titer of the virion population obtained after each selection round will increase, since mutants with a sufficient binding affinity to the target antibody should be enriched. In case of the selection against Omalizumab, however, no such increase of genomic titers of the recovered AAV particles could be observed. The titers remained more or less constant after all selection rounds and the selection behaviour based on the genomic titer was similar to the PBS control. From these findings it was expected that no specific sequences recognized by Omalizumab were enriched during the selection procedure. Therefore, about 100 sequences cloned after each single selection round were analyzed by sequencing of the 587 region. A total of 3 individual sequences was identified which were highly repetitive with frequencies of 12 to 95% after a given selection round. However, only one sequence – VYSPTGK – was clearly enriched during the four rounds of selection. Two sequences occurred early in the selection process and then disappeared again, others appeared later during the selection process, and one

sequence even popped up after only the third selection round. All selected sequences were tested for IgE specific binding in Dot Blot experiments. Clear and IgE-specific signals with different intensity were obtained for selected AAV in the performed Dot Blot. Interestingly, the only sequence which was continuously enriched during the selection process was not recognized by Omalizumab. Perhaps AAV particles encoding this cap sequence have only a comparable low affinity to Omalizumab, but its genome is excellently taken up by and reamplified in the transduced cells. Also the fact that the selected mutants did not show increasing titers in the continuous selection rounds might be explained by a weaker affinity to Omalizumab combined with an efficient replication in HeLa cells.

As a completely independent experiment and to confirm the usefulness of a coupled library for the selection of anti-idiotypic AAV particles, selection of AAV variants on a anti-KLH antibody (mouse IgG₁), known to recognize a linear epitope of KLH, was performed. Interestingly, in this experiment increasing genomic titers after each of the three selection rounds performed were detectable, in agreement with our hypothesis, indicating that selection of one or a few specific sequences and their enrichment had indeed taken place. 50 to 100 clones obtained after the first and second selection round were sequenced. This analysis revealed that five sequences were prominent after the first selection round, but only two of them prevailed (95%) after the second selection round. Dot Blot experiments indicated that AAV particles with those 5 sequences have different affinity for the anti-KLH antibody. Two of them bind with a rather high efficacy, two of them have intermediate to low affinity and one has no detectable affinity at all. Interestingly, only one of the two sequences left after the second round of selection belongs to the high-affinity binders, whereas the other sequence has only little affinity for anti-KLH IgG. This seems to confirm the theory that there is the interplay of binding affinity for the target antibody on the one hand and amplification efficiency in the cell on the other hand. For this reason, it seems very important to investigate all repetitive sequences obtained after each selection step for their respective affinity in Dot Blot experiments.

The selections of coupled AAV libraries performed on the antibodies Omalizumab and anti-KLH IgG showed that the selection of a specific mutant is possible. However, the experiments have also shown that repeated selections will not lead to the isolation of only one high affinity binding mutant. In contrast, several sequences with different affinities for

the respective antibodies are being identified. Although a preselection of suitable mutants can be performed based on *in vitro* assays such as Dot Blot, animal vaccination experiments are indispensable to finally identify the one AAV variant which is best suited to induce polyclonal antibodies against the target antigen with all desired and required properties also carried by the monoclonal selection antibody.

The production of sufficient antibody titers for an active immunization approach highly depends on the immunogenicity of the viral structure. Several studies have determined a high prevalence of serum antibodies (Ab) against the AAV capsid in the human population. They could show that between 30 and 96% of human beings are seropositive for AAV specific Ab and that 18 to 67.5% of them are neutralizing antibodies, depending on age and ethnic group. (Blackow et al. 1968; Chirmule et al. 1999; Erles et al. 1999; Moskalenko et al. 2000). These neutralizing Ab can cause considerable problems, especially when readministration of the vector is required in gene therapy applications. Acute inflammation due to activation of the innate immune system, and expression of chemokines and cytokines, which has been strongly observed for adenovirus, does take place very gentle after AAV transduction and is only very short lived (Zaiss et al. 2002). Therefore, AAV vectors seem to have markedly reduced inflammatory properties compared to other viral vectors such as adenovirus. For many viral vectors, a strong cellular immune response against the vector and the delivered transgene, which can cause severe complications for the treated patient, has been observed. This was probably the case for Jesse Gelsinger, who died in a Phase I gene therapy trial after application of an adenoviral vector (for further information see Teichler Zallen 2000). In contrast, after *in vivo* gene transfer of rAAV vectors, apparently no evidence for a cellular immune response to the transgene product, elicited by the presence of AAV, has been reported (Chirmule et al. 1999; Hernandez et al. 1999; Jooss et al. 1998; Chirmule et al. 2000). This may be due to the fact that rAAV fails to infect mature dendritic cells capable of stimulating antigen-specific T-cell responses and therefore, the presentation of neoantigens might be inefficient (Jooss et al. 1998), but that rather high numbers of immature dendritic cells are transducible with AAV *in vitro*, a situation which is unlikely to occur *in vivo*. The study describes the *in vitro* transduction of immature dendritic cells by AAV which initiated subsequently a CD40-ligand dependent T-cell response against transduced cells (Zhang et al. 2000). The role of such immature dendritic cells for eliciting a cellular immune response after AAV transduction *in vivo* has to be further elucidated.

Manno et al. recently described an immune response against recombinant AAV capsids, in a phase 1 study in severe hemophilia B (2006). Preclinical studies in dogs revealed no immune response against the transgene or vector, but administration in humans showed a destruction of transduced hepatocytes by cell-mediated immunity targeting antigens of the AAV capsid. These events occurred 4 – 6 weeks after administration of the vector and in consequence led to decreasing titers of Factor IX expression.

All these observations point towards a mainly humoral response against the AAV capsid, while a cellular immune response to the virion or to the delivered gene product is rare.

The conflicting data presented by several studies indicate that the CTL as well as the humoral response to the delivered gene and the AAV capsid depends on a number of variables, including the nature of the transgene, the route and site of injection, the age, health and immunological background of the subject, the degree of contamination with helper virus proteins, and even the maturation state of antigen presenting cells exposed to rAAV administration. This implies the need for a better understanding of the immune response against AAV. Nevertheless, the studies indicate that AAV is able to elicit a humoral immune response and therefore can be used for active immunization approaches, where an polyclonal antibody response is to be provoked. The efficiency and the magnitude of antibody response have still to be elucidated, and importantly, the AAV vaccine has to have the potential to break tolerance against self-antigens such as IgE described in this thesis. If the particular structure and repetitiveness of the epitopes exposed on AAV should not be sufficient to break tolerance against the antigen, which is very unlikely, the immunogenicity of the viral capsid can be further improved by the addition of adjuvants such as Freund's Complete Adjuvants (FCA) in mouse or CpG in human, both stimulating T_H1 immune responses.

Other vaccination approaches for allergy include the design of IgE-based synthetic peptide immunogens (Wang et al. 2003). The known epitope for the binding of IgE to its high affinity receptor $Fc\epsilon RI$ was synthesized and immunopotiated by linkage to a combinatorial T helper epitope derived from measles virus, UBITH[®]A, to provoke an immune response and allow active immunization. Wang et al. could show that a polyclonal antibody response could be generated in dogs and these antibodies blocked binding to the high affinity receptor $Fc\epsilon RI$, and were sufficiently immunogenic to evoke functional anti-dog IgE immune responses in dog. Besides the design and synthesis of immunogenic peptides, the target epitope has to be known in this approach. The coupled AAV library

allows the mapping of unknown epitopes and the selection of high affinity peptides in one step and in addition provides the polymeric structure to evoke a polyclonal immune response.

Outlook

Although we could demonstrate that the AAV library currently available is already suitable for the selection of AAV variants with the specific affinity for a target antibody of choice, there are several ways to improve the library on the one hand and the selection methodology on the other hand. For further improvements of the AAV library an extension of the insertion sequence from currently 7 to at least 12 up to about 34 amino acids should be feasible as a 34mer sequence directly cloned into this insertion site was well tolerated by AAV (Ried et al., 2001). This could increase the diversity of the library dramatically (whereupon a biodiversity of 1×10^8 to 1×10^9 will be the upper limit due to the restrictions such as cloning efficiencies and scale feasible) and allow the formation of secondary structures within the inserted sequence to expose more complex epitopes. The production of a library with an insertion sequence of 14 amino acids is on the way to widen the diversity of the library. Other insertion sites suitable to express foreign peptide sequences on the virus capsid have been identified and libraries cloned into these sites are currently in preparation. Another approach is the insertion of 14 random amino acids flanked by two cysteines residues on each side which would lead to formation of loop structure of the inserted random sequence due to disulfide bridging (Shi and Bartlett, 2003). With the insertion of an RGD-4C motif in position 520 and/or 584, AAV vectors could be generated which show eliminated heparin binding ability and a novel tropism to endothelial cells (Shi et al. 2006). The advantage of an extra loop mediated by flanking cysteine residues could be that such a structure would be protruding from the rest of the capsid and, therefore, could allow a better contact to the target antibodies in the selection process and a better presentation of the selected sequence later on in the vaccination step.

The selection of AAV mutants on antibodies widens the application of the AAV library and allows selection of specific mutants for vaccination approaches. Extending the size of the insertion peptide of the library will provide a library with greater diversity for new selection approaches.

4. Chapter III - Application of the coupled AAV library for selection of gene therapy vectors

4.1. Introduction

The coupled AAV library, which was required for AAV anti-idiotypic selection, is also a very useful tool for selection of gene therapy vectors. A major problem for application of AAV in gene therapy is the broad tropism of the vector *in vivo*. The primary receptor of AAV, HSPG (Summerford and Samulski 1998), a widely distributed negatively charged cell surface molecule, is thought to be responsible for this broad tropism. This hampers selective transduction of target tissue. Vectors aiming to redirect the tropism of AAV have been generated by insertion of ligands at position 587/588 of the AAV capsid (Büning et al. 2003a; Büning et al. 2003b). This is likely to interfere with the HSPG binding of at least two (R585 and R588) of the five positively charged amino acids of the recently identified HSPG binding motif (Kern et al. 2003; Opie et al. 2003), explaining the ablation of HSPG binding of some targeting vectors (Girod et al. 1999; Grifman et al. 2001; Nicklin et al. 2001; Perabo et al. 2003; Ried et al. 2002). In some cases, however, binding was only partially affected (White et al. 2004), or even restored (Grifman et al. 2001; Perabo et al. 2003; Work et al. 2004).

AAV heparin Binder and Nonbinder pool

With the coupled AAV library, the mutants can be differentiated into heparin Binder and Nonbinder and facilitate the selection of HSPG independent vectors. To investigate molecular mechanisms responsible for these differences in HSPG binding behaviour, the combinatorial library of AAV capsids carrying insertions of 7 randomized amino acids at position 587 (Perabo et al. 2003) and coupled by infection was applied to a heparin affinity column to separate heparin/HSPG binding from non-binding mutants.

In the following the separation of Binders and Nonbinders is described and a selection on primary Hepatocytes as target cells was performed to show that by utilizing the Nonbinder pool a highly selective and efficient retargeting vector can be obtained.

4.2. Results

Separation of Binders and Nonbinders by Heparin binding affinity

In a first step the AAV library was coupled by infection of HeLa cells as described in **Coupling of geno- and phenotype by infection**. Briefly, HeLa cells were infected with a GPC of 1000 in presence of adenovirus and harvested after 48h. The cell pellet was submitted to repeated thaw/freeze cycles and the lysate was then purified by Iodixanol step gradient purification. To separate the mutants displaying sequences able to restore HSPG binding ability from mutants displaying peptides which ablate HSPG binding, the coupled library (about a total of 1×10^{11} genomic particles) was applied to a Heparin column (HiTrap, Amersham Bioscience).

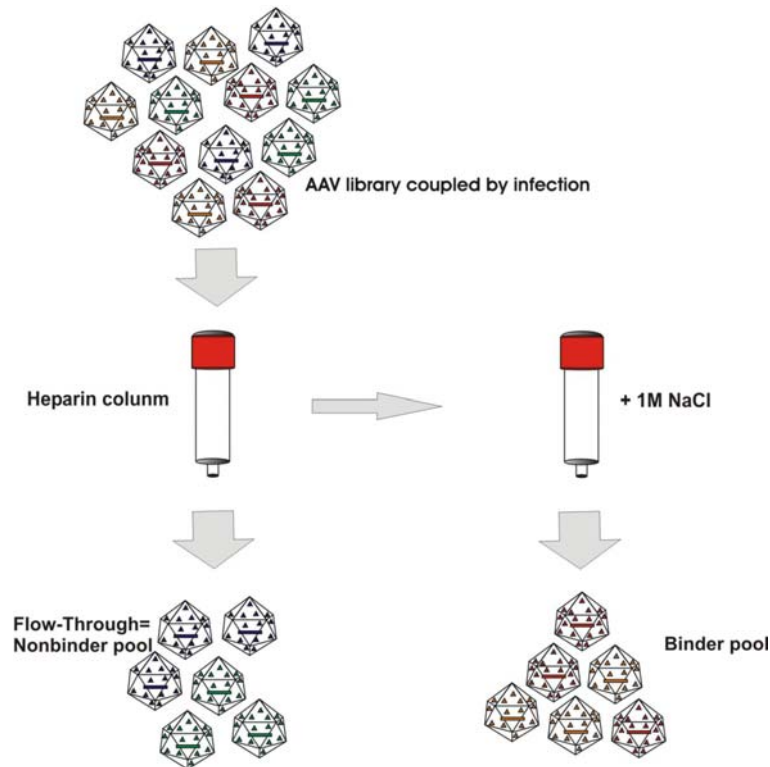


Figure 1: Separation of Binder and Nonbinder pool

The AAV library coupled by infection is separated by Heparin column. The flow-through was termed as Nonbinder pool and the Binder pool was eluted with 1M NaCl.

The flow-through contained the Nonbinders, whereas the Binders were eluted from the column by 1M NaCl. Then both fractions were again purified by Iodixanol step gradient to concentrate the virions. Thereafter genomic titers of both pools were determined by Light Cycler PCR.

After the second purification step still genomic titers of 1×10^7 per μl (500 μl total) were obtained. The Binder and the Nonbinder libraries were then characterized by sequencing. Therefore, viral DNA was amplified by PCR and cloned into the AAV pRC vector. The plasmids were transfected into bacteria and one hundred single clones were picked and sequenced. In addition, the viral DNA library and the AAV library after packaging were also sequenced and analyzed.

A)

DNA – library	AAV - library	B -pool	NB -pool
R	R	R	R
H	H	H	H
K	K	K	K
E	E	E	E
D	D	D	D
N	N	N	N
S	S	S	S
T	T	T	T
G	G	G	G
A	A	A	A
P	P	P	P
C	C	C	C
Q	Q	Q	Q
I	I*	I	I
L	L	L	L
M	M	M	M
F	F	F	F
W	W*	W	W*
Y	Y	Y	Y
V	V	V	V

B)

B - pool	net charge	NB - pool	net charge
DRDRPQR	+	ADRQEAN	-
KSSDLSR	+	ADSDHSS	-
HPSGVGK	+	ASLSHDD	-
SGVEGGR		GSGTTQA	
KKPSGAV	+	DRAYGEQ	-
PPKVAQT	+	DSQGEAE	-
SPRSDRP	+	EALSTRD	-
ARDPGKA	+	EPTGSDL	-
SSRATAD		GASSVSG	
AGRITIE		GLDGQEQ	-
VKSRDQQ	+	GPGATST	
CDQRDRC		HTTSAAS	(+)
APEARLS		DHDDPEW	-
NSATGSK	+	NTAGANA	
PNPAAVH	(+)	QDTPPA	-
ASLGGRP	+	SNADKVS	
DRATPTR	+	TEDSEPD	-
ALTGAPG		TERPGAD	-
ASQQHAH	(+)	TTPSPHA	(+)
RVDPEAK		VGSDPSV	-

Table 1: A) Statistical analysis of the frequency of amino acids.

Based on the χ^2 -test, the colours indicate a higher (red), lower (blue) or expected (black) frequency of each amino acid in the analyzed populations ($P=0.0001$). For each population >80 clones were sequenced. *These amino acids were found at clearly lower frequencies than expected but statistical assessment of the significance was not possible without sequencing a higher number of clones.

B) Representative example of 20 peptides detected in B-AAV and NB-AAV pool.

Net charge of the insertions is provided. Parentheses indicate a weak charge considering the low pKa of histidine

The AAV DNA library showed a higher than expected statistical presence of alanines which originates from the chemical features of the oligonucleotides synthesis procedure. Occurrence of every other amino acid met statistical expectations.

The AAV viral library showed an excess of the amino acids proline (P), glycine (G) and, alanine (A) and a defect of cysteine (C), leucine (L), phenylalanine (F), tryptophan

(W) and tyrosine (Y) (Table 1A). Since P, G, and A are three of the four smallest amino acids, whereas F, Y and W are three of the four biggest, this bias suggests that the packaging process selects against bulky inserts which would introduce dramatic structural rearrangements and have a deleterious effect on capsid structure. In addition, prolines could favour spatial accommodation of the peptide by introducing kinks and reducing its bulkiness. Cysteine on the other hand might lead to structural problems due to disulfide bridging with other cysteine residues of the AAV capsid.

The Binder pool showed a significant increase of arginine residues (Figure 1B). Strikingly, arginines were particularly frequent at the 7th position of the peptide (30%). In contrast, in the AAV display library and the Nonbinder pool, the frequency of arginine at this position (15% and 9%, respectively) was equal or lower than the expectation for a randomized distribution (14.3%).

Interestingly, Binder pool insertions carrying no positive amino acids displayed an exceptionally high amount of alanine (A), glycine (G) and serine (S) (data not shown), the three smallest amino acids, suggesting a reduced impact on the wild-type capsid three-dimensional structure, which is less likely to interfere with binding of heparin.

The Nonbinder pool showed clearly a higher presence of negative charged amino acids [aspartic acid (D) and glutamic acid (E)] (Table 1A, B). Moreover, although the number of negative residues observed in the Binder pool matched statistical expectations, only 2% of the clones carried a net negative charge in its insertion, while 76% carried a positive and 21.5% a neutral charge. In clear contrast, the Nonbinder pool consisted of 53% negative, 8% positive and 39% neutral net charged inserts. This bias becomes even clearer if histidine is considered neutral due to its low pKa: Binder pool insertions would then be 2% negative, 64% positive and 34% neutral while Nonbinder pool consisted of 64% negative, 2% positive and 34% neutral. These observations strongly suggest that the presence of negative charges is deleterious for functional binding of AAV vectors to negatively charged heparin/HSPG.

Infection and uptake experiments on HeLa cells with the Binder and the Nonbinder pool packaged with scGFP as transgene reflected the different binding behaviour. While uptake of the Binder and Nonbinder pool should only show minor differences in AAV-mediated GFP expression, the infection experiment should reveal significant differences in GFP expression for the Binder and the Nonbinder pool, since the Binder pool should be much more efficient in infecting HeLa cells, because of their ability to interact with HSPG, AAV's primary receptor. To analyze this, HeLa cells were infected with 1×10^3 genomic

particles per cell of the Binder/GFP, Nonbinder/GFP pool and rAAV/GFP (as control), and incubated for 48h. The GFP expression level was determined by FACS analysis. For the uptake experiments, plates were coated with the A20 antibody recognizing the intact AAV capsid. Unbound A20 was washed away and the plate was then incubated with rAAV/GFP, the Binder library or the Nonbinder library with 1×10^3 genomic particles per cell. After incubation and a washing step, HeLa cells were seeded into the plates and incubated for further 48h. Transduction efficiency was determined by FACS analysis.

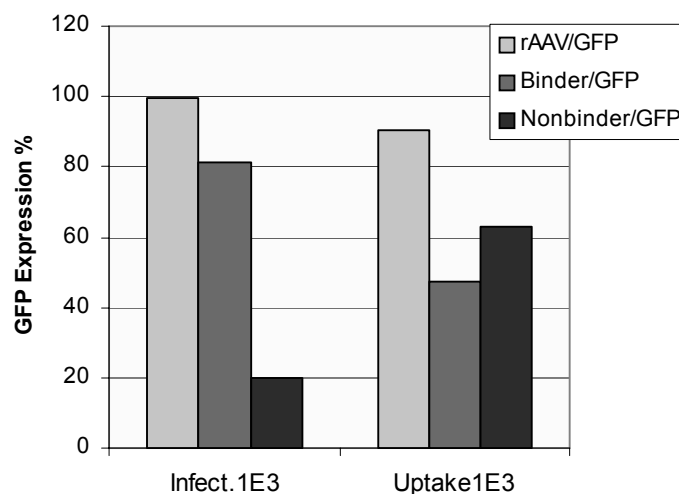


Figure 2: Infection and Uptake experiment with Binder and Nonbinder fractions

For uptake wells were coated with A20 and incubated with rAAV/GFP as control, the Binder or the Nonbinder pool (GPC of 1×10^3). After washing of unbound virus, HeLa cells were seeded into the wells and analyzed by FACS after 48h. For infection HeLa cells were seeded into wells and infected with rAAV/GFP, the Binder or the Nonbinder pool. Cells were analyzed by FACS 48h later.

The Binder pool behaved similar to rAAV/GFP when infecting HeLa, both reaching up to 80 to 99% transduction efficiency on HeLa, using 1×10^3 GPC. rAAV/GFP reached 90% transduction efficiency by uptake with 1×10^3 GPC, whereas Binder and Nonbinder pool showed both similar transduction efficiencies with 50 to 60%. For infection, however, the Nonbinder pool showed transduction efficiency of only 20% using 1×10^3 GPC in clear contrast to the Binder pool with 80% indicating that the Binder pool was clearly better infecting HeLa cells than the Nonbinder pool as expected.

Competition experiments with heparin and the Binder and the Nonbinder pool were carried out. HeLa cells were transduced with 1×10^3 infectious particles per cell of rAAV-

RC, Binder pool and Nonbinder pool, preincubated with heparin (25U/ml). After 48h the transduction efficiency was measured by FACS analysis (Figure 3).

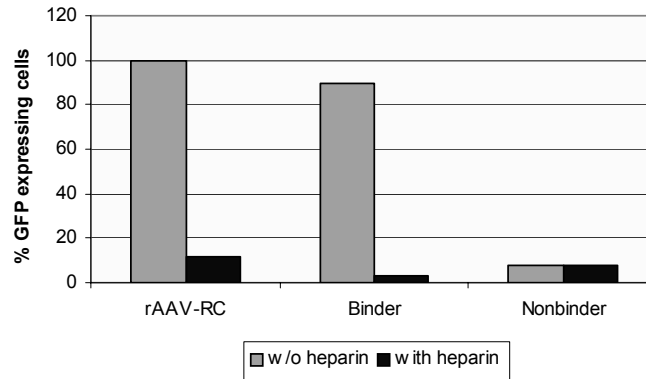


Figure 3: Competition of transduction on HeLa cells

HeLa cells were seeded into 24well plates. rAAV-RC, Binder pool and Nonbinder pool were preincubated with and without heparin and the cells were transduced with 1×10^3 infectious particles per cell. After 48h cells were analyzed by FACS for GFP expressing cells.

rAAV-RC and Binder transduced HeLa 90 to 100% when not preincubated with heparin. In heparin competition, transduction efficiency of both rAAV-RC and Binder pool could be blocked by heparin to 11% (rAAV-RC) and 2% (Binder pool), respectively. In contrast to the Nonbinder pool, which transduction efficiency was unaffected by the incubation with heparin, transducing HeLa with 8% with or without heparin, and indicating that the Nonbinder pool is heparin independent.

In vivo biodistribution of heparin Binders and Nonbinders

Previously an AAV targeting vector was described, rAAV-MTP, that allowed systemic vascular targeting (White et al. 2004). Simultaneous detargeting of this vector from liver and spleen was observed. This vector showed a reduced ability to bind to heparin (White et al. 2004). Here, it was analysed whether the inability of AAV insertion mutants to bind heparin directly correlates with detargeting from liver and spleen. Therefore, Binder and Nonbinder pools were produced as beta-galactosidase expressing recombinant AAV vectors (rAAV) as previously described (Work et al. 2005). rAAV with wild-type capsid (rAAV-RC) was used as a control. First, the ability to infect the hepatocellular carcinoma cell line HepG2 was determined (Figure 4).

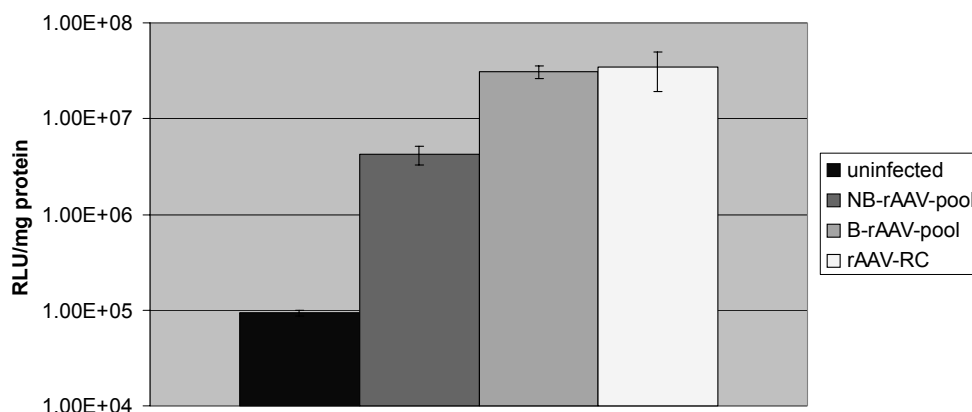


Figure 4: Transduction efficiency of rAAV-RC, B-rAAV-pool and NB-rAAV-pool on HepG2.

HepG2 were infected in the presence of adenovirus (1 pfu/cell) with 1000 genomic particles per cell of rAAV-RC, B-rAAV-pool or NB-rAAV-pool and analysed 48 h p.i. Cells were lysed in Galactolight Plus beta galactosidase lysis buffer (Tropix, USA) and betagalactosidase expression was determined by Galactolight Plus beta galactosidase assay according to manufacturer instructions. Detection was performed using a Wallac 1420 (Victor2) multilabel counter with beta-galactosidase as standard. Gene expression was normalized for total protein using BCA (Perbio, UK) and expressed as RLU/ mg protein.

All three viral preparations were able to transduce HepG2. rAAV-RC and Binder pool showed a comparable transduction efficiency whereas the Nonbinder pool was about 10-fold less efficient as expected. Since the addition of heparin completely abolished rAAV-RC mediated transduction (data not shown), it can be assumed that AAV infection of this cell line depends on HSPG binding.

Thereafter, 4×10^9 genomic particles were injected intravenously into C57/B6 mice (n=4) and biodistribution studies were performed as described (White et al. 2004). Animals injected with rAAV-RC and Binder pool showed a comparable biodistribution with the highest vector DNA level in spleen and liver (Figure 5).

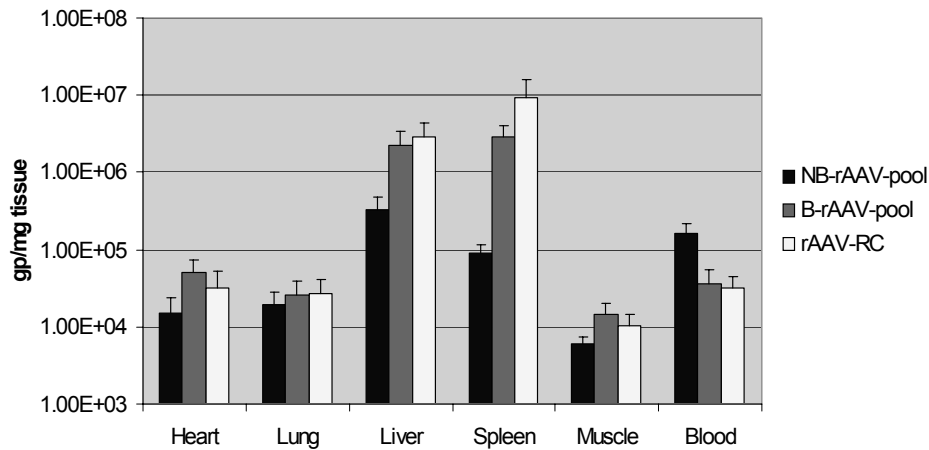


Figure 5: Biodistribution of rAAV-RC, B-rAAV-pool and NB-rAAV-pool in C57/B6 mice
 4×10^9 genomic particles of the different vector preparations were injected into the tail vein of 12 week old C57/B6 mice. 24 h p.i. mice were sacrificed. DNA was extracted from blood and tissues. Vector genomes per tissue were quantified by PCR (Taqman).

In contrast, the Nonbinder rAAV-pool showed a 102- and 31.8-fold reduction of vector DNA level in the spleen in comparison to rAAV-RC and Binder pool, respectively, whereas in the liver an 8.8- and 6.7-fold reduction was detected. In addition, elevated levels of viral DNA in the blood were measured for the Nonbinder pool consistently with the level of liver and spleen detargeting.

Selection on Hepatocytes with the Nonbinder library

Recombinant AAV and targeting mutants within the binder pool are sequestered in the liver due to an unspecific interaction with heparin. This is not the case with targeting mutants within the Nonbinder pool. A possible application for HSPG-independent AAV vectors lies in the therapy of hemophilia A or B (VandenDriessche and Collen et al. 2001; Chuah and Collen et al. 2001). Gene therapy for hemophilia demands a selective targeting of the liver while other organs are detargeted. In addition, a high expression level should be reached. The Nonbinder pool consists of a pool of mutants, which have in common their inability to bind to heparin and therefore their inability to be unspecifically requested in the liver. By AAV display selection on hepatocytes, a targeting mutant should be selectable out of this pool which is able to efficiently and receptor-specifically transduce

hepatocytes. Besides an efficient and specific cell entry, the mutant is also selected for optimized intracellular processes since only if a mutant is able to reach the nucleus progeny production will occur during selection. For this, an AAV mutant was to be obtained for efficient retargeting of a primary hepatocytic cell line kindly provided by Thierry VandenDriessche and Marinee Khim Chuah (Leuven, Belgium).

Selection procedure on Hepatocytes

Hepatocytes were seeded into cell dishes and one day later infected with the AAV Nonbinder library applying a GPC of 1. Cells were incubated for two more days in the presence of adenovirus to allow replication and packaging of mutants that infected the hepatocytes.

Four rounds of selection were performed whereas in the following rounds a GPC of 100 was used. Viral DNA was extracted from cell lysate after each round and amplified by PCR. The DNA was cloned into the AAV pRC vector and the plasmids were transformed into bacteria. At least one hundred single clones from each round were sequenced and analyzed.

Already after the second round of selection one sequence was remarkably outweighing all others.

	I. Round	II. Round	III.Round	IV. Round
VGDSTRD	14.1%	97.6% ▲	100% ▲	100% ▲
GGGVSTG	68%	0% ▼	0% ▼	0% ▼
TGASPRD	5.1%	0% ▼	0% ▼	0% ▼
others	12.8%	2.4% ▼	0% ▼	0% ▼

Table 2: Frequency of identified sequences

At least one hundred clones were sequenced and analyzed after round I to IV in selection of Nonbinder pool on hepatocytes. The amount of each selected sequence was set in relation to the total of sequences analyzed.

The strongly selected sequence VGDSTRD was cloned into an AAV helper plasmid and used to package the respective recombinant AAV mutant with GFP as transgene (HepIV) for transduction experiments.

Transduction experiments are currently carried out in our group in Cologne and in collaboration with the group of Thierry VandenDriessche in Leuven.

4.3. Discussion and Outlook

AAV Library can be divided into heparin/HSPG binders and Nonbinders with specific binding properties

The insertion of a peptide sequence into position 587 of the AAV capsid interferes with the binding site for the primary receptor of AAV, the heparan sulphate proteoglycan (HSPG) (Perabo et al. 2003). However, the binding to HSPG is only ablated in some mutants of the AAV library, not in all. Based on our hypothesis that peptides containing a net negative charge are prone to confer a HSPG non-binding phenotype and that a net positive charge can contribute to a restored heparin binding site, the coupled library was separated into a Binder and a Nonbinder pool.

This was done by a heparin column. The flow through was considered as Nonbinder pool and the eluted fraction as Binder pool. Clones from both fractions were then sequenced and analyzed as done for the libraries coupled through uptake and infection. Small amino acids seemed to be preferred. In the Binder pool a clear prevalence for the positively charged amino acid arginine was found and strikingly arginine mostly occurred in amino acid position 7 of the inserted sequence. The proximity of R588 to the last position of the inserted peptide could facilitate reconstitution of a functional motif if an arginine is present at this latter position. Insertion of positively charged peptides could lead to a HSPG binding phenotype by reconstituting a binding motif in combination with one of the original arginines or independently from them (compare **Chapter II, Figure 12**) explaining the good transduction efficiency, compared to rAAV/GFP, in the infection experiment described below (compare **Figure 3**). In contrast, the Nonbinder pool, showed clearly a higher frequency of negatively charged amino acids, especially of aspartic acid and glutamic acid. These observations strongly suggest that the presence of negative charges is deleterious for functional binding of AAV vectors to negatively charged heparin/HSPG.

To reflect the binding properties of the Binder and the Nonbinder pool, both libraries were packaged with scGFP as transgene and submitted to infection and uptake experiments on HeLa cells, expecting that the Binder pool would show higher binding affinity to HSPG and therefore higher transduction efficiencies. This experiment clearly demonstrated that, as expected with uptake, no major difference in the transduction efficiency of Binders and Nonbinders could be seen, but the Binders were clearly more potent in infecting HeLa cells than the Nonbinders, which underlines that the HSPG

binding plays a major role in AAV infection. Heparin competition experiments emphasized that the Nonbinder pool transduces cells independent from HSPG and that it provides clear advantages for selection of a real retargeting mutant since the natural HSPG binding phenotype is ablated.

***In vivo* biodistribution of Binder and Nonbinder pool**

Biodistribution studies with wildtype AAV2 showed that vector genomes were predominantly found in liver and spleen after tail vein injections in mice (Nathwani et al. 2001). Efforts have been made to identify receptor molecules on the cellular surface responsible for transduction of a certain cell type. For AAV-2, heparan sulphate proteoglycan (HSPG) has been shown to act as a primary receptor, next to its secondary receptors, $\alpha_v\beta_5$ integrin, human fibroblast growth factor receptor I (FGFR) and the hepatocyte growth factor receptor (HGFR). (Summerford and Samulski 1998; Summerford et al. 1999; Qing et al. 1999; Kashiwakura et al. 2005). Systematic deletions of potential heparin-binding motifs on the AAV capsid indicated that heparin binding is a prerequisite for efficient transduction of liver, but not kidney, heart or lung tissue (Kern et al. 2003).

In this study a heparin Binder and Nonbinder pool of the AAV library were isolated by heparin column chromatography and tested for their ability to transduce HepG2 cells, a hepatocellular carcinoma cell line. Producing recombinant AAV from both libraries and using a vector with a wild-type capsid (rAAV-RC) as control, all three viral preparations were able to transduce HepG2. rAAV-RC and Binder pool showed comparable transduction efficiencies. Since the addition of heparin completely abolished rAAV-RC mediated transduction (data not shown), it can be assumed that AAV infection of this cell line depends on HSPG binding. The mutants within the Nonbinder pool were unable to bind to HSPG. This suggests that capsid variants of the Nonbinder pool are able to transduce HepG2 cells by other means than HSPG binding, pointing towards new and specific ligand-receptor interactions.

C57/B6 mice were injected with rAAV-RC, Binder pool and the Nonbinder pool and analyzed for distribution of the vectors in the mouse organs. Thereby animals injected with rAAV-RC and Binder pool showed a comparable biodistribution with the highest vector DNA levels seen in spleen and liver.

In contrast, the Nonbinder pool showed a 102- and 31.8-fold reduction in vector DNA level in the spleen in comparison to rAAV-RC and Binder pool, respectively,

whereas in the liver an 8.8- and 6.7-fold reduction was detected. In addition, elevated levels of viral DNA in the blood were measured for the Nonbinder pool being consistent with the level of liver and spleen detargeting. This suggests an unspecific HSPG-dependent retention of rAAV and HSPG-binding of rAAV-targeting vectors in liver and spleen on the one hand and an HSPG-independent infection of cells in the liver mediated by some peptide insertions of the Nonbinder pool on the other hand. This hypothesis is in agreement with results previously obtained for a HSPG-knock-out mutant (Kern et al. 2003) and explains the liver and spleen detargeting observed for rAAV-MTP (White et al. 2004).

Furthermore, our studies revealed different ways by which an inserted peptide is able to confer HSPG-binding abilities to AAV targeting vectors (compare **Chapter II, Figure 12**) and may help to fine tune the peptide insertion in order to ablate HSPG binding and to obtain tissue specific vectors. This knowledge could also improve targeting mutants where R585 and/or R588 are substituted by other amino acids, since even in this case, some peptides (**Chapter II, Figure 12G**) would restore HSPG binding.

Nonbinder library allows the selection of heparin/HSPG-independent targeting mutants on Hepatocytes

To underline the advantages of a Nonbinder library for selection of heparin independent retargeting mutants, a selection on primary Hepatocytes was performed with the Nonbinder library. Heparin binding mutants and, therefore, mutants with the natural tropism were excluded from the selection in the first place. Four selection rounds were performed on Hepatocytes, starting with a strong selection pressure of one genomic particle per cell in the first round of selection. The mutant which became prominent already after the second round of selection on Hepatocytes, with the insertion sequence VGDSTRD, was cloned into the pRC AAV vector and packaged with self complementary GFP (scGFP) as transgene (HepIV). For rAAV packaged with scGFP higher transduction efficiencies were expected, since the self complementary transgene can bypass the rate-limiting step of second-strand synthesis (McCarty et al. 2001). This vector is now analyzed in comparison to recombinant AAV with unmodified capsid for its efficiency *in vitro* and *in vivo*.

Outlook

An optimally designed gene therapy vector is able to find and transduce only its target tissue after intravenous injection of this vector (systemic application). With recombinant AAV carrying wildtype capsids, most of the virus is filtrated from the blood by the liver, based on its interaction with HSPG, before the virus has even a chance to find the target tissue of choice. In addition, binding to HSPG expressing cells outside the liver like endothelia cells of the vessels will sequester AAV. Ideally, the targeting variant will only transduce the target tissue whereas no other tissues are affected. Retargeting of AAV vectors to the liver by means of specific but HSPG independent transduction of Hepatocytes makes sense for gene therapy applications where i) the transgene has to be solely expressed in the liver and ii) the transfer vector has to be optimized for efficient transgene expression. One example for such a gene therapy application is the delivery of Factor VIII and Factor IX for the treatment of hemophilia A and B patients, as it was shown that the highest expression levels of the blot clotting factors was achieved in cases where the rAAV vector was injected directly into the liver (compared to e.g. salvary glands, or muscle transduction) (VandenDriessche and Collen 2001). To make a hemophilia gene therapy more convenient for both, the patient and the physician, systemic application of gene therapy vectors encoding for Factor VIII and Factor IX finding only their target –the hepatocytes of the liver- by themselves, will be desirable.

Further experiments have to prove that the selected mutant HepIV results in a better transduction efficiency on hepatocytes and shows HSPG independent behaviour at the same time. In vivo biodistribution studies have to show the advantage of HepIV in comparison to wtAAV. For the selection of new mutants the selection pressure can be tightened by a negative selection round on HeLa cells, where the supernatant with non-infectious virions will be used for selection on Hepatocytes, further reinforcing the selection cell-specific mutants (targeting mutants which are able to infect HeLa cells independent of HSPG will be lost in this process).

5. Material and Methods

5.1. Material

Cell lines

Hek 293

Cell type: human embryonic kidney cells
Medium: DMEM with GlutaMAX1 (Invitrogen) + 10% FCS + 1% P/S
Origin: AG Hallek, Gene Center LMU München

HeLa

Cell type: human cervix carcinoma cell line
Medium: DMEM with GlutaMAX1 (Invitrogen) + 10% FCS + 1% P/S
Origin: AG Hallek, Gene Center LMU München

Hepatocytes

Cell type: human primary hepatocytes
Medium: DMEM with GlutaMAX1 (Invitrogen) + 10% FCS + 1% P/S
Origin: provided by Thierry Vandendriessche, Leuven, Belgium

HT29

Cell type: epithelial colon carcinoma
Medium: RPMI (Invitrogen) + 10% FCS + 1% P/S
Origin: ATCC cell bank

SVEC

Cell type: SV40-transformed axillary lymph node endothelia
Medium: DMEM (Invitrogen) + 10% FCS + 1% P/S
Origin: ATCC cell bank

MCF-7

Cell type: epithelial mammary gland adenocarcinoma
 Medium: MEM + 10% FCS + 1% P/S
 Origin: provided by Hauke Lilie, Halle

Viruses and vectorswtAAV

The recombinant AAV with unmodified capsid with GFP transgene will in the following be termed as rAAV/GFP. rAAV/GFP was packaged in 293 cells as described below.

Recombinant AAV

The modification and use of the rAAV vectors are described in the respective chapters. All rAAVs were packaged in 293 cells and purified by Iodixanol step gradient if not stated otherwise.

Wt-adenovirus was generated with the plasmid pG3602 and propagated in HeLa cells.

Bacteria

The used plasmids were amplified in *E. coli* TOP10F' and *E. coli* DH10B bacteria. For electroporation XL-1 Blue MRF were used.

TOP10F':

F' {*lacI^qTn10*(Tet^R)} *mcrA* Δ(*mrr-hsdRMS-mcrBC*) Φ80*lacZ*ΔM15 Δ*lacX74* *recA1*
araD139 Δ (*ara-leu*)7697 *galU galK rpsL endA1 nupG*
 (Invitrogen Corp., Karlsruhe)

DH10B:

F' *mcrA* Δ(*mrr-hsdRMS-mcrBC*) Φ80*lacZ*ΔM15 Δ*lacX74* *recA1 end A1 araD139* Δ (*ara-leu*)7697 *galU galK λ-rpsL nupG*
 (Invitrogen Corp., Karlsruhe)

XL-1 blue MRF

$\Delta(mcrA)183 \Delta(mcrCB-hsdSMR-mrr)173 endA1 supE44 thi-1 recA1 gyrA96 relA1 lac$ [F' *proAB lacI^qZ* $\Delta M15Tn10$ (Tet^r)].

(Stratagene, USA)

Plasmids

pRC, pRC99, pRC-Kotin and pGFP were provided by AG Hallek, Gene Center. pXX6-80 was kindly made available by Prof. Jude Samulski (Chapel Hill, University of North Carolina, USA).

pGFP

The pGFP plasmid is an AAV-based vector plasmid in which the AAV ITR sequences are flanking the hygromycin selectable marker gene controlled by the thymidine kinase promoter and the *Aequorea victoria* Green Fluorescence Protein (GFP) gene regulated by the cytomegalovirus promoter. pGFP was generated by inserting the Asp718-Not I fragment of pEGFP-N1 (Clontech) into the Asp718-Not I sites of psub/CEP4 (Sal invers). psub/Cep4 (Sal invers) is a derivative of psub201(+) (Samulski et al. 1987), which was digested with Xba I, blunt ended and ligated to blunt ended 3923 bp Sal I-Nru I-Fragment of pCEP4 (Sal inverse). pCEP4 (Sal inverse) differs from pCEP4 (Invitrogen) by inversion of the Sal I (8)-Sal I (1316)-fragment.

pRC

The pRC plasmid was constructed as previously described (Girod et al. 1999). Briefly, the 4.5 kb Xba I-fragment of psub201(+) (Samulski et al. 1987), containing the *rep* and *cap* ORFs of AAV was subcloned into the Pst I and BamH I sites of pSV40oriAAV (Chiorini et al. 1995).

pRC99

Variant of pRC containing a multiple cloning site in position 587, cleavable by AscI and MluI.

P587Lib7

AAV library plasmid, generated as described in Perabo et al. 2003

pRC-Kotin

pRC lacking ITRs with an additional single cleaving site for SnaBI.

pXX6-80

Adeno-Helperplasmid: Expression plasmid for the adenoviral proteins VA, E2A und E4, which are needed for packaging of AAV next to E1a und E1b.

Enzymes

Benzonase	Merck, Darmstadt
Proteinase K	Sigma, Deisenhofen

All restriction enzymes were obtained by New England Biolabs, Schwalbach

Antibodies

A20 (AAV2-capsid antibody)	DKFZ Heidelberg, Arbeitsgruppe Prof. Dr. J. Kleinschmidt
B1 (AAV VP-specific Antibody)	DKFZ Heidelberg, Arbeitsgruppe Prof. Dr. J. Kleinschmidt
B3 (Lewis)-antibody	University of Halle, Hauke Lilie
Omalizumab (Xolair [®])	Novartis, Germany
Mouse IgG1 Isotype Control	R&D Systems, Germany
Monoclonal Antibody to CETP	Acris Antibodies, Hiddenhausen

Synthetic Oligonucleotides

All synthetic oligonucleotides were obtained by Metabion in Martinried.

Chemicals and other Material

Agarose	Sigma, Deisenhofen
Ampicillin	Sigma, Deisenhofen
Benzonase	Merck, Darmstadt

Biomax Light Film	Kodak, Stuttgart
Blocking-Reagenz Boehringer Mannheim	Boehringer, Mannheim
DIG-DNS Labeling and Detection Kit	Boehringer, Mannheim
DMEM mit GlutaMAX1	Invitrogen Corporation, Karlsruhe
DMSO (Dimethylsulfoxid)	Merck, Darmstadt
EDTA	AppliChem, Darmstadt
Ethidiumbromid	Roth, Karlsruhe
Formamid	Fluka ChemieAG, Buchs, Schweiz
FCS (Fetal Calf Serum)	Invitrogen Corporation, Karlsruhe
HEPES	Roth, Karlsruhe
λ DNA Hind III	New England Biolabs, Schwalbach
Molecular Weight Marker for 1kb	New England Biolabs, Schwalbach
Molecular Weight Marker λ Hind III	New England Biolabs, Schwalbach
Nylonmembran	Roche, Mannheim
OptiPrep TM (Iodixanol)	Sigma, Deisenhofen
PBS	Invitrogen Corporation, Karlsruhe
Primer	Metabion, Martinsried
Restriktion enzymes	New England Biolabs, Schwalbach
RPMI 1640 mit GlutaMAX1	Invitrogen Corporation, Karlsruhe
SDS (Natriumdodecylsulfat)	Merck, Darmstadt
SSC (Salines Sodium Citrate)	Merck, Darmstadt
Tris	Merck, Darmstadt
Trypsin-EDTA	Invitrogen Corporation, Karlsruhe

Primers

4066 BACK

5'- ATG TCC GTC CGT GTG TGG -3'

3201 FOR

5'- GGT ACG ACG ACG ATT GCC -3'

BsiW back

5'- TAC CAG CTC CCG TAC GTC CTC GGC -3'

New SnaBI 1

5'- CGC CAT GCT ACT TAT CTA CG -3'

New SnaBI 2

5'- AA GAT TAA CCC GCC ATC C -3'

For the PCR cloning of the AAV Cys mutants, pRC backbone and the following primers were used:

Outer primer: 4066Back and 3201For

Inner primer:

S452C For 5'-AACACTCCATGCGGAACCA-3'

S452C Back 5'-GTGGTTCCGCATGGAGTGT-3'

G453C For 5'-CACTCCAAGTTGCACCACCA-3'

G453C Back 5'-TGGTGGTGCAACTTGGAGTG-3'

N587C For 5'-CAGAGAGGCTGCAGACAAG-3'

N587C Back 5'-GCTTGTCTGCAGCCTCTCT-3'

The mutants G265C, S384C, and A667C were cloned by Florian Kreppel in Ulm.

Standards and Kits

DNeasy®Tissue Kit	Qiagen, Hilden
EndoFree® Plasmid Kits	Qiagen, Hilden
PCR Purification Kit	Qiagen, Hilden
Gel Extraction Kit	Qiagen, Hilden
Light-Cycler-FastStart DNA Master SYBR Green I	Roche, Mannheim

Buffer and Solutions

Ampicillin: Stock Solution: 50 mg/ml in H₂O, sterile filtered

Used concentration: 50 µg/ml

EB-Puffer: Tris/HCl, pH 8.0 10 mM

10x TBE: Tris 890 mM
Boric Acid 890 mM
EDTA 20 mM

Freeze Medium: FCS 50 %
DMEM 40 %
DMSO 10 %

15 % Iodixanol-Solution 1x PBS 10 %
MgCl₂ 1 mM
KCl 2.5 mM
NaCl 1 M
Optiprep 15 %
Phenolrot 0.075 %
H₂O ad 500 ml

25 % Iodixanol-Solution 1x PBS 10 %
MgCl₂ 1 mM
KCl 2.5 mM
Optiprep 25 %
Phenolrot 0.01 %
H₂O ad 500 ml

40 % Iodixanol-Solution 1x PBS 10 %
MgCl₂ 1 mM
KCl 2.5 mM
Optiprep 40 %
H₂O ad 500 ml

60 % Iodixanol-Solution MgCl₂ 1 mM
KCl 2.5 mM
Optiprep 60 %
Phenolrot 0.025 %
H₂O ad 500 ml

Loading buffer Agarosegel	Glycerin	50 %
	EDTA, pH 8.0	100 mM
	Bromphenolblau	0.25 %
	Xylencyanol FF	0.25 %
Loading buffer SDS gel	Tris/HCl pH 6.8	200 mM
	Glycerol	25 %
	SDS	5 %
	Bromphenolblau	0.025 %
	β -Mercapto EtOH	0,5 M
LB-Medium:	Bacto Trypton	1 %
	Yeast Extract	0.5 %
	NaCl	0.5 %
	NaOH	1 mM
	Bacto Agar (bei Platten)	1.5 %
Lysis buffer	NaCl	150 mM
	Tris/HCl, pH 8.5	50 mM
Transfection buffer (HBS) for Virus production:	HEPES, pH 7.2	50 mM
	NaCl	280 mM
	Na ₃ P	1.5 mM
CaCl₂-solution	CaCl ₂	250 mM
10xTBS	Tris pH8.0	100 mM
	NaCl	1.5 M
TBST	TBS	100 ml
	Tween20	0.5 ml
	ad H ₂ O	1000 ml

Equipment

For the equipment used, please refer to the corresponding chapters.

5.2. Methods

General Methods

Cultivation of Microorganism (Bacteria)

Cultivation on Agar plates

Bacteria were plated onto a sterile LB-agar plate with a sterile Drygalski-spatula and cultivated over night at 37°C.

For production of agar plates, LB medium was poured after sterilization by autoclave into sterile Petri plates and left for cooling. Plates were kept at 4°C.

For selection of plasmids the corresponding antibiotic was put into the medium before pouring the plates.

Liquid bacteria culture

Single bacteria colonies were cultivated in 5ml LB-medium and the corresponding antibiotic over night at 37°C and 220 rpm. Over night cultures were then used for inoculation of larger cultures or used for Mini preps.

Preparation and analysis of nucleid acids

Isolation of plasmids from bacteria

Isolation by QIAGEN Mini Prep Kit

Plasmids for sequencing were prepared and purified by QIAGEN Mini Prep Kit using the Mini prep protocol using a microcentrifuge.

Endotoxin-free isolation by QIAGEN Mega prep kit

Plasmids for packaging of wtAAV and rAAV were prepared and purified by QIAGEN EndoFree Mega Kit using the QIAGEN EndoFree Plasmid Mega protocol.

Isolation of DNA from cells with QIAGEN DNeasy Tissue Kit

DNA from cell lysates was extracted and isolated using the QIAGEN DNeasy Tissue Kit. The kit was applied as described in the protocol for cultured from animal cells.

Separation of DNA by electrophoresis in agarose gel

For preparative separation and control of DNA size after digest with restriction enzymes, DNA and DNA fragments were separated in agarose gel by electrophoresis.

For this 0.5 - 1% agarose was heated in Tris-Borat-EDTA- (TBE; 89mM Tris, 89mM boric acid, 2mM EDTA) buffer and ethidium bromide was added for detection of DNA. The hot gel was poured into the gel chamber and left for cooling. 0.1 volumes of loading buffer was added to the DNA samples and the samples were put onto the gel in TBE buffer and run at 60 – 120 Volt. DNA was made visible by UV absorption of ethidium bromide at 366nm. For determination of DNA fragment size a DNA marker was run with the samples.

Isolation and purification of DNA with QIAquick Gel Extraction Kit

For isolation and purification of DNA from agarose gels the QIAquick Gel Extraction Kit was applied. DNA was prepared using the QIAquick Gel Extraction Kit protocol using a microcentrifuge.

Purification of DNA by QIAGEN PCR Purification Kit

For purification of DNA from enzymatic reactions the QIAquick PCR Purification Kit was applied using the QIAquick PCR Purification Kit protocol using a microcentrifuge.

Determination of DNA concentration

Nucleid acid concentrations were determined by photometer analysis and evaluated by computer. The ratio of OD260/OD280 determines the purity of DNA with ratio of 1.8-2.0 for good purity. Ratios below 1.8 point to contaminations through protein.

Enzymatic reactions with plasmids and DNA-fragments

Digestion of DNA with restriction enzymes

The cleavage of DNA with restriction enzymes was used for vector cloning and for control cleavage of the obtained insertions or deletions. For complete cleavage 0.2 to 10 µg DNA were used with 1 to 30 U enzyme. DNA was incubated for 1.5 – 2 h at the given temperature in 20 to 50 µl volume. The necessary conditions like restriction buffer, temperature and restriction activity was obtained by the manufacture's manual and adapted. Cleavage was controlled by agarose gel analysis.

Dephosphorylation with alkaline phosphatase

To avoid intra molecular religation of linearised vector plasmids during cloning, the 5'-phosphoric acid was cleaved by alkaline phosphatase (CIP). After restriction cleavage 1 µl of Calf Intestinal Phosphatase (CIP) was added to a total volume to 50 µl sample and incubated at 37°C for 30 min. For further reactions CIP was then removed by DNA purification with the QIAGEN PCR Purification Kit.

Ligation of DNA-fragments

T4-DNA-Ligase was used for cloning of DNA fragments and plasmids. Usually 100 -200 ng dephosphorylated plasmid backbone was ligated with 3 to 5 times more molar insert. Ligation was carried out in a total volume of 20 µl with ligase buffer and 10 U T4-Ligase. Ligation was incubated at 16°C over night or at room temperature for 2 h. After ligation the ligase was inactivated by incubation at 65°C for 10min and the DNA was submitted to dialysis for 3 h and then transformed into electro competent bacteria. As negative control a CIP treated plasmid backbone incubated without the insert was used.

Electroporation of bacteria

Ligated plasmids were transformed into bacteria by electroporation. 5µl of ligated DNA was mixed with 40µl MRF XL-1 Blue bacteria and submitted to BioRad cuvettes. Electroporation conditions were set to 1.85kb (600Ohm) and the electroporated DNA was then diluted in 1ml LB medium without antibiotics and submitted to shaking at 37°C for 1h. After that the bacteria containing medium was diluted 1:1000 and distributed onto agar

plates containing Ampicillin. Plates were controlled for colonies the next day after incubation at 37°C over night.

DNA-Sequencing

Sequence analyses for control of cloned plasmids were carried out by Laboratory for Functional Genome Analysis (LaFuga) in the Gene Center. Sequence analysis for the single insertion sequences obtained in the selection procedure was carried out by AGOWA, Berlin. For this, single bacteria colonies were picked and resuspended in 96well plate in 100µl LB medium and sent to the AGOWA.

Cultivation of cell lines

Cell Culture

All cell lines mentioned in Material were kept at 37°C and 5% CO₂ in the respective medium. All cell lines used were adherent cells and were kept as "monolayer"-cultures in plastic cell culture vessels (TPP). Cells were splitted with Trypsin after washing with PBS and medium was changed at least every three days.

Cell stocks

About 10⁷ cells were suspended in cold freeze medium, distributed in 1ml Cryo-tubes (Nunc) and cooled on ice for at least one hour. Stocks were then cooled in the -80°C freezer and later stored in liquid nitrogen.

For recultivation Cryo-tubes were thawed in warm water and cells were quickly suspended in the according medium. Medium was changed after one day to remove remainders of DMSO.

Adenovirus-free Production of AAV vector particles and purification by Iodixanol density gradient

The packaging and purification of AAV vectors were carried out under the laminar flow and only sterile buffers were used.

Cells for packaging

For packaging HEK 293 cells were used in 15cm² cell culture plates, 15 plates for one produced vector. 24h before transfection 7.5x10⁶ 293 cells were seeded into plates.

Transfection

The medium was changed 3hs before transfection. The transfection was carried out in Ca₃(PO₄)₂ medium at 70% confluent cells. For each plate a solution of 1ml 250mM CaCl₂ with 7.5µg helperplasmid (e.g. pGFP as transgene), 7.5µg vector plasmid (e.g. pRC for packaging of AAV with wt capsid) and 22.5µg Adeno-helper plasmid pXX6-80 was prepared and 1ml transfection buffer HBS was added (for packaging of the AAV library 15µg of library plasmids were transfected with 22,5µg pXX6-80). The solution was incubated for 2min at room temperature and then pipetted onto the plate while cautious mixing with the medium. Cells were incubated for 24h at 37°C and 5%CO₂ and then the medium was changed to DMEM with 2% FCS and cells were kept for another 24h before harvesting.

Harvest of virus producing cells

293 cells were harvested with a cell lifter, transferred into GSA tubes and centrifuged at 3000g and 4°C for 10min. The cell pellet was resuspended in 2.5 ml lysis buffer and objected to three rounds of freeze and thaw cycles. Cells were again pelleted by centrifugation and the supernatant was used for further purification.

Purification of AAV vectors by Iodixanol density gradient

The supernatant after cell lysis was centrifuged again for greater purity in SS34 tubes and then transferred to ultra centrifugation tubes (26x77mm, Beckman). Iodixanol solutions of different concentrations were layered beneath the virus containing solution. By this an Iodixanol gradient was created, with 6ml 60% on the bottom, 5ml 40%, 6ml 25% and 9ml 15% going upwards and the virus solution on top. The gradient was centrifuged in an ultra centrifuge at 65.000rpm for 1.5h and at 18°C. The 40% phase was then extracted with a cannula by puncturing the tube underneath the 40% phase and allowing the solution to drip

into a Falcon tube until the 25% phase was reached. Genomic and capsid titers were then determined for experiments or the 40% phase was objected to further purification by gel filtration when necessary.

Evaluation of AAV titers

Evaluation of AAV genomic titers Dot Blot

For determination of the genomic titer, the virus samples were digested with proteinase K (Merck). For this 2 to 10 μ l of virus sample were added to 95 μ l PK buffer (75mM Tris pH8.0, 25mM EDTA) and ad 180.5 μ l PBS. The sample was incubated at 70°C for 10min and 9.5 μ l proteinase K was added and incubated at 50°C. After 2h 10 μ l NaOH were added and the samples were diluted in a 96well plate 1:2 and incubated for 1h at 37°C. Samples were blotted to nylon membrane using a Dot Blot apparatus. The membrane was cross-linked by incubation at 80°C for 2h or 15min at 120°C. The membrane was treated with SDS-hybridization solution for 15min at 42°C and then incubated with SDS-hybridization solution plus the DNA probe (the labeling of the DNA probes was conducted as recommended by the manufacturer in the standard protocol of the DIG DNA labeling kit (Roche, Mannheim)) over night at 42°C. The membrane is washed and then incubated with blocking buffer (blocking reagent in maleic acid) for 30min at room temperature. The blocking buffer is exchanged with 1.5 μ l anti-DIG antibody (Roche) in blocking buffer and incubated for 1h at room temperature. The membrane is washed again and the signals are detected by incubation of the membrane in detection buffer (100mM Tris pH9.5 and 100mM NaCl) and CSPD for 20min at 37°C. The membrane is exposed to film and signals are visible on the developed film and compared to the according standard.

Evaluation of AAV genomic titers by Light Cycler PCR

For determination of genomic titers 50 μ l of virus solution were used for isolation of viral DNA by DNeasy Tissue Kit. DNA was eluted in 200 μ l Tris/pH 7.5, differing from the DNeasy Tissue Kit protocol. 2 μ l viral DNA were applied to the Light Cycler PCR Master Mix using the Light Cycler FastStart DNA Master SYBR Green I Kit. Primers were used according to the vector preparation (GFP-primer for GFP transgene and 4066Back/3201For-primer for the AAV library). Titters were determined by computer evaluation using the program provided with the Roche Light Cycler 2.0 and compared to an according standard.

Evaluation of AAV capsid titers by A20 ELISA

For determination of capsid titers 10 to 20 μ l of virus solution were coated to 96-well plates in serial dilution at 4°C over night. Wells were then washed and blocked with 3% BSA/5% Saccharose/0.05% Tween20 blocking buffer for 2h at room temperature. Bound virions were incubated with 50 μ l of the AAV recognizing antibody A20, derived from hybridom supernatant (kindly provided by the group of Jürgen Kleinschmidt) for 1h at room temperature. Wells were washed 3x with PBS/0.05% Tween20 and A20 was incubated with anti-mouse IgG-Biotin (Dianova, 1:50000) for 1h at room temperature. Wells were washed again and incubated with Streptavidin-POD antibody (Dianova, 1:1000) for 1h at room temperature and quantified by an enzymatic reaction (Tetramethylbenzidin (TMB) in 100 μ l DMSO and 10ml 0.1M NaOAc pH6.2 and 1 μ l H₂O₂ 30%). OD was determined by an ELISA reader and the titers were calculated using Origin 6.0, compared to an according standard.

Established Methods

Conjugation of AAV-Glu and SIG peptide

The conjugation of AAV-Glu to the SIG peptide was performed in 0.02M Tris/HCl (pH 7.4)/ 200mM NaCl/ 5% Glycerol/ 1mM CaCl₂/ 1.6mM GSSG/ 0.4mM GSH. The SIG peptide, designed with and without a linker region, was incubated with AAV-Glu at a 10-fold molar excess for 5h at 10°C. After coupling the reaction mixture was dialyzed against ice cold PBS over night in Slide-A-Lyzer cassettes (Pierce). The genomic titers were determined by Dot Blot.

Conjugation of AAV-Glu and B3 (Lewis)-antibody using DTP

For conjugation with the B3 (Lewis)-antibody AAV-Glu was purified by anion exchange chromatography and eluted in the reaction buffer (25mM Na₂HPO₄/ 25mM KH₂PO₄ (pH8)/ 2mM EDTA/ 0.5M NaCl) and dialyzed against the same buffer without NaCl. B3-antibody was also dialyzed against 25mM Na₂HPO₄/ 25mM KH₂PO₄ (pH8)/ 2mM EDTA and both were incubated with 1mM GSH for 2h. Both proteins were shifted to pH 5.0 by addition of buffer with pH 4.5 and dialyzed over night against 25mM Na₂PO₄/ 25mM KH₂PO₄ (pH 4.5)/ 2mM EDTA. The pH was shifted back to pH 8.0 by addition of buffer pH 8.0. B3-antibody was then incubated with 10-fold molar excess of Dithiopyridin

(DTP) for 1h at pH 8.0. Excess DTP was removed by dialysis against the buffer. For conjugation AAV-Glu and the activated B3-antibody were incubated at a molar ratio of 1:1 for 4h at 20°C. Uncoupled and coupled AAV-Glu was separated by gefiltration and eluted in PBS. Fractions were collected, genomic titers determined by Dot Blot and tested for transduction efficiency on MCF-7 cells.

Transduction experiments Chapter I

For testing if coupling was successful, the coupled vectors were submitted to transduction experiments. AAV-Glu coupled with SIG peptide was tested on SVEC and AAV-Glu coupled to B3-antibody was tested on MCF-7 cells.

The respective cells were seeded into 24 well plates, 1×10^5 or 2×10^5 in 1ml of medium. Cells were rested for 24h and then counted. According to the cell number, the respective genomic particles per cell were used for transduction after medium change. Cells were incubated for 48h at 37°C and then washed once with PBS and harvested by Trypsin detachment. After pelleting the cells were washed again and then resuspended in 500 μ l PBS. GFP expression was determined in FACS analysis.

Conjugation with Oregon Green

For conjugation with Oregon Green (Molecular Probes), the protocol for Thiol-Reactive Probes from the Molecular Probes handbook was used. Briefly the vector was purified by gel filtration and eluted with PBS. 10-fold molar excess of reducing agent TCEP was added and then incubated with 10-fold molar excess of the Oregon Green dye for 2h at room temperature in the dark. Excess dye was removed by dialysis against PBS using Slide-A-Lyzer cassettes.

Western Blot

Proteins were separated in a reducing SDS gel, consisting of a 4% Polyacrylamide (PAA) gel and a 10% PAA separation gel. Loading buffer (Fermentas) with β -MercaptoEtOH was added to the samples and heated at 95°C for 5min for denaturation of the proteins. Rainbow Marker (Amersham Biosciences) was used as marker. The gel was run at 20mA. The proteins were then transferred to a nitrocellulose membrane (Protan) in a semi-dry transfer chamber.

For detection of AAV VP proteins, the membrane was developed with B1 antibody. In detail, the membrane was blocked with 0.2% I-Block in TBST for 1h at room temperature and then incubated with B1 antibody 1:20 in blocking buffer. The membrane was washed 3x with TBST and then incubated with anti-mouse IgG-Peroxidase (Sigma) 1:5000 in blocking buffer at room temperature for 1h. The membrane was washed 3x in TBST and 1x in H₂O and then developed using the Super Signal West Pico developing solution by Pierce. The membrane was wrapped in transparent foil and the signal was detected by Kodak film and developed in the dark room.

Silver Staining

For detection of proteins by silver staining, the proteins were separated in a reducing SDS gel as described above. The gel was fixed in a solution of 250ml EtOH, 60ml acetic acid, and 250 μ l formaldehyde 37% ad 500ml H₂O for 1h. The gel was washed 3x in 50% EtOH for 20min and then pretreated for 5-10sec in 500ml H₂O with 0.1g Na-thiosulphate. The gel was again washed 3x in H₂O for 20min and then stained in freshly produced 100ml H₂O with 0.2g AgNO₃ and 73 μ l formaldehyde 37% for 10min. The gel was washed in H₂O for 10sec and the developed in 100ml H₂O containing 0.4mg Na-thiosulphate, 50 μ l formaldehyde 37%, and 6g Na-carbonate till protein bands were visible. The development was stopped by 250ml EtOH and 60ml acetic acid ad 500ml H₂O for 10min. and then dried and conserved.

Transduction experiments Chapter II

The titers of the applied vectors were determined by Light Cycler PCR (genomic titer) or by A20 ELISA (capsid titer). For transduction, cells were seeded into cell culture plates (TPP), 4x10⁵ cells in 24 wells in 1ml of medium. Cells were rested for 24h and infected after the medium was changed. For the amount of vector please refer to the corresponding chapters. Usually genomic particles per cells (GPC) were used. Cells were incubated for 48h at 37°C.

For uptake the wells were coated with 100 μ l A20 antibody (hybridoma supernatant) and incubated for 1h at room temperature or at 4°C over night. Wells were washed twice with 300 μ l PBS and then incubated with blocking solution (Milk Powder 1%/Tween20 1%) for 2h. The vector was diluted in 200 μ l blocking solution and incubated for at least 1h at room

temperature. Wells were washed with 500 μ l PBS/1%Tween20 at least 15x. HeLa cells were seeded into the wells in 1ml medium and incubated for 48h at 37°C.

Cells were washed once with PBS and then harvested by Trypsin (200 μ l/well) detachment. The cells were washed again with PBS and then resuspended in 500 μ l PBS for FACS analysis (FacsCalibur, Beckman).

Uptake and infection experiments

For uptake and infection experiments, as well as for the selections, 15cm² cell culture plates (TPP) were used. The genomic titer of the AAV library was determined by Light Cycler PCR.

For infection 2x10⁶ HeLa cells were seeded in 15ml medium in cell culture plates and rested for 24h. Medium was changed and the cells were infected with genomic particles per cell (GPC) of 10, 100 and 1000 and incubated for 48h.

For uptake the wells were coated with A20 antibody for 1h at room temperature or at 4°C over night. Plates were 2 – 3 times washed with PBS/Tween20 1% and then incubated with 10ml blocking buffer (Milk Powder 10%/Tween20 1%) at room temperature for 2h. The AAV library was then, diluted in 5ml blocking buffer submitted to the plates and incubated for 1 – 2 h at room temperature. Plates were then washed with 10ml PBS/Tween20 1% at least 15 – 20 times and 4x10⁶ HeLa cells were seeded into the plates in 10ml medium. 10ml fresh medium was added the next day and the cells were incubated at 37°C and 5% CO₂ for another 24h. Cells were then harvested by scratching and the cell pellet was washed once with PBS and then resuspended in 500 μ l lysis buffer. The pellet was submitted to three rounds of freeze and thaw cycles and the supernatant was used for further analysis. Compare **Cloning of insertion sequences of the AAV library into AAV vectors for sequencing.**

Selection of AAV library mutants on solid phase antibodies

For selection the respective antibodies were coated to 15cm² cell culture plate (TPP) at a concentration of 10 - 50 μ g/15cm² per plate at 4°C over night. Plates were 2 – 3 times washed with PBS/Tween20 1% and then incubated with 10ml blocking buffer (Milk Powder 10%/Tween20 1%) at room temperature for 2h. The AAV library was then, diluted in 5ml blocking buffer submitted to the plates and incubated for 1 – 2 h at room temperature. Plates were then washed with 10ml PBS/Tween20 1% at least 15 – 20 times

and 4×10^6 HeLa cells were seeded into the plates in 10ml medium. 10ml fresh medium was added the next day and the cells were incubated at 37°C and 5% CO₂ for another 24h. Cells were then harvested by scratching and the cell pellet was washed once with PBS and then resuspended in 500µl lysis buffer. The pellet was submitted to three rounds of freeze and thaw cycles and the supernatant was used for further analysis. Compare **Cloning of insertion sequences of the AAV library into AAV vectors for sequencing.**

Cloning of insertion sequences of the AAV library into AAV vectors for sequencing

DNA from 50µl from the supernatant after lysis and centrifugation was extracted by Qiagen DNeasy Tissue Kit and used for determination of genomic titers and amplification by PCR for further analysis. For genomic titers see **Evaluation of AAV titers by Light Cycler PCR**. For sequence analysis the DNA was amplified by PCR with the high fidelity Platinum Pfx DNA polymerase (Invitrogen) using 2µl each of the primers New SnaBI 1 and BsiWI Back (each 10mM), usually with 5µl of the isolated DNA in a total volume of 50µl. After PCR the DNA was purified by PCR Purification using the QIAGEN PCR Purification Kit, eluting the DNA in 40µl NEB4 buffer diluted 1:10 in two steps. 2µl were run on an agarose gel to control the PCR product. The purified DNA was then digested with SnaBI according to the manufacturer's manual (1.5-2h at 37°C) in a total volume of 50µl. For digestion with BsiWI the DNA was purified again by PCR Purification Kit and eluted in 40µl NEB3, diluted 1:10. BsiWI was applied according to the manufacturer's manual (1.5-2h at 55°C) and again purified by PCR Purification. AAV backbone, pRC-Kotin without ITR's or pwt with ITR's, was digested at the same time, 1µl of CIP was added before purification and incubated for 1h at 37°C for dephosphorylation. DNA concentration was determined by photometer and ligated with the AAV backbone, in most cases the pRC-Kotin, as described in **Ligation of DNA fragments**. After inactivation of Ligase activity, the ligated DNA was desalted by dialysis against H₂O for 3h and then electroporated into XL-1 Blue MRF bacteria. After electroporation bacteria were suspended in 1ml of LB medium without antibiotics and put into the shaker for 1h. Bacterial solution was then diluted 1:1000 and applied to agar plates and incubated over night at 37°C. Single colonies were picked the next day and prepared for sequencing as described in **DNA-Sequencing** and sent to AGOWA. The sequences obtained by AGOWA were evaluated by computer using BioEdit.

For the statistical verification of the frequency of the amino acids the χ^2 -test was applied.

Antibody-specific Dot Blot

The AAV library mutants fished in selection on Omalizumab or anti-KLH, were packaged with GFP transgene and purified by Iodixanol density gradient and the capsid titers were determined by A20 ELISA. 1×10^5 and 5×10^5 capsid particles were dotted to a nitrocellulose membrane (Hybond, Amersham) using Dot Blot equipment. As positive control IgE antibody and KLH peptide are dotted, respectively, using $1 \mu\text{g}$ protein in the first dilution step. The membrane is blocked in 5% Milk Powder/ PBS/ 1% Tween20 for 1h at room temperature and then incubated with Omalizumab or anti-KLH antibody, respectively, in a 1:1000 dilution in blocking solution overnight at 4°C . The membrane is washed 3x in PBS/1%Tween20 for 5min and then incubated with secondary antibody anti mouse IgG γ HRP control in a dilution of 1: 20000 for 1h at room temperature. The membrane is again washed with PBS/1%Tween20 and then developed in ECL advance solution (Amersham) for 5min at room temperature. The membrane is exposed to Hyperfilm (Amersham) and developed. After developing the membrane is stripped with a solution of 100mM Glycin pH2.5, 3x for 15min at room temperature and 3x in PBS/1%Tween20 for 15min at room temperature. The membrane is then again incubated with A20 antibody for detection of AAV capsids for 1h at room temperature. The membrane is washed and then incubated with secondary antibody anti mouse IgG γ HRP control in a dilution of 1: 20000 for 1h at room temperature and developed in ECL advance aolution (Amersham) and exposed to hyperfilm as above.

6. Abbreviations

aa	amino acid	BSA	bovine serum albumine
AAV	adeno-associated virus, specifically adeno-associated virus type 2	bp	base pair
Ab	antibody	Cap	capsid protein
Ad	Adenovirus	CLL	chronic lymphocytic leukemia
		CMV	cytomegalovirus
		Da	Dalton
		DMEM	Dulbecco's Modified Eagle Medium
<u>Amino acids</u>		e.g.	for example (Lat.: <i>exempli gratia</i>)
A (Ala)	alanine		
C (Cys)	cysteine	ELISA	enzyme-linked immunosorbent assay
D (Asp)	aspartate		
E (Glu)	glutamate	FACS	fluorescence-activated cell sorting
F (Phe)	phenylalanine		
G (Gly)	glycine	FCS	fetal calf serum
H (His)	histidine	FGFR	fibroblast growth factor receptor 1
I (Ile)	isoleucine		
K (Lys)	lysine	Fig.	figure
L(Leu)	leucine	GFP	green fluorescence protein
M (Met)	methionine	GPC	genomic particles per cell
N (Asn)	asparagine	h	hour
P (Pro)	proline	HGFR	hepatocyte growth factor receptor
Q (Gln)	glutamine		
R (Arg)	arginine	HSPG	heparan sulphate proteoglycan
S (Ser)	serine	ITR	inverted terminal repeat
T (Thr)	threonine	kb	kilobases
V (Val)	valine	mAb	monoclonal antibody
W (Trp)	tryptophan	KLH	keyhole limpet hemocyanin
Y (Tyr)	tyrosine		

MHC	major histocompatibility komplex	Rep	viral regulatory protein
min	minute	RT	room temperature
MP	milk powder	SDS	sodium dodecyl sulphate
MOI	multiplicity of infection	Strep-POD	Streptavidin-Peroxidase
NPC	nuclear pore complex	TRS	terminal resolution site
nt	nucleotide	VP	viral protein (AAV capsid protein)
ori	origin of replication	wtAAV	wild-type AAV
ORF	open reading frame		
PEG-mal	polyethylenglycol-maleimide		
rAAV	recombinant AAV		

7. References

- Agbandje, M., Kajigaya, S., McKenna, R., Young, N. S., and Rossmann, M. G. (1994). The structure of human parvovirus B19 at 8 Å resolution. *Virology* **203**(1), 106-15.
- Agbandje-McKenna, M., Llamas-Saiz, A. L., Wang, F., Tattersall, P., and Rossmann, M. G. (1998). Functional implications of the structure of the murine parvovirus, minute virus of mice. *Structure* **6**(11), 1369-81.
- Atchison, R. W., Casto, B. C., and Hammon, W. M. (1965). Adenovirus-associated defective virus particles. *Science* **149**, 754-756.
- Bartlett, J. S., Kleinschmidt, J., Boucher, R. C., and Samulski, R. J. (1999). Targeted adeno-associated virus vector transduction of nonpermissive cells mediated by a bispecific F(ab'γ)2 antibody. *Nat Biotechnol* **17**(2), 181-6.
- Bartlett, J. S., Wilcher, R., and Samulski, R. J. (2000). Infectious entry pathway of adeno-associated virus and adeno-associated virus vectors. *J Virol* **74**(6), 2777-85.
- Berns, K. I., Bergoin, M., Bloom, M. E., Lederman, M., Muzyczka, N., Siegl, N., Tal, G., and Tattersall, P. (2000). Parvoviridae. VIIth Report of the International Committee on Taxonomy of Viruses. In "Virus Taxonomy: Classification and Nomenclature of Viruses." (M. H. V. van Regenmortel, C. M. Fauquet, D. H. L. Bishop, E. B. Carstens, M. K. Estes, S. M. Lemon, J. Maniloff, M. A. Mayo, D. J. McGeoch, C. R. Pringle, and R. B. Wickner, Eds.), pp. 311-323. Academic Press, San Diego.
- Berns, K. I., and Giraud, C. (1996). Biology of adeno-associated virus. *Curr Top Microbiol Immunol* **218**, 1-23.
- Berns, K. I., and Linden, R. M. (1995). The cryptic life style of adeno-associated virus. *Bioessays* **17**(3), 237-45.
- Bessis, N., GarciaCozar, F. J., and Boissier, M. C. (2004). Immune responses to gene therapy vectors: influence on vector function and effector mechanisms. *Gene Ther* **11 Suppl 1**, S10-7.
- Blacklow, N. R., Hoggan, M. D., Kapikian, A. Z., Austin, J. B., and Rowe, W. P. (1968). Epidemiology of adenovirus-associated virus infection in a nursery population. *Am J Epidemiol* **88**(3), 368-78.
- Blacklow, N. R., Hoggan, M. D., Sereno, M. S., Brandt, C. D., Kim, H. W., Parrott, R. H., and Chanock, R. M. (1971). A seroepidemiologic study of adenovirus-associated virus infection in infants and children. *Am J Epidemiol* **94**(4), 359-66.
- Bleker, S., Sonntag, F., and Kleinschmidt, J. A. (2005). Mutational analysis of narrow pores at the fivefold symmetry axes of adeno-associated virus type 2 capsids reveals a dual role in genome packaging and activation of phospholipase A2 activity. *J Virol* **79**(4), 2528-40.
- Brinkmann, U., Pai, L. H., FitzGerald, D. J., Willingham, M., and Pastan, I. (1991). B3(Fv)-PE38KDEL, a single-chain immunotoxin that causes complete regression of a human carcinoma in mice. *Proc Natl Acad Sci U S A* **88**(19), 8616-20.
- Brockstedt, D. G., Podsakoff, G. M., Fong, L., Kurtzman, G., Mueller-Ruchholtz, W., and Engleman, E. G. (1999). Induction of immunity to antigens expressed by recombinant adeno-associated virus depends on the route of administration. *Clin Immunol* **92**(1), 67-75.
- Buning, H., Nicklin, S. A., Perabo, L., Hallek, M., and Baker, A. H. (2003a). AAV-based gene transfer. *Curr Opin Mol Ther* **5**(4), 367-75.
- Buning, H., Ried, M. U., Perabo, L., Gerner, F. M., Huttner, N. A., Enssle, J., and Hallek, M. (2003b). Receptor targeting of adeno-associated virus vectors. *Gene Ther* **10**(14), 1142-51.

- Carter, B. J., and Rose, J. A. (1974). Transcription in vivo of a defective parvovirus: sedimentation and electrophoretic analysis of RNA synthesized by adenovirus-associated virus and its helper adenovirus. *Virology* **61**(1), 182-99.
- Carter, P. J., and Samulski, R. J. (2000). Adeno-associated viral vectors as gene delivery vehicles. *Int J Mol Med* **6**(1), 17-27.
- Chang, S. F., Sgro, J. Y., and Parrish, C. R. (1992). Multiple amino acids in the capsid structure of canine parvovirus coordinately determine the canine host range and specific antigenic and hemagglutination properties. *J Virol* **66**(12), 6858-67.
- Chapman, M. S., and Rossmann, M. G. (1993). Structure, sequence, and function correlations among parvoviruses. *Virology* **194**(2), 491-508.
- Chejanovsky, N., and Carter, B. J. (1989). Replication of a human parvovirus nonsense mutant in mammalian cells containing an inducible amber suppressor. *Virology* **171**(1), 239-47.
- Chipman, P. R., Agbandje-McKenna, M., Kajigaya, S., Brown, K. E., Young, N. S., Baker, T. S., and Rossmann, M. G. (1996). Cryo-electron microscopy studies of empty capsids of human parvovirus B19 complexed with its cellular receptor. *Proc Natl Acad Sci U S A* **93**(15), 7502-6.
- Chirmule, N., Propert, K., Magosin, S., Qian, Y., Qian, R., and Wilson, J. (1999). Immune responses to adenovirus and adeno-associated virus in humans. *Gene Ther* **6**(9), 1574-83.
- Chirmule, N., Xiao, W., Truneh, A., Schnell, M. A., Hughes, J. V., Zoltick, P., and Wilson, J. M. (2000). Humoral immunity to adeno-associated virus type 2 vectors following administration to murine and nonhuman primate muscle. *J Virol* **74**(5), 2420-5.
- Chuah, M. K., Collen, D., and VandenDriessche, T. (2001). Gene therapy for hemophilia. *J Gene Med* **3**(1), 3-20.
- Cosset, F. L., and Russell, S. J. (1996). Targeting retrovirus entry. *Gene Ther* **3**(11), 946-56.
- de la Maza, L. M., and Carter, B. J. (1981). Inhibition of adenovirus oncogenicity in hamsters by adeno-associated virus DNA. *J Natl Cancer Inst* **67**(6), 1323-6.
- Dubielzig, R., King, J. A., Weger, S., Kern, A., and Kleinschmidt, J. A. (1999). Adeno-associated virus type 2 protein interactions: formation of pre-encapsulation complexes. *J Virol* **73**(11), 8989-98.
- Erles, K., Sebokova, P., and Schlehofer, J. R. (1999). Update on the prevalence of serum antibodies (IgG and IgM) to adeno-associated virus (AAV). *J Med Virol* **59**(3), 406-11.
- Fisher, K. J., Jooss, K., Alston, J., Yang, Y., Haecker, S. E., High, K., Pathak, R., Raper, S. E., and Wilson, J. M. (1997). Recombinant adeno-associated virus for muscle directed gene therapy. *Nat Med* **3**(3), 306-12.
- Flannery, J. G., Zolotukhin, S., Vaquero, M. I., LaVail, M. M., Muzyczka, N., and Hauswirth, W. W. (1997). Efficient photoreceptor-targeted gene expression in vivo by recombinant adeno-associated virus. *Proc Natl Acad Sci U S A* **94**(13), 6916-21.
- Flotte, T. R., and Carter, B. J. (1995). Adeno-associated virus vectors for gene therapy. *Gene Ther* **2**(6), 357-62.
- Gao, G., Vandenberghe, L. H., Alvira, M. R., Lu, Y., Calcedo, R., Zhou, X., and Wilson, J. M. (2004). Clades of Adeno-associated viruses are widely disseminated in human tissues. *J Virol* **78**(12), 6381-8.
- Gao, G. P., Alvira, M. R., Wang, L., Calcedo, R., Johnston, J., and Wilson, J. M. (2002). Novel adeno-associated viruses from rhesus monkeys as vectors for human gene therapy. *Proc Natl Acad Sci U S A* **99**(18), 11854-9.

- Girod, A., Ried, M., Wobus, C., Lahm, H., Leike, K., Kleinschmidt, J., Deleage, G., and Hallek, M. (1999). Genetic capsid modifications allow efficient re-targeting of adeno-associated virus type 2. *Nat Med* **5**(9), 1052-6.
- Grifman, M., Trepel, M., Speece, P., Gilbert, L. B., Arap, W., Pasqualini, R., and Weitzman, M. D. (2001). Incorporation of tumor-targeting peptides into recombinant adeno-associated virus capsids. *Mol Ther* **3**(6), 964-75.
- Grimm, D., Kern, A., Pawlita, M., Ferrari, F., Samulski, R., and Kleinschmidt, J. (1999). Titration of AAV-2 particles via a novel capsid ELISA: packaging of genomes can limit production of recombinant AAV-2. *Gene Ther* **6**(7), 1322-30.
- Heilbronn, R., Schlehofer, J. R., Yalkinoglu, A. O., and Zur Hausen, H. (1985). Selective DNA-amplification induced by carcinogens (initiators): evidence for a role of proteases and DNA polymerase alpha. *Int J Cancer* **36**(1), 85-91.
- Hermonat, P. L. (1989). The adeno-associated virus Rep78 gene inhibits cellular transformation induced by bovine papillomavirus. *Virology* **172**(1), 253-61.
- Hermonat, P. L., Labow, M. A., Wright, R., Berns, K. I., and Muzyczka, N. (1984). Genetics of adeno-associated virus: isolation and preliminary characterization of adeno-associated virus type 2 mutants. *J Virol* **51**(2), 329-39.
- Hernandez, Y. J., Wang, J., Kearns, W. G., Loiler, S., Poirier, A., and Flotte, T. R. (1999). Latent adeno-associated virus infection elicits humoral but not cell-mediated immune responses in a nonhuman primate model. *J Virol* **73**(10), 8549-58.
- Hoggan, M. D., Blacklow, N. R., and Rowe, W. P. (1966). Studies of small DNA viruses found in various adenovirus preparations: physical, biological, and immunological characteristics. *Proc Natl Acad Sci U S A* **55**(6), 1467-74.
- Hoque, M., Ishizu, K., Matsumoto, A., Han, S. I., Arisaka, F., Takayama, M., Suzuki, K., Kato, K., Kanda, T., Watanabe, H., and Handa, H. (1999). Nuclear transport of the major capsid protein is essential for adeno-associated virus capsid formation. *J Virol* **73**(9), 7912-5.
- Im, D. S., and Muzyczka, N. (1990). The AAV origin binding protein Rep68 is an ATP-dependent site-specific endonuclease with DNA helicase activity. *Cell* **61**(3), 447-57.
- Im, D. S., and Muzyczka, N. (1992). Partial purification of adeno-associated virus Rep78, Rep52, and Rep40 and their biochemical characterization. *J Virol* **66**(2), 1119-28.
- Jonkers, R. E., and van der Zee, J. S. (2005). Anti-IgE and other new immunomodulation-based therapies for allergic asthma. *Neth J Med* **63**(4), 121-8.
- Jooss, K., Yang, Y., Fisher, K. J., and Wilson, J. M. (1998). Transduction of dendritic cells by DNA viral vectors directs the immune response to transgene products in muscle fibers. *J Virol* **72**(5), 4212-23.
- Kaplitt, M. G., Leone, P., Samulski, R. J., Xiao, X., Pfaff, D. W., O'Malley, K. L., and Doring, M. J. (1994). Long-term gene expression and phenotypic correction using adeno-associated virus vectors in the mammalian brain. *Nat Genet* **8**(2), 148-54.
- Kashiwakura, Y., Tamayose, K., Iwabuchi, K., Hirai, Y., Shimada, T., Matsumoto, K., Nakamura, T., Watanabe, M., Oshimi, K., and Daida, H. (2005). Hepatocyte growth factor receptor is a coreceptor for adeno-associated virus type 2 infection. *J Virol* **79**(1), 609-14.
- Kern, A., Schmidt, K., Leder, C., Muller, O. J., Wobus, C. E., Bettinger, K., Von der Lieth, C. W., King, J. A., and Kleinschmidt, J. A. (2003). Identification of a heparin-binding motif on adeno-associated virus type 2 capsids. *J Virol* **77**(20), 11072-81.
- Khleif, S. N., Myers, T., Carter, B. J., and Trempe, J. P. (1991). Inhibition of cellular transformation by the adeno-associated virus rep gene. *Virology* **181**(2), 738-41.

- King, J. A., Dubielzig, R., Grimm, D., and Kleinschmidt, J. A. (2001). DNA helicase-mediated packaging of adeno-associated virus type 2 genomes into preformed capsids. *Embo J* **20**(12), 3282-91.
- Kreppel, F., Gackowski, J., Schmidt, E., and Kochanek, S. (2005). Combined genetic and chemical capsid modifications enable flexible and efficient de- and retargeting of adenovirus vectors. *Mol Ther* **12**(1), 107-17.
- Krieg, A. M. (2002). CpG motifs in bacterial DNA and their immune effects. *Annu Rev Immunol* **20**, 709-60.
- Kronenberg, S., Kleinschmidt, J. A., and Bottcher, B. (2001). Electron cryo-microscopy and image reconstruction of adeno-associated virus type 2 empty capsids. *EMBO Rep* **2**(11), 997-1002.
- Kyostio, S. R., Owens, R. A., Weitzman, M. D., Antoni, B. A., Chejanovsky, N., and Carter, B. J. (1994). Analysis of adeno-associated virus (AAV) wild-type and mutant Rep proteins for their abilities to negatively regulate AAV p5 and p19 mRNA levels. *J Virol* **68**(5), 2947-57.
- Labow, M. A., and Berns, K. I. (1988). The adeno-associated virus rep gene inhibits replication of an adeno-associated virus/simian virus 40 hybrid genome in cos-7 cells. *J Virol* **62**(5), 1705-12.
- Lux, K., Goerlitz, N., Schlemminger, S., Perabo, L., Goldnau, D., Endell, J., Leike, K., Kofler, D. M., Finke, S., Hallek, M., and Buning, H. (2005). Green fluorescent protein-tagged adeno-associated virus particles allow the study of cytosolic and nuclear trafficking. *J Virol* **79**(18), 11776-87.
- Manning, W. C., Paliard, X., Zhou, S., Pat Bland, M., Lee, A. Y., Hong, K., Walker, C. M., Escobedo, J. A., and Dwarki, V. (1997). Genetic immunization with adeno-associated virus vectors expressing herpes simplex virus type 2 glycoproteins B and D. *J Virol* **71**(10), 7960-2.
- Manno, C. S., Arruda, V. R., Pierce, G. F., Glader, B., Ragni, M., Rasko, J., Ozelo, M. C., Hoots, K., Blatt, P., Konkle, B., Dake, M., Kaye, R., Razavi, M., Zajko, A., Zehnder, J., Nakai, H., Chew, A., Leonard, D., Wright, J. F., Lessard, R. R., Sommer, J. M., Tigges, M., Sabatino, D., Luk, A., Jiang, H., Mingozzi, F., Couto, L., Ertl, H. C., High, K. A., and Kay, M. A. (2006). Successful transduction of liver in hemophilia by AAV-Factor IX and limitations imposed by the host immune response. *Nat Med* **12**(3), 342-347.
- Mayor, H. D., Houlditch, G. S., and Mumford, D. M. (1973). Influence of adeno-associated satellite virus on adenovirus-induced tumours in hamsters. *Nat New Biol* **241**(106), 44-6.
- McCarty, D. M., Monahan, P. E., and Samulski, R. J. (2001). Self-complementary recombinant adeno-associated virus (scAAV) vectors promote efficient transduction independently of DNA synthesis. *Gene Ther* **8**(16), 1248-54.
- McCarty, D. M., Pereira, D. J., Zolotukhin, I., Zhou, X., Ryan, J. H., and Muzyczka, N. (1994). Identification of linear DNA sequences that specifically bind the adeno-associated virus Rep protein. *J Virol* **68**(8), 4988-97.
- McKenna, R., Olson, N. H., Chipman, P. R., Baker, T. S., Booth, T. F., Christensen, J., Aasted, B., Fox, J. M., Bloom, M. E., Wolfenbarger, J. B., and Agbandje-McKenna, M. (1999). Three-dimensional structure of Aleutian mink disease parvovirus: implications for disease pathogenicity. *J Virol* **73**(8), 6882-91.
- McLaughlin, S. K., Collis, P., Hermonat, P. L., and Muzyczka, N. (1988). Adeno-associated virus general transduction vectors: analysis of proviral structures. *J Virol* **62**(6), 1963-73.
- Miller, A. D. (1996). Cell-surface receptors for retroviruses and implications for gene transfer. *Proc Natl Acad Sci U S A* **93**(21), 11407-13.

- Monahan, P. E., and Samulski, R. J. (2000). Adeno-associated virus vectors for gene therapy: more pros than cons? *Mol Med Today* **6**(11), 433-40.
- Moskalenko, M., Chen, L., van Roey, M., Donahue, B. A., Snyder, R. O., McArthur, J. G., and Patel, S. D. (2000). Epitope mapping of human anti-adeno-associated virus type 2 neutralizing antibodies: implications for gene therapy and virus structure. *J Virol* **74**(4), 1761-6.
- Mori, S., Wang, L., Takeuchi, T., and Kanda, T. (2004). Two novel adeno-associated viruses from cynomolgus monkey: pseudotyping characterization of capsid protein. *Virology* **330**(2), 375-83.
- Muller, O. J., Kaul, F., Weitzman, M. D., Pasqualini, R., Arap, W., Kleinschmidt, J. A., and Trepel, M. (2003). Random peptide libraries displayed on adeno-associated virus to select for targeted gene therapy vectors. *Nat Biotechnol* **21**(9), 1040-6.
- Muzyczka, N., and Berns, K. I. (2001). Parvoviridae: The viruses and their replication. 4th ed. In "Fields Virology" (D. M. Knipe, P. M. Howley, D. E. Griffin, R. A. Lamb, M. A. Martin, B. Roizman, and S. E. Straus, Eds.), Vol. 2, pp. 2327-2359. 2 vols. Lippincott Williams & Wilkins, Philadelphia.
- Nathwani, A. C., Davidoff, A., Hanawa, H., Zhou, J. F., Vanin, E. F., and Nienhuis, A. W. (2001). Factors influencing in vivo transduction by recombinant adeno-associated viral vectors expressing the human factor IX cDNA. *Blood* **97**(5), 1258-65.
- Nicklin, S. A., Buening, H., Dishart, K. L., de Alwis, M., Girod, A., Hacker, U., Thrasher, A. J., Ali, R. R., Hallek, M., and Baker, A. H. (2001). Efficient and selective AAV2-mediated gene transfer directed to human vascular endothelial cells. *Mol Ther* **4**(3), 174-81.
- Ohno, K., Sawai, K., Iijima, Y., Levin, B., and Meruelo, D. (1997). Cell-specific targeting of Sindbis virus vectors displaying IgG-binding domains of protein A. *Nat Biotechnol* **15**(8), 763-7.
- Opie, S. R., Warrington, K. H., Jr., Agbandje-McKenna, M., Zolotukhin, S., and Muzyczka, N. (2003). Identification of amino acid residues in the capsid proteins of adeno-associated virus type 2 that contribute to heparan sulfate proteoglycan binding. *J Virol* **77**(12), 6995-7006.
- Perabo, L., Buning, H., Kofler, D. M., Ried, M. U., Girod, A., Wendtner, C. M., Enssle, J., and Hallek, M. (2003). In vitro selection of viral vectors with modified tropism: the adeno-associated virus display. *Mol Ther* **8**(1), 151-7.
- Perabo, L., Endell, J., King, S., Lux, K., Goldnau, D., Hallek, M., and Buning, H. (2006). Combinatorial engineering of a gene therapy vector: directed evolution of adeno-associated virus. *J Gene Med* **8**(2), 155-62.
- Qing, K., Mah, C., Hansen, J., Zhou, S., Dwarki, V., and Srivastava, A. (1999). Human fibroblast growth factor receptor 1 is a co-receptor for infection by adeno-associated virus 2. *Nat Med* **5**(1), 71-7.
- Rabinowitz, J. E., and Samulski, R. J. (2000). Building a better vector: the manipulation of AAV virions. *Virology* **278**(2), 301-8.
- Rabinowitz, J. E., Xiao, W., and Samulski, R. J. (1999). Insertional mutagenesis of AAV2 capsid and the production of recombinant virus. *Virology* **265**(2), 274-85.
- Raj, K., Ogston, P., and Beard, P. (2001). Virus-mediated killing of cells that lack p53 activity. *Nature* **412**(6850), 914-7.
- Redemann, B. E., Mendelson, E., and Carter, B. J. (1989). Adeno-associated virus rep protein synthesis during productive infection. *J Virol* **63**(2), 873-82.
- Ried, M. U., Girod, A., Leike, K., Buning, H., and Hallek, M. (2002). Adeno-associated virus capsids displaying immunoglobulin-binding domains permit antibody-mediated vector retargeting to specific cell surface receptors. *J Virol* **76**(9), 4559-66.

- Ruffing, M., Zentgraf, H., and Kleinschmidt, J. A. (1992). Assembly of viruslike particles by recombinant structural proteins of adeno-associated virus type 2 in insect cells. *J Virol* **66**(12), 6922-30.
- Russell, D. W., Alexander, I. E., and Miller, A. D. (1995). DNA synthesis and topoisomerase inhibitors increase transduction by adeno-associated virus vectors. *Proc Natl Acad Sci U S A* **92**(12), 5719-23.
- Samulski, R. J., Chang, L. S., and Shenk, T. (1987). A recombinant plasmid from which an infectious adeno-associated virus genome can be excised in vitro and its use to study viral replication. *J Virol* **61**(10), 3096-101.
- Sarukhan, A., Camugli, S., Gjata, B., von Boehmer, H., Danos, O., and Jooss, K. (2001). Successful interference with cellular immune responses to immunogenic proteins encoded by recombinant viral vectors. *J Virol* **75**(1), 269-77.
- Shi, W., Arnold, G. S., and Bartlett, J. S. (2001). Insertional mutagenesis of the adeno-associated virus type 2 (AAV2) capsid gene and generation of AAV2 vectors targeted to alternative cell-surface receptors. *Hum Gene Ther* **12**(14), 1697-711.
- Shi, W., and Bartlett, J. S. (2003). RGD inclusion in VP3 provides adeno-associated virus type 2 (AAV2)-based vectors with a heparan sulfate-independent cell entry mechanism. *Mol Ther* **7**(4), 515-25.
- Shi, X., Fang, G., and Shi, W. (2006). Insertional Mutagenesis at Positions 520 and 584 of Adeno-Associated Virus Type 2 (AAV2) Capsid Gene and Generation of AAV2 Vectors with Eliminated Heparin-Binding Ability and Introduced Novel Tropism. *Hum Gene Ther*.
- Sieczkarski, S. B., and Whittaker, G. R. (2002). Dissecting virus entry via endocytosis. *J Gen Virol* **83**(Pt 7), 1535-45.
- Sinha, P., Sengupta, J., and Ray, P. K. (1999). Functional mimicry of protein A of *Staphylococcus aureus* by a proteolytically cleaved fragment. *Biochem Biophys Res Commun* **260**(1), 111-6.
- Smith, R. H., and Kotin, R. M. (1998). The Rep52 gene product of adeno-associated virus is a DNA helicase with 3'-to-5' polarity. *J Virol* **72**(6), 4874-81.
- Smith, R. H., and Kotin, R. M. (2000). An adeno-associated virus (AAV) initiator protein, Rep78, catalyzes the cleavage and ligation of single-stranded AAV ori DNA. *J Virol* **74**(7), 3122-9.
- Smith, T. J. (2001). Antibody interactions with rhinovirus: lessons for mechanisms of neutralization and the role of immunity in viral evolution. *Curr Top Microbiol Immunol* **260**, 1-28.
- Smuda, J. W., and Carter, B. J. (1991). Adeno-associated viruses having nonsense mutations in the capsid genes: growth in mammalian cells containing an inducible amber suppressor. *Virology* **184**(1), 310-8.
- Snyder, R. O., Im, D. S., and Muzyczka, N. (1990). Evidence for covalent attachment of the adeno-associated virus (AAV) rep protein to the ends of the AAV genome. *J Virol* **64**(12), 6204-13.
- Snyder, R. O., Im, D. S., Ni, T., Xiao, X., Samulski, R. J., and Muzyczka, N. (1993). Features of the adeno-associated virus origin involved in substrate recognition by the viral Rep protein. *J Virol* **67**(10), 6096-104.
- Snyder, R. O., Miao, C. H., Patijn, G. A., Spratt, S. K., Danos, O., Nagy, D., Gown, A. M., Winther, B., Meuse, L., Cohen, L. K., Thompson, A. R., and Kay, M. A. (1997). Persistent and therapeutic concentrations of human factor IX in mice after hepatic gene transfer of recombinant AAV vectors. *Nat Genet* **16**(3), 270-6.
- Stachler, M. D., and Bartlett, J. S. (2006). Mosaic vectors comprised of modified AAV1 capsid proteins for efficient vector purification and targeting to vascular endothelial cells. *Gene Ther*.

- Strassheim, M. L., Gruenberg, A., Veijalainen, P., Sgro, J. Y., and Parrish, C. R. (1994). Two dominant neutralizing antigenic determinants of canine parvovirus are found on the threefold spike of the virus capsid. *Virology* **198**(1), 175-84.
- Stubenrauch, K., Gleiter, S., Brinkmann, U., Rudolph, R., and Lilie, H. (2001). Conjugation of an antibody Fv fragment to a virus coat protein: cell-specific targeting of recombinant polyoma-virus-like particles. *Biochem J* **356**(Pt 3), 867-73.
- Summerford, C., Bartlett, J. S., and Samulski, R. J. (1999). AlphaVbeta5 integrin: a co-receptor for adeno-associated virus type 2 infection. *Nat Med* **5**(1), 78-82.
- Summerford, C., and Samulski, R. J. (1998). Membrane-associated heparan sulfate proteoglycan is a receptor for adeno-associated virus type 2 virions. *J Virol* **72**(2), 1438-45.
- Tal, J. (2000). Adeno-associated virus-based vectors in gene therapy. *J Biomed Sci* **7**(4), 279-91.
- Teichler Zallen, D. (2000). US gene therapy in crisis. *Trends Genet* **16**(6), 272-5.
- Tratschin, J. D., Miller, I. L., and Carter, B. J. (1984). Genetic analysis of adeno-associated virus: properties of deletion mutants constructed in vitro and evidence for an adeno-associated virus replication function. *J Virol* **51**(3), 611-9.
- Tsao, J., Chapman, M. S., Agbandje, M., Keller, W., Smith, K., Wu, H., Luo, M., Smith, T. J., Rossmann, M. G., Compans, R. W., and et al. (1991). The three-dimensional structure of canine parvovirus and its functional implications. *Science* **251**(5000), 1456-64.
- VandenDriessche, T., Collen, D., and Chuah, M. K. (2001). Viral vector-mediated gene therapy for hemophilia. *Curr Gene Ther* **1**(3), 301-15.
- Walter, W., and Stein, U. (1996). Cell type specific and inducible promoters for vectors in gene therapy as an approach for cell targeting. *J Mol Med* **74**, 379-392.
- Wang, C. Y., Walfield, A. M., Fang, X., Hammerberg, B., Ye, J., Li, M. L., Shen, F., Shen, M., Alexander, V., and MacGlashan, D. W. (2003). Synthetic IgE peptide vaccine for immunotherapy of allergy. *Vaccine* **21**(15), 1580-90.
- Wang, M., Hemminki, A., Siegal, G. P., Barnes, M. N., Dmitriev, I., Krasnykh, V., Liu, B., Curiel, D. T., and Alvarez, R. D. (2005). Adenoviruses with an RGD-4C modification of the fiber knob elicit a neutralizing antibody response but continue to allow enhanced gene delivery. *Gynecol Oncol* **96**(2), 341-8.
- Warrington, K. H., Jr., Gorbatyuk, O. S., Harrison, J. K., Opie, S. R., Zolotukhin, S., and Muzyczka, N. (2004). Adeno-associated virus type 2 VP2 capsid protein is nonessential and can tolerate large peptide insertions at its N terminus. *J Virol* **78**(12), 6595-609.
- White, S. J., Nicklin, S. A., Buning, H., Brosnan, M. J., Leike, K., Papadakis, E. D., Hallek, M., and Baker, A. H. (2004). Targeted gene delivery to vascular tissue in vivo by tropism-modified adeno-associated virus vectors. *Circulation* **109**(4), 513-9.
- Wistuba, A., Kern, A., Weger, S., Grimm, D., and Kleinschmidt, J. A. (1997). Subcellular compartmentalization of adeno-associated virus type 2 assembly. *J Virol* **71**(2), 1341-52.
- Wobus, C. E., Hügler-Dorr, B., Girod, A., Petersen, G., Hallek, M., and Kleinschmidt, J. A. (2000). Monoclonal antibodies against the adeno-associated virus type 2 (AAV-2) capsid: epitope mapping and identification of capsid domains involved in AAV-2-cell interaction and neutralization of AAV-2 infection. *J Virol* **74**(19), 9281-93.
- Work, L. M., Nicklin, S. A., Brain, N. J., Dishart, K. L., Von Seggern, D. J., Hallek, M., Buning, H., and Baker, A. H. (2004). Development of efficient viral vectors selective for vascular smooth muscle cells. *Mol Ther* **9**(2), 198-208.

- Work, L. M., Buning, H., Hunt, E., Nicklin, S. A., Denby, L., Britton, N., Leike, K., Odenthal, M., Drebber, U., Hallek, M., and Baker, A. H. (2005). Vascular bed-targeted in vivo gene delivery using tropism-modified adeno-associated viruses. *Mol Ther*.
- Wu, P., Xiao, W., Conlon, T., Hughes, J., Agbandje-McKenna, M., Ferkol, T., Flotte, T., and Muzyczka, N. (2000). Mutational analysis of the adeno-associated virus type 2 (AAV2) capsid gene and construction of AAV2 vectors with altered tropism. *J Virol* **74**(18), 8635-47.
- Xiao, X., Li, J., and Samulski, R. J. (1996). Efficient long-term gene transfer into muscle tissue of immunocompetent mice by adeno-associated virus vector. *J Virol* **70**(11), 8098-108.
- Xie, Q., Bu, W., Bhatia, S., Hare, J., Somasundaram, T., Azzi, A., and Chapman, M. S. (2002). The atomic structure of adeno-associated virus (AAV-2), a vector for human gene therapy. *Proc Natl Acad Sci U S A* **99**(16), 10405-10.
- Yakobson, B., Hrynko, T. A., Peak, M. J., and Winocour, E. (1989). Replication of adeno-associated virus in cells irradiated with UV light at 254 nm. *J Virol* **63**(3), 1023-30.
- Yakobson, B., Koch, T., and Winocour, E. (1987). Replication of adeno-associated virus in synchronized cells without the addition of a helper virus. *J Virol* **61**(4), 972-81.
- Yalkinoglu, A. O., Heilbronn, R., Burkle, A., Schlehofer, J. R., and zur Hausen, H. (1988). DNA amplification of adeno-associated virus as a response to cellular genotoxic stress. *Cancer Res* **48**(11), 3123-9.
- Yalkinoglu, A. O., Zentgraf, H., and Hubscher, U. (1991). Origin of adeno-associated virus DNA replication is a target of carcinogen-inducible DNA amplification. *J Virol* **65**(6), 3175-84.
- Yang, Q., Mamounas, M., Yu, G., Kennedy, S., Leaker, B., Merson, J., Wong-Staal, F., Yu, M., and Barber, J. R. (1998). Development of novel cell surface CD34-targeted recombinant adenoassociated virus vectors for gene therapy. *Hum Gene Ther* **9**(13), 1929-37.
- Yuasa, K., Sakamoto, M., Miyagoe-Suzuki, Y., Tanouchi, A., Yamamoto, H., Li, J., Chamberlain, J. S., Xiao, X., and Takeda, S. (2002). Adeno-associated virus vector-mediated gene transfer into dystrophin-deficient skeletal muscles evokes enhanced immune response against the transgene product. *Gene Ther* **9**(23), 1576-88.
- Zaiss, A. K., Liu, Q., Bowen, G. P., Wong, N. C., Bartlett, J. S., and Muruve, D. A. (2002). Differential activation of innate immune responses by adenovirus and adeno-associated virus vectors. *J Virol* **76**(9), 4580-90.
- Zhang, Y., Chirmule, N., Gao, G., and Wilson, J. (2000). CD40 ligand-dependent activation of cytotoxic T lymphocytes by adeno-associated virus vectors in vivo: role of immature dendritic cells. *J Virol* **74**(17), 8003-10.
- Zhou, X., Zolotukhin, I., Im, D. S., and Muzyczka, N. (1999). Biochemical characterization of adeno-associated virus rep68 DNA helicase and ATPase activities. *J Virol* **73**(2), 1580-90.

Curriculum Vitae

Persönliche Daten

Daniela Goldnau
Karneidplatz 32
81547 München
geboren am 9.Juli 1975 in Duisburg
ledig

Schulausbildung und Studium

1985-1994 altsprachliches Gymnasium Adolfinum, Moers
1991-1992 1-jähriger **Auslandsaufenthalt**, Highschooljahr mit
Graduation in Acton, Massachusetts, USA

Hochschulausbildung

1995-2000 Studium der **Pharmazie** an der Johannes Gutenberg-
Universität, Mainz
August 1998 Abschluß des Grundstudiums mit dem 1. Abschnitt der
Pharmazeutischen Prüfung
Mai 2000 2. Abschnitt der Pharmazeutischen Prüfung
Juni 2001 3. Staatsexamen Pharmazie in Mainz
Erteilung der Approbation als Apothekerin

Praktische Tätigkeiten

Arbeit als Apothekerin

Juli-Dezember 2001 Apothekerin in der Sonnen-Apotheke in Gröbenzell
Seit Dez 2001 als Teilzeitbeschäftigung bis heute
fortgesetzt

Promotion

Seit Dezember 2001 **Promotion am Genzentrum** der LMU München in der
Arbeitsgruppe von Prof. Michael Hallek
Thema der Arbeit: "**New strategies for the application
of AAV-2 targeting vectors**"

Publikationen

Kerstin Lux, Nico Görlitz, Stefanie Schlemminger, Luca Perabo, **Daniela Goldnau**, Jan Endell, Kristin Leike, David M. Kofler, Stefan Finke, Michael Hallek, Hildegard Büning
"Green Fluorescent Protein-Tagged Adeno-Associated Virus (AAV) Particles Allow the Study of Cytosolic and Nuclear Trafficking"; J Virol. 2005 Sep; 79(18):11776-87

Luca Perabo, Jan Endell, Susan King, Kerstin Lux, **Daniela Goldnau**, Michael Hallek, Hildegard Büning
"Combinatorial engineering of a gene therapy vector: directed evolution of adeno-associated virus"; J Gene Med. 2006 Feb; 8(2):155-62

Daniela Goldnau, Jan Endell, Luca Perabo, and Kathryn White, Sibille Humme, Lorraine Work, Hanna Janicki, Michael Hallek, Andrew H. Baker, Hildegard Büning
"HSPG binding properties of adeno-associated virus (AAV) retargeting mutants and consequences for their in vivo tropism"; J Virol, in revision March 2006

Hildegard Büning, John Nieland, Luca Perabo, Daniela Goldnau, Kerstin Lux, and Michael Hallek
"AAV anti-idiotypic vaccine", eingereicht als Erfindungsmeldung, 2005
